Characterising the Role of mTORC1 in Myeloid Cells

Lamya Zohair Yamani

A thesis submitted for the degree of Doctor of Philosophy

at Queen Mary University of London

January 2017

Centre for Cancer and Inflammation
Bart and the London School of Medicine and Dentistry
Queen Mary University of London
3rd Floor, John Vane Science Centre
Charterhouse Square
London, EC1M 6BQ

Statement of Originality

I, Lamya Yamani, confirm that the research included within this thesis is my own work or that where it has been carried out in collaboration with, or supported by others, that this is duly acknowledged below and my contribution indicated.

I attest that I have exercised reasonable care to ensure that the work is original, and does not to the best of my knowledge break any UK law, infringe any third party's copyright or other intellectual Property Right, or contain any confidential material.

I accept that the College has the right to use plagiarism detection software to check the electronic version of the thesis.

I confirm that this thesis has not been previously submitted for the award of a degree by this or any other university.

Signature:

Date:

Abstract

The mammalian target of rapamycin (mTOR) signalling pathway takes part in both extracellular and intracellular signals. It is a major regulator of cell metabolism, growth, proliferation and survival. mTOR also regulates critical processes such as cytoskeletal organization, ribosomal biogenesis, transcription and protein synthesis. The mTOR pathway has been implicated in many diseases such as cancer, neurodegeneration and diabetes, which impact homeostasis and cellular functions. Moreover, mTOR has also been shown to play a critical role in immune cell regulation of T and B cells together with neutrophils and antigen presenting cells, as it integrates signals between them extending to the entire immune microenvironment.

The aim of my study was to investigate the role of a component of the mTOR complex 1, Raptor, in myeloid cells. My findings show that the absence of Raptor knock out (KO) does not affect bone marrow derived macrophage (BMDM) differentiation and maturation. However, the absence of Raptor influences BMDM polarisation towards an inflammatory phenotype, at least at the level of transcription as observed by increases in mRNA expression of inflammatory cytokines such as *TNFα, IL-12β,* and *IL-6*. This finding was consolidated by an increase in NFκB pathway signalling in Raptor KO BMDMs.

Downstream intracellular signalling in myeloid cells was affected by deletion of Raptor as I found reduced S6K phosphorylation in Raptor KO BMDMs compared to wild type (WT) BMDMs. As a consequence of Raptor absence in BMDMs, STAT3 phosphorylation was also reduced. Raptor deletion did not impact the PI3K/Akt signalling pathway, but decreased phosphorylation of ERK. BMDMs lacking Raptor had reduced phagocytic activity as they were also observed to migrate less towards a pancreatic cancer cell line. However preliminary experiments in pancreatic cancer models did not indicate a major role for Raptor in the activity of tumour associated myeloid cells. My results demonstrate that Raptor and by implication mTORC1, is involved in macrophage polarisation and function.

Acknowledgments

In the Name of Allah, The Most Gracious, The Most Merciful….

It is strange how it is time for me to write the acknowledgments, but I am finding it the hardest part to write, there are so many people that I would like to thank and I am sure words alone are not enough…

I start off by thanking my supervisor Professor Frances Balkwill, it was a pleasure working under her guidance. Her constant motivation and belief in my capabilities are things I will never forget. Her high standards and work ethics inspired me to give my all in the research and thesis writing. I would also like to thank my second supervisor Dr. Melania Capasso, for all her help and constant championing.

I would like to thank my guardian angel these past 4 years, Dr. Eleni Maniati, she has taught me so much over the course of my research, she taught me to be humble when things were working and how to get up and keep moving without looking back when things were not going as planned. I thank her for just being around whenever I needed advice. Dr. Juliana Candido, I would like to thank her for the constant motivation that she has provided over the years, her help and constant cheering are unforgettable. I would also like to thank Dr. Maryam Jangani for her support and advice. I would not forget to thank my second family, all the amazing individuals at the Centre of Cancer and Inflammation (including past members), it was a delight coming in daily smiling at your faces, you made every day worthwhile.

Dr. Esther Castellano Sanchez, I thank her with all my heart for being a great friend over these years, there are so many memories I will cherish. Dr. Sarah Spear, her friendship is of great value to me, I thank her for all the help and support she offered me professionally and all the fun times we had together in between. I hope our friendship will continue for as long as we both can still remember. Laura Lecker, I thank her for her friendship and her constant positivity. I will never forget all the great times we had together, she was an inspiration to always stay happy no matter what, I am sure this friendship will continue for the longest time. Thank you to ATS staff for all their help you guys were amazing.

Agata Krygowska, “My Aggie”, I really don’t know where and how to begin thanking her, but I will start by saying, that I thank her for being a perfect friend, it was pure joy

sitting next to her for these 4 years, she turned from friend to sister quite quickly and I am glad that she came into my life. I am sure that we will have each other always and forever.

Dr. Layla Al-Bashawri, I thank her for the constant support and love she has given me throughout these years, she was one of the reasons I wanted to pursue a PhD degree.

I would like to also thank the Kingdom of Saudi Arabia, and the University of Dammam with the department of Clinical Laboratory Sciences, for the opportunity of a scholarship that helped me pursue this PhD degree.

I would like to thank my friends, Hend AlKraidees, Yasmeen AlSoufi, Sarah AlHumaid, Maha AlSaif, Nora AlWatban, Saja AlRayes, Afnan AlJaffari, Summaya AlRuwaie, and Amjad AlQahtani, for being true friends no matter how far the distances or the busy lives we have that keep us from seeing each other as often as we would like.

Many thanks to Yasmeen AlDawsari for all her help and constant cheering, also thanks for the times where I would come home with stiches in my stomach from all the laughter. I am so happy I got to know such a person.

To my darling Maha AlMadhi, I thank her greatly for all that she has done for me over these years, I was truly blessed having her in my life, she became a sister to me, from day one. Her constant support and belief in me was so heart-warming. Honestly, herself and her lovely family are a constant reminder that humans may very much be angels.

To my one and only sister Najla Yamani and brother AbdulRahman Yamani, I thank them for their love and support, I love them and keep them implanted deep in my heart. No matter how rough the weather may be, looking at their faces reminds me everything will be alright.

Last but definitely not least, I would like to thank “the crown on top of my head” my father, Dr. Zohair A. Yamani, and “my eyes and heart” my mother Maha AlKhrieji, if it wasn’t for their constant prayers for me I would not be where I am today, I am so proud to have them as my parents, they are more than anyone could wish for. They have taught me to break all barriers and to go above and beyond in pursue of knowledge. I hope that I am doing them proud.

Table of Contents

List of Figures

List of Tables

Abbreviations

4E-BP1	Eukaryotic translation initiation factor 4E eIF4E-binding protein 1
AGC	Protein kinase C kinase
Akt	Protein kinase B (PKB)
AMP	Adenosine monophosphate
AMPK	5' AMP-activated protein kinase
APCs	Antigen presenting cells
Atg13	Autophagy related 13
ATP	Adenosine triphosphate
BALB/c	Mouse model
B-CLL	B cell chronic lymphoblastic leukaemia
BCR	B cell antigen receptor
BM	Bone marrow
BMDMs	Bone marrow derived macrophages
C57Bl/6	Mouse model commonly known as black 6
CAFs	Cancer associated fibroblasts
cAMP	Cyclic adenosine monophosphate
CD	Cluster of differentiation
CD19	B cell marker
CD3	T cell marker
CD4	T helper cell marker
CD8	T cytotoxic cell marker
cGMP	Cyclic guanosine monophosphate

CMP	Common myeloid progenitors
Cre	Cre recombinase
Cre/LoxP	Cre/Loxp recombination
CSF1R	Colony stimulating factor 1 receptor
DEPTOR	DEP domain containing mTOR interacting protein
eIF4E	Eukaryotic translation initiation factor 4E
ERK	Extracellular signal regulated kinase
f/f	LoxP site
F480	Macrophage marker
FACS	Fluorescence activated cell sorting
FAT	FK506 binding protein 12 rapamycin associated protein 1 (FRAP), Ataxia telangiectasia mutated (ATM), Transcription factor co-activator (TRRAP)
FATC	FRAP, TRRAP, and ATM C-terminal domain
Fc	Fragment crystallizable
FKBP12	FK binding protein 12
FOXO1	Forkhead box protein O1
FRB	FKBP12 rapamycin binding domain
GAP	GTPase activating protein
GDP	Guanosine diphosphate
GM-CSF	Granulocyte macrophage colony stimulating factor
GSK3β	Glycogen synthase kinase 3 beta
GTP	Guanosine 5' triphosphate
HEAT	Huntingtin , elongation factor 3 (EF3), protein phosphatase 2A (PP2A), yeast kinase (TOR1)
HIF-1α	Hypoxia inducible factor 1 alpha

HSC	Hematopoietic stem cells
I.P	intraperitoneal
IFN	Interferon
IL-	Interleukin
iNOS	Nitric oxide synthase
IκBα	Inhibitor of κB
KO	Knock out
LD	Lethal dose
LIN	Lineage marker
LPS	Lipopolysaccharides
M0	Unstimulated macrophages
M1	Inflammatory macrophages (classical)
M2	Immunomodulatory macrophages (alternative)
MAPK	Mitogen activated protein kinase
MDSCs	Myeloid derived suppressor cells
MEFs	Mouse embryonic fibroblasts
MEK	Mitogen activated protein kinase kinase
MHCII	Major histocompatibility complex class II
mLST8	Mammalian lethal with sec13 protein 8
MMPs	Matrix metalloproteinases
MRC1	Mannose receptor C type 1
mRNA	Messenger ribonucleic acid
mSIN1	Mammalian stress activated protein kinase interacting protein 1
mTOR	Mammalian target of rapamycin
mTORC1	Mammalian target of rapamycin complex 1

mTORC2	Mammalian target of rapamycin complex 2
NFκB	Nuclear factor kappa light chain enhancer of activated B cell
NO	Nitric oxide
PanINs	Pancreatic intraepithelial neoplasias
PDAC	Pancreatic ductal adenocarcinoma
PDCD4	Programmed cell death 4
PDK1	3-Phosphoinositide dependent protein kinase 1
PDL1	Programmed death ligand 1
PGC-1β	Peroxisome proliferator activated receptor gamma coactivator 1 beta
Phalloidin	F-actin
PI3K	Phosphatidylinositol 4,5, bisphosphate 3 kinase
PIKK	Phosphoinositide 3 kinase family
PIP2	Phosphatidylinositol 4,5 bisphosphate
PIP3	Phosphatidylinositol 3,4,5 triphosphate
PKCα	Protein kinase C alpha
PPAR	Peroxisome proliferator activated receptor
PRAS40	Proline rich Akt substrate 40 kDa
PROTOR	Protein observed with RICTOR
PTEN	Phosphatase and tensin homolog
Rag	Ras related GTP binding protein
RAPTOR	Regulatory associated protein of mTOR
REDD1	Hypoxia induced factor protein regulated in the development of DNA damage response 1
RHEB	Ras homolog enriched in brain
RICTOR	Rapamycin insensitive companion of mTOR

S6K (S6)	Ribosomal S6 kinase beta 1
SGK1	Serum glucocorticoid regulated kinase 1
STAT	Signal transducer and activator of transcription
T regs	T regulatory cells (T cells)
TAMs	Tumour associated macrophages
TB32047	Murine pancreatic cancer cell line
TB32048	Murine pancreatic cancer cell line
TCR	T cell receptor
TGF-β	Transforming growth factor beta
TH	T helper cells (T cells)
TLRs	Toll like receptors
TNFα	Tumour necrosis factor alpha
TOS	TOR signalling motif
TSC1/2	Tuberous sclerosis complex 1 and 2
UTRs	Untranslated regions
VEGF	Vascular endothelial growth factor
WT	Wild type

1 Introduction

Over the millennia organisms have evolved mechanisms allowing them to utilise cues from their environment for growth and survival. Living organisms rely on continuous biochemical reactions that need constant nutrient and energy availability. This is to permit synthesis of new cellular components such as nucleic acids, proteins and lipids leading to an increase in cell size and number. However, these organisms must also cope with times of reduced nutrient and energy accessibility and this necessitates their adaptation to stress signals accordingly, in order to balance anabolic and catabolic processes. In times of stress, organisms begin to gradually slow down proliferation and start recycling organelles and aged proteins that will provide them with new metabolites to remain alive.

The mechanistic target of rapamycin, previously known as the mammalian target of rapamycin (mTOR), is a major component of a signalling pathway that enables multicellular organisms to sense environmental cues that promote growth and survival [1]. As this pathway supports cell growth, it also provides homeostasis by balancing growth and starvation signals. Deregulation of mTOR has been implicated in many diseases in which homeostasis becomes compromised, such as cancer, neurodegeneration, and diabetes. mTOR increases longevity by controlling rates of cellular maturation [1]. Furthermore, mTOR is capable of integrating signals occurring within the immune microenvironment and plays a major role in regulating immune cells, particularly T cells, B cells, neutrophils and antigen presenting cells (APCs) [2 3 4]. mTOR acts as a central link between cellular metabolism and immune cell function, as it regulates many aspects of immune cell differentiation, growth and development [5].

Given the significance of this pathway in controlling major facets of cell survival and disease states, targeting mTOR as a therapeutic approach has been a focus for many years in regards to cancer, ageing, metabolic and neurodegenerative diseases.

1.1 mTOR

mTOR is an evolutionary conserved serine/threonine protein kinase that has a molecular weight of 289 kDa. It is constitutively expressed and usually regulated post-translationally [6]. It is part of the phosphoinositide 3-kinase family (PIKK) [1 7]. mTOR was discovered as the target of the immunosuppressive drug rapamycin, thereby it was given the name of 'mechanistic target of rapamycin'. Rapamycin was discovered in a search for new antibiotics; it is produced from *streptomyces hygroscopicus* extracted from soil samples taken in Easter Island (the island is named Rapa Nui in native Polynesian, hence the name rapamycin) [8]. Scientists found rapamycin to possess growth retardation properties as it has inhibitory effects on the cell cycle. It also has immunosuppressive and anti-tumour activities [9]. Rapamycin inhibits mTOR function by binding to the FK binding protein 12 (FKBP12), which in turn binds mTOR through the FKBP12-rapamycin-binding (FRB) domain. Rapamycin induces a conformational change in the mTOR-RAPTOR complex by binding to the kinase domain found on mTOR in a mechanism that is still not thoroughly understood. This conformational change potentially destabilizes mTOR-RAPTOR complex leading to an impairment of the coupling between mTORC1 and its substrates. Hence this prevents the recruitment of key substrates such as S6 kinase 1 (S6K) and eukaryotic translation initiation factor 4E eIF4E-binding protein 1 (4E-BP1), thereby inhibiting the phosphorylation of these substrates. Hindering the phosphorylation of these substrates impedes mRNA translation and subsequent protein synthesis [10 11]. From the time rapamycin was discovered, many other drugs have been developed, known as rapalogs, which also block mTOR [12].

1.1.1 mTOR structure

Structurally mTOR has 2 terminals that take on different roles. The N terminus is composed of cluster of HEAT repeats, containing binding domains of Huntingtin, elongation factor 3 (EF3), protein phosphatase 2A (PP2A), and the yeast kinase TOR1. HEAT repeats are needed for protein-protein interactions. mTOR also has a FAT domain that contains portions of FK506- binding protein 12-rapamycin associated protein 1 (FRAP), ataxia telangiectasia mutated (ATM), and transcription factor co-activator (TRRAP). Adjacent to the FAT domain is an FRB domain, constituted of the FKBP 12-rapamycin binding domain, which is next to the kinase domain. This kinase domain is necessary for the kinase activity of mTOR. The C terminus is required for mTOR

structural integrity and is composed of portions of FRAP, TRRAP, and ATM C-terminal (FATC) domain [13] (Figure 1.1).

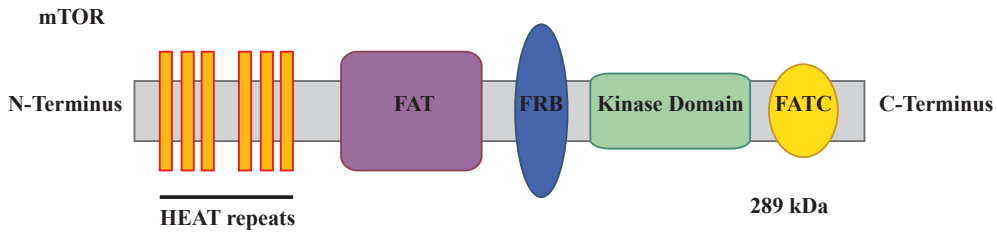

Figure 1.1 Structure of mTOR

mTOR is a 289 kDa protein composed of HEAT repeats, FAT and FRB domain, which are important for protein to protein interactions. The kinase domain is needed for mTOR's kinase activity. FATC domain is important for the structure integrity.

1.1.2 mTOR complexes

mTOR is the catalytic subunit of two complexes known as mTORC1 and mTORC2. Unique proteins distinguish the two complexes. mTORC1 is composed of regulatory associated protein of mTOR (RAPTOR) a scaffolding protein vital for assembly of the complex, proline-rich Akt substrate 40 kDa (PRAS40), mammalian lethal with Sec13 protein 8 (mLST8), and DEP domain-containing mTOR- interacting protein (DEPTOR). The presence of RAPTOR and PRAS40 distinguish mTORC1. RAPTOR and mLST8 are adaptor proteins needed for protein-protein interactions, while PRAS40 and DEPTOR constrain mTORC1 activity. PRAS40 has been shown to inhibit mTORC1 as it binds to RAPTOR through what is known as a TOR signalling motif (TOS) that is found on mTORC1 substrates (4E-BP1 and S6K). PRAS40 is said to compete with these substrates for binding and phosphorylation of mTORC1 thereby constraining its activation [14]. As mTORC1 activity decreases DEPTOR is recruited to the complex along with PRAS40 where they promote inhibition of the complex [15]. mTORC2 comprises the adaptor protein rapamycin insensitive companion of mTOR or RAPTOR independent companion of TOR (RICTOR), also a scaffolding protein needed for complex assembly. mTORC2 also contains the mammalian stress-activated protein kinase interacting protein 1 (mSIN1), which is essential for targeting mTORC2 to the plasma membrane, allowing interaction with Akt. Another adaptor protein is the protein observed with RICTOR (PROTOR). mTORC2 also includes both mLST8 and DEPTOR. Therefore, mTORC2 is defined by

the presence of RICTOR, mSIN1 and PROTOR. mTORC1 and mTORC2 complexes are needed for intracellular signalling abilities, each having specific substrates [13].

Activation of mTORC1 strictly depends on the interaction of mTOR and RAPTOR. As mentioned previously, rapamycin and the rapalogs destabilise the mTOR-RAPTOR interaction and therefore deactivate this complex, halting the downstream signalling pathway [16]. Rapamycin does so by binding to FKBP12, which in turn binds to the mTOR FRB domain, leading to a conformational change weakening the connection between mTOR and RAPTOR, perturbing recruitment and access to substrates, diminishing further complex activation [17]. This rapamycin sensitivity is seen in mTORC1 and to a lesser extent mTORC2. mTORC2 sensitivity to rapamycin is observed in prolonged usage of rapamycin, this may be due to a sequestration of mTOR making it less accessible for mTORC2 assembly [18] (Figure 1.2).

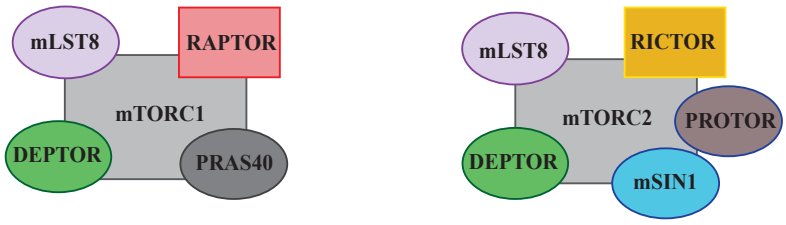

Figure 1.2 mTOR complexes

mTOR can form two complexes, mTORC1 and mTORC2. Each complex has different functions and downstream signalling substrates. mTORC1 is composed of a scaffolding protein RAPTOR, the protein mLST8, also an adaptor protein, PRAS40 and DEPTOR, other constituents of the complex needed to constrain the activity of the complex by competing with substrates for binding and phosphorylation sites, thereby inhibiting mTORC1 and substrate interactions. mTORC2 comprises RICTOR, a scaffolding protein, the adaptor protein PROTOR and mSIN1, essential for translocating the complex to the membrane, where it interacts with Akt. This complex also contains DEPTOR and mLST8, which serve the same purposes as in mTORC1.

1.1.3 Regulation of mTOR activity

mTOR is capable of integrating signals from the surrounding environment in the form of nutrients or growth factors thereby regulating cell growth and survival. There are many positive and negative regulators to this signalling pathway that will either activate or suppress mTORC1, respectively [19]. Ras homolog enriched in brain (RHEB) lies directly upstream of mTORC1 and positively regulates signalling through the complex [20]. This upstream regulator is a GTPase that is active when bound to GTP and inactive when

bound to GDP. Additionally, tuberous sclerosis complex 1 and 2 (TSC1 and TSC2) negatively regulates RHEB [19]. TSC2 is a tumour suppressor forming a heterodimeric complex with TSC1. Mutations in either TSC1 or TSC2 give rise to TSC hamartoma syndrome and a lung disorder known as lymphangioleiomyomatosis. TSC2 contains a GTPase activating protein (GAP) domain that activates the GTPase activity of RHEB, thereby inactivating it and consequently, the TSC complex is a negative regulator of mTORC1 activity[21].

The upstream signalling cascade leading to mTORC1 activation relies on recruitment of PI3K by growth factors, which in turn phosphorylates phosphatidylinositol 4,5-bisphosphate (PIP_2), forming phosphatidylinositol 3,4,5-trisphosphate (PIP_3). Formation of PIP_3 recruits Akt to the membrane, where it is phosphorylated by 3-phosphoinositide dependent protein kinase-1 (PDK1) at position T308. Active Akt will phosphorylate TSC1, disrupting the TSC1/TSC2 complex, inhibiting its GAP function, therefore allowing stabilization of GTP-RHEB and consequently activation of mTORC1 [22] [20]. Extracellular signal-regulated kinases (ERK1/2), part of the mitogen-activated protein kinases (MAPK) pathway, also has an inhibitory role on the TSC1/TSC2 complex [23]. By phosphorylating TSC2, it causes a similar disruption of the complex, promoting mTORC1 activation.

Apart from growth factors, amino acids are essential for mTORC1 activation [24]. Amino acids promote RHEB and mTORC1 interaction and therefore are necessary for its activation [25]. Amino acids, mainly leucine, exert their function by activating Rag GTPases. These proteins are constituted of a heterodimer of RagA or RagB and RagC or RagD. In their inactive form, RagA (or RagB) are loaded with GDP and RagC (or RagD) are bound to GTP. Once amino acids are present, a switch to an active conformation takes place and RagA (or RagB) is loaded with GTP and RagC (or RagD) with GDP. The Rag heterodimer interacts with RAPTOR, thereby promoting RHEB-mTORC1 contact by allowing mTORC1 to reach surfaces of late endosomes and lysosomes where Rag GTPases are found [26]. Other molecules related to the immune system may also play a role in mTORC1 activation. CD28, a costimulatory molecule on T cells needed for their activation and survival, is a strong activator of mTORC1 [27] [28]. Interleukin 2 and 4 (IL-2 and IL-4) activate PI3K, which in turn activates mTORC1 in T cells. On the other hand,

programmed death ligand 1 (PDL1) binds to PD1 on T cells, leading to mTORC1 inhibition [17] [29].

At times of nutrient deprivation, low energy and oxygen levels, stress signals activate the TSC1/TSC2 complex, leading to mTORC1 deactivation. When energy levels are low, the adenosine triphosphate:adenosine monophosphate (ATP:AMP) ratio is lower, AMP-activated protein kinase (AMPK) is activated by higher levels of AMP and in turn phosphorylates TSC1/TSC2, enhancing its GAP activity, which deactivates mTORC1 [30] [31]. This will in turn halt cellular growth and proliferation. The Wnt pathway also activates mTORC1, but in stressful conditions glycogen synthase kinase 3β (GSK3β) phosphorylates TSC1/TSC2, inducing inhibition of mTORC1 [32]. During times of low oxygen levels the hypoxia-induced factor protein regulated in the development of DNA damage response 1 (REDD1) is upregulated, REDD1 supports TSC1/TSC2 assembly and heightens its inhibitory role on mTORC1 [33]. REDD1 does so by liberating TSC2 from its interaction with 14-3-3 proteins (proteins that bind to various signalling proteins) during scarce oxygen conditions [34]. Less is known about regulation of mTORC2 activation and inhibition. Upon receiving growth signals, PI3K activation leads to Akt phosphorylation at T308, however, full activation of Akt happens after, phosphorylation at position S473, which is mediated by mTORC2 [35] it has also been suggested that mSIN1 promotes translocation of mTORC2 to the membrane where it phosphorylates Akt at S473 that may lead to mTORC2 activation by Akt itself which might occur through a positive loop mechanism, though this model needs to be supported by more work [36] (Figure 1.3).

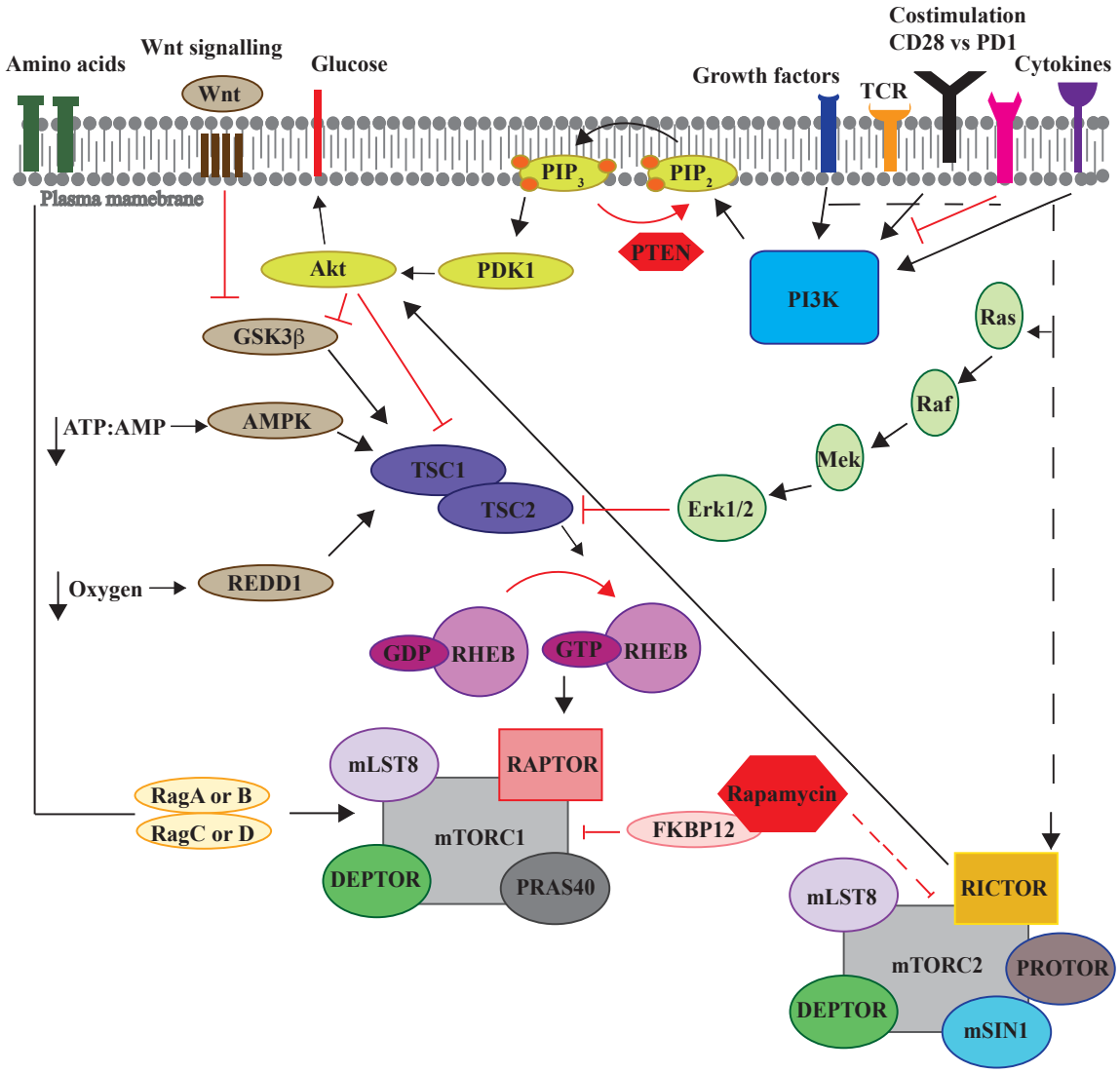

Figure 1.3 mTOR regulation

mTORC1 is activated by growth factor signalling and in the presence of nutrient abundance, especially amino acids. PI3K phosphorylates PIP2 making PIP3, which recruits Akt to the membrane and thereupon is phosphorylated by PDK1. Activated Akt inactivates GSK3β and phosphorylates the negative regulator of RHEB, the TSC1/2 complex, leading RHEB to change from an inactive GDP state to an active GTP state. RHEB positively regulates mTORC1 when it is in a GTP state. Amino acid presence leads to activation of Rag complexes by switching them to an active conformation loaded with GTP and therefore activates mTORC1. The MAPK pathway also leads to mTORC1 activation since Erk1/2 phosphorylates TSC1/2, thereupon activating RHEB. In times of amino acid depletion, Rag complexes are loaded with GDP and exist as inactive heterodimers. During oxygen deprivation REDD1 activates TSC1/2 complex, keeping RHEB and therefore inactive. When the ratio of ATP:AMP is low, AMPK also activates the TSC1/2 complex, diminishing mTORC1 activity. The Wnt pathway activates mTORC1 but in times of nutrient scarcity GSK3β, which is downstream of Wnt, activates TSC1/2 and therefore inactivates RHEB. Rapamycin inhibits mTORC1 activation by binding to FKBP12, which causes a conformational change in the complex, preventing mTOR-RAPTOR interaction. PTEN also inhibits mTORC1 activation by dephosphorylating PIP3. mTORC2 regulation is less understood, it activates Akt leading to many downstream effects such as its regulation of the cell cytoskeleton through stimulation of F-actin stress fibres (my own diagram but contents adapted from Powell et al 2012 37).

1.1.4 Downstream mTOR signalling

Actions of mTORC1 and mTORC2 are dictated by their substrate specificities. mTORC1 activation leads to increased protein synthesis and is involved in upregulation of genes needed for glucose metabolism, lipid metabolism and mitochondrial biosynthesis [38]. Furthermore, it results in inhibition of catabolic pathways such as autophagy [39] [40]. mTORC1 has two known substrates, S6K1 and 4E-BP1 [41]. These two substrates associate with mRNAs in order to control protein synthesis by regulating mRNA initiation, transcription and progression. 4E-BP1 in its unphosphorylated form suppresses cap dependent mRNA translation. Once it becomes phosphorylated by mTORC1, 4E-BP1 separates from eukaryotic translation initiation factor 4E (eIF4E). eIF4E recruits eIF4G, a translation initiation factor, to the 5' end of mRNAs, promoting translation of mRNAs that contain 5' untranslated regions (UTRs) [42]. S6K1 phosphorylates eIF4B leading to its activation; this allows eIF4A to unwind 5' UTRs of most mRNAs, enhancing protein synthesis. S6K1 assists eIF4A in degrading programmed cell death 4 (PDCD4), which inhibits the interaction of eIF4A with the translation pre-initiation complex, allowing protein synthesis [43]. In terms of its regulation of autophagy, mTORC1 suppresses it by inhibiting the production of autophagosomes, achieved through phosphorylation of autophagy related 13 (Atg13). This phosphorylation event interrupts the formation of the complex composed of Atg1-Atg13-Atg17, which is needed for the generation of autophagosome [40] [44].

mTORC2 activation leads to cellular polarization and actin cytoskeletal reorganization [45] [46]. It also plays a role in cell growth and survival [47]. mTORC2 phosphorylates Akt at S473 [35]. Once Akt is phosphorylated it is able to regulate forkhead box protein O1 (FOXO1) and FOXO3 transcription factors by phosphorylating them, thereby inhibiting their release and recruitment to the nucleus, where they are able to activate genes needed for apoptosis. In their phosphorylated state, they are sequestered in the cytoplasm [48]. Another mTORC2 target is serum glucocorticoid-regulated kinase 1 (SGK1), which is a cAMP- and cGMP-dependent protein. Downstream of SGK1 is the transcription factor FOXO1. As SGK1 is activated it phosphorylates FOXO1 thereby inhibiting it through its relocation from the nucleus to the cytoplasm where it is ubiquitinated and degraded. FOXO1 degradation leads to cell survival and growth [49]. Protein kinase C kinase (AGC) is also an mTORC2 target that phosphorylates and inhibits FOXO transcription factors [50]

[51]. Furthermore, mTORC2 is known to phosphorylate protein kinase C alpha (PKCα), which leads to reorganization of the actin cytoskeleton [52] (Figure 1.4).

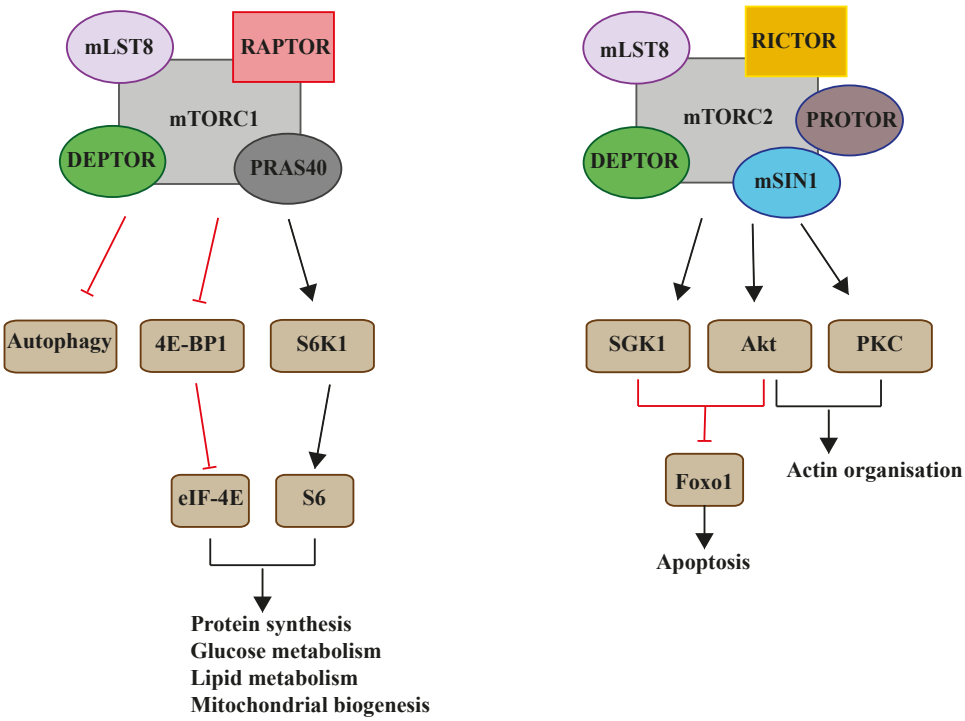

Figure 1.4 mTOR downstream signalling pathways

mTORC1 phosphorylates a number of substrates, which leads to an increase in protein synthesis, glucose and lipid metabolism and mitochondrial biogenesis. It phosphorylates 4E-BP1which is needed to negatively regulate transcription and therefore once it is phosphorylated protein synthesis and cellular growth is increased. mTORC1 also phosphorylates a substrate inhibiting autophagy in times of excess nutrients. mTORC1 phosphorylates S6K also leading to an increase in mRNA translational and subsequent protein synthesis. mTORC2 phosphorylates both Akt and SGK1 which in turn phosphorylate FOXO1 inhibiting apoptosis thereby initiating cell survival and growth. PKC is phosphorylated by mTORC2 initiating cytoskeletal organisation through f-actin polymerisation.

1.1.5 mTOR inhibitors and their applications

The mTOR pathway plays a central role in key cellular processes such as growth, survival and proliferation and is hyper-activated in many human malignancies such as melanoma and ovarian cancer [53]. Aberrant mTOR signalling in tumours may be due to either loss of function of tumour suppressor proteins for example TSC1/2 or PTEN, or activation of oncogenes such as PI3K, Akt, and Ras, which activate the mTOR complexes [54]. Therefore, in recent years the mTOR pathway has become an attractive target for anti-tumour therapy.

Rapamycin, also known as sirolimus, is a naturally occurring macrolide, as described earlier. It has diverse usage as an antifungal, immunosuppressive and anti-proliferative drug [8]. Rapamycin and derivatives known as rapalogs, temsirolimus (CCI-779), AP23573 and everolimus (RAD001), inhibit tumour cell proliferation [10]. These rapalogs were developed since rapamycin was less bioavailable *in vivo* with poor solubility [55].

Rapamycin, as well as the rapalogs, halts B cell chronic lymphocytic leukemia (B-CLL) proliferation by inhibiting cells in the G1 phase [56], which would likely induce apoptosis. Evaluation of this mechanism was carried out on different tumour cell lines. Luo *et al* showed that the antiproliferative ability of rapamycin was due to the inhibitory affect it has on cell cycle progression. Rapamycin prevents the downregulation of cyclin-dependent kinase inhibitor $p27^{kip1}$ and regulation of $p27^{kip1}$ levels seem to be important in determining rapamycin antiproliferative activity [57].

In addition to rapamycin's anti-proliferative effects *in vitro*, it also affected tumour growth and angiogenesis *in vivo*. Guba *et al* treated CT-26 cells derived from colon adenocarcinomas and B16-B10 melanoma cells with rapamycin intraperitoneally on day 0 or day 7 after tumour implantation, and showed a decrease in tumour growth and neovascularization of the tumours [58].

1.2 mTOR and immune cell regulation

1.2.1 Introduction to inflammation

During times of infection and tissue injury, inflammatory responses enable maintenance of homeostasis and survival of the host. Inflammation has been known for many centuries and scientific contributions over the years have led to milestones in understanding this important aspect of immunity [59]. Inflammation comes in many forms leading to different pathways being activated that in turn, determine the type of response produced by the host. The level of severity of inflammation can either be acute, for example during infections, or chronic, as observed in neurodegenerative diseases and cancer [60]. Acute inflammation is the initial response to the foreign stimuli and involves many cells such as neutrophils and macrophages along with mediators as cytokines, working together to eliminate the foreign body and consequently reduce inflammation. Chronic inflammation on the other hand occurs as these cells and mediators are unable to resolve inflammation leading to adverse effects on the host. Inflammation is considered a generic response and associates with innate immunity as opposed to adaptive immunity that responds in a specific manner to a particular target [59].

The inflammatory response comprises several constituents; inducers, sensors, mediators and target tissues. These components form different combinations, depending on pathways triggered by the inducers [61]. Bacterial pathogens are recognized by Toll like receptors (TLRs), which are part of the innate immune response [62]. These receptors are found on macrophages, which in turn induce cytokine production e.g. tumor necrosis factor alpha (TNFα), IL-1β, IL-6, as well as mediators such as nitric oxide (NO) and chemokines such as CCL2. Leukocytes are able to move and migrate actively through blood vessels and into surrounding tissues as they receive cues from their surroundings. Cytokine release results in vasodilation and extravasation of neutrophils to the site of inflammation and both extravasated and resident macrophages help destroy the pathogen [63]. Macrophages also produce IL-12 and IL-23 to assist TH1 and TH17 T cell differentiation to promote the inflammatory response even further [64]. Resolution of this inflammatory response occurs as the trigger subsides and clearing of the infection ensues, accompanied by tissue repair and regaining of active homeostatic functions. If the pathological trigger is not eliminated and the response proceeds, this usually leads to chronic inflammatory responses that could be detrimental to the host [65].

Chronic inflammation can be detrimental to the host, as tissue damage is caused by excessive reactive oxygen and nitrogen species along with TH1 and TH17 bi-products, thereby increasing pathogenic and disease progression. Macrophages are able to halt the inflammatory response by upregulating apoptotic signals or suppress the inflammatory cascade by dampening the response by producing pro-resolving (resolvins) factors, aiding tissue repair [66]. This scenario differs during viral infections, in which interferons alpha (IFNα) and beta (IFNβ) are produced from the infected cells, inducing expansion of cytotoxic T cells that are able to destroy the virally infected cells [67].

Additional cells that play an important role in immunity and inflammation are mast cells and basophils, which regulate allergy responses and clearing of parasitic infections as they release histamine, along with IL-4 and IL-13 [68] [69].

1.2.2 Interactions between macrophages and T and B cells

Macrophages are known as antigen presenting cells; they interact with T cells by presenting processed proteins to the cell surface and along with MHC class II, they bind to the T cell receptor (TCR) thereby activating T cells. Macrophages have also been shown to produce cytokines that are needed for T and B cell development and maturation [70] [71] [72].

How mTOR takes part in this inflammatory process will be described below according to different cell types.

1.2.3 mTOR and macrophages

As macrophages are a major topic of this thesis, this section will focus on the role of the mTOR pathway in regulating macrophage polarization in different metabolic statuses, and disease [73].

Macrophages are multifaceted cells that play major roles in the immune system. They are professional phagocytes and they also take part in homeostasis, development and tissue repair. Macrophages are found in all tissues. They display versatility in their functions according to the specific tissue they reside in. They acquire specialized characteristics based on the tissue of residence, for example in the brain they are microglia cells and specify a function of microglia (i.e. aid neuronal function); in the liver they are Kupffer

cells and specialize in breaking down blood cells by their phagocytic actions [74]. Ontologically macrophages arise from the yolk sac during early embryogenesis, as the embryo develops hematopoiesis takes place in the fetal liver, in which macrophages are formed. Postnatal bone formation leads to a reduction in fetal liver hematopoiesis, replaced by bone marrow hematopoiesis [75] [76]. Macrophages can also differentiate from monocytes, which develop from bone marrow progenitors. Monocytes circulate in the periphery until they receive activation signals leading to extravasation and differentiation into macrophages [73]. Regardless of their origin, most macrophages have a major lineage regulator known as colony stimulating factor 1 receptor (CSF1R). It is a transmembrane tyrosine kinase receptor, necessary for macrophage differentiation [77]. Macrophages also participate in adaptive immune responses and can act as APCs [78].

Macrophages are able to keep the balance between inflammatory responses and immunomodulatory functions, depending on the environmental signals they receive. In terms of their phenotype, many publications have described how macrophages can assume two opposing phenotypes, one more inflammatory and aimed at eradication of microbes, called M1 (classical) and one that aids tissue repair and restoration of homeostasis, called M2 (alternative) [78] [79] [80] [81] (Figure 1.5). Since macrophages are heterogeneous in nature, this classification is very general and it should be noted that macrophages lie within a spectrum of subtypes. However, for simplification in this thesis I will describe macrophages as M1 or M2 [64]. M1 macrophages can be activated by lipopolysaccharides (LPS) alone or in the presence of IFNγ and exert proinflammatory functions by secreting cytokines and enabling tissue inflammation. The M1 or classical macrophages are known for their cytotoxic abilities and are the first line of defence observed in innate immunity. They have a proinflammatory role, being able to engulf foreign entities and through a respiratory burst (releasing of reactive oxygen species) will destroy them spreading products of inflammation into their surroundings. A specific marker that is expressed by the M1 phenotype is nitric oxide synthase (iNOS) which is needed to metabolize arginine into nitric oxide (NO). Cytokines that are produced are IL-6, IL-12 and TNF-α [82]. M2 macrophages are activated through IL-4 and IL-13 [78] [83], these activate signal transducer and activator of transcription 6 (STAT6) a transcription factor along with nuclear receptors peroxisome proliferator-activated receptor gamma (PPARγ and PPARδ), which are all needed for full M2 activation and immunomodulation [84]. A specific marker pertaining to this phenotype is mannose receptor C type 1 MRC1, and the

usual cytokines produced are IL-10 and transforming growth factor beta (TGF-β) [83]. In relation to M2 polarization there is an increase in arginase 1 expression and activity that promotes tissue repair through conversion of L-arginine to L-ornithine and subsequent polyamine synthesis [85].

Macrophages need to maintain specific metabolic programs to support energy utilization. M1 macrophages use the glycolytic metabolic pathway supported by hypoxia inducible factor 1 alpha (HIF-1α), whereas M2 macrophages use fatty acid oxidation mediated by the transcriptional activator peroxisome proliferator-activated receptor gamma coactivator 1-beta (PGC-1β) and PPARγ [86]. These data suggest a link between both macrophage metabolism and inflammation and regulatory mechanisms needed for macrophage control.

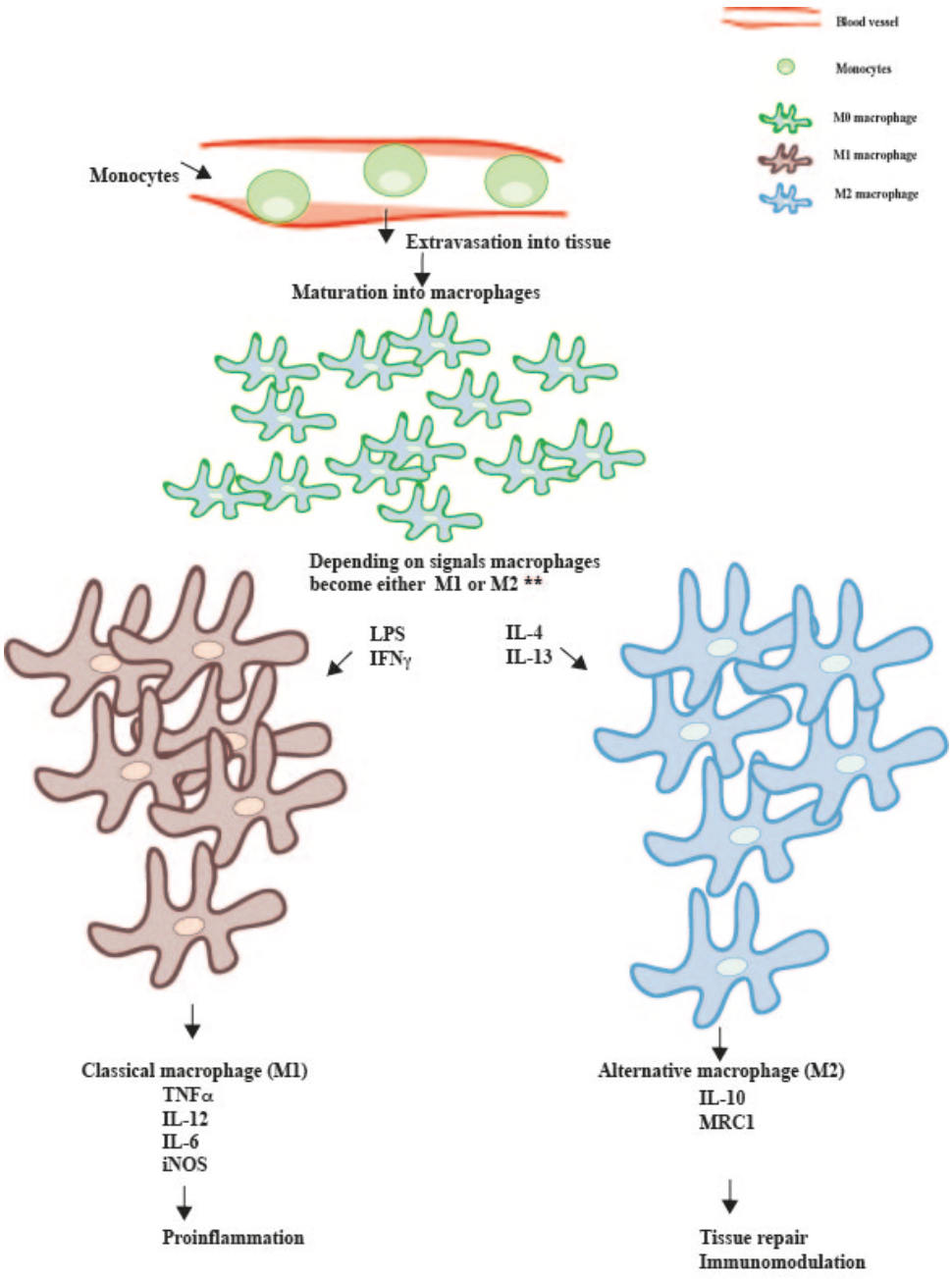

Figure 1.5 Macrophage development *in vivo*

In vivo bone marrow myeloid progenitors are released into the periphery where monocytes continuously circulate, once an activation signal is intercepted these monocytes extravasate into the peripheral tissue, where they become macrophages in the presence of monocyte colony stimulating factor (MCSF). Depending on the signals received, macrophages carry on different functions. Macrophages receiving signals through LPS/IFNγ for instance become what are known as the classical or M1 macrophages and release inflammatory cytokines such as TNFα and IL-12 which help fight against foreign bodies. If they receive signals through IL-4/IL-13 they become alternative or M2 macrophages and are needed for tissue repair and immunomodulation restoring balance and homeostasis.

Previous publications have shown that constitutive mTORC1 activation in macrophages through deletion of the negative regulator of mTOR TSC1 leads to an increase in proinflammatory cytokine production while IL-10 is decreased. M2 polarization in these macrophages was defective, as M2 markers had reduced expression. Akt activation was reduced at both phosphorylation sites T308 and S473, which contributed to impaired M2 polarization, highlighting the importance of the mTOR pathway in macrophage polarization and regulation [87].

Another group published that TSC1/2 is a regulator of macrophage polarization through different signalling pathways independent from mTOR [88]. Mice that had specific myeloid cell TSC1 deficiency were used to assess the role of mTOR in macrophage polarization. Mice were highly sensitive to LPS shock; macrophages from these mice produced increased amounts of proinflammatory cytokines such as TNFα, IL-12 and NO. This suggests that these macrophages have an increased ability to differentiate into M1 macrophages[88]. Macrophages from TSC1 knockout (KO) mice had reduced Akt activation but higher MEK/ERK activity. Upon mTOR inhibition with rapamycin, macrophages deficient in TSC1 or mTOR showed a slight increase in inflammatory cytokine production [88] accompanied by enhanced macrophage activation of NFκB and decreased STAT3 activation [88]. After an addition of LPS to either TSC1 KO or mTOR KO macrophages, there was a continuous increase in their inflammatory response, suggesting the existence of mTOR independent pathways, consistent with data obtained with rapamycin [88].

This group also showed a decrease in M2 response and few immune cell infiltrates, when TSC1 KO mice were challenged with OVA-induced allergic asthma. It was confirmed by the decrease of M2 expression markers Arg1, Ym1, Fizz1 after IL-4 treatment. This was an important observation, since IL-4 drives M2 polarization and plays a major role in allergic asthma pathogenesis. But after mTOR inhibition with rapamycin, the M2 defects were almost completely rescued by increase in Arg1, Ym1 and Fizz1. This in itself indicates that rapamycin-sensitive mTOR functions negatively regulate M2 polarization [88].

Weichhart *et al* also demonstrated that inhibiting mTOR in macrophages leads to an increase in proinflammatory cytokines by activation of NFκB with a decrease in IL-10 due to reduction of the transcription factor STAT3. In contrast to previous results, Weichhart *et al* showed that deleting the negative regulator of mTOR TSC1/2 reverses the proinflammatory cytokine shift, which is in direct contrast to data reported by *Byles et al* and Zhu *et al* [89] [87]. In an attempt to understand more on how mTOR regulates innate immunity, Weichhart *et al* challenged BALB/c mice with *Listeria monocytogenes* (L.m), an infection they normally succumb to due to low IL-12, IL-6 and IFNγ secretion [89]. In another experiment, mice were treated with rapamycin 3 days prior to the bacterial challenge with a lethal dose (LD_{50} OR LD_{100}) of *Listeria monocytogenes* (L.m), these mice demonstrated improved survival which was shown by less bacterial burden in liver and spleen, with an increased production of NO. In order to prove innate cell dependency for this survival pattern, macrophages and dendritic cells were depleted using clodronate this abolished resistance to infection the mice had shown and emphasized that myeloid cells are important for the *in vivo* effects that were observed [89].

Festuccia *et al* investigated the role mTORC2 has on inflammation and macrophage stimulation. The PI3K/Akt axis is central to reducing inflammation as macrophages are stimulated by TLR ligands. It is well known that the PI3K pathway and Akt activation dampens TLR activation and therein decreases the inflammatory response via mTORC2 in order to restore balance after TLR activation and inflammation [90].

mTORC2 activates Akt and indirectly the PI3K signalling pathway therefore it was important to know how mTORC2 may regulate inflammation. Macrophages isolated from mice with a specific myeloid deletion of Rictor, demonstrated high expression of M1 genes as compared to M2 genes once stimulated with TLR ligands. *In vivo* experiments were also performed to mimic an acute or chronic inflammatory state as mice were fed a high fat diet (chronic inflammation) or were injected with LPS (acute inflammation). In the absence of Rictor mice with the high fat diet were observed to have a gradual increase in inflammation but was not as high as those mice receiving LPS injections that showed a higher sensitivity. This led to a heightened TLR signalling upon infection, with macrophages skewed to a M1 phenotype with excessive inflammatory responses. An increase in TNFα production was observed, and that a reduction of inflammation was seen with deletion of PTEN which is a negative regulator of the PI3K pathway. In general

these findings reiterate the point that mTOR regulates macrophage polarization as mTORC2 negatively regulates TLR signaling [91].

Others have shown that PI3K promotes an inflammatory response in LPS stimulated THP-1 derived macrophages by increasing proinflammatory cytokines as IL-1β, IL-6, IL-8, and TNFα, consequently as PI3K is inhibited by LY (pan-PI3K inhibitor) secretion of these cytokines was reduced, therefore giving PI3K an important role in macrophage regulation [92]. Usage of PI3K inhibitors LY294002 (LY) and Wortmannin or mTOR inhibitors AZD8055 (AZD) and rapamycin, to test the mechanisms of cytokine secretion in Jurkat cells (that have constitutively active Akt phosphorylation), was investigated. Phosphorylation of Akt, GSK-3β and p70S6K were assessed. The PI3K and mTOR inhibitors reduced phosphorylation of Akt and p70S6K while no reduction was observed in phosphorylation of GSK-3β (only slightly with mTOR inhibitors) [92]. In THP-1 derived macrophages phosphorylation of p70S6K was also reduced thus restricting proinflammatory cytokine production [92] .

To identify the role of PI3K in macrophage motility, THP-1 derived macrophages were stimulated with LPS and placed on transwells treated with or without PI3K inhibitor (LY); different proinflammatory cytokines were added as chemoattractants. Migration of macrophages treated with PI3K inhibitor (LY) was reduced, highlighting PI3K involvement in macrophage motility and subsequently mTOR involvement in macrophage regulation [92].

mTOR plays a major role in differentiating macrophages into tumour-associated macrophages (TAMs) promoting tumour development and progression mainly by encouraging tumour angiogenesis. Published data showed that human monocytes stimulated with LPS either lacking mTORC1 activity by its inhibition through rapamycin or activated using RNAi mediated knockdown of TSC2, regulated monocyte differentiation. Rapamycin instigated differentiation of macrophages to an M1 phenotype where IL-12 production was increased and IL-10 was reduced. Knockdown of TSC2 caused macrophages to develop into M2 macrophages and had the opposite cytokine readout more IL-10 production and reduced IL-12 [93].

Ai et al, have also shown that by inhibiting mTORC1 in macrophages by rapamycin decreases chemokine expression and atherosclerosis, this result may be used as a

treatment for atherosclerotic plaques [94]. They used bone marrow from mice with myeloid specific RAPTOR KO (Mac-RapKO) and transplanted it into mice deficient of low-density lipoprotein receptor (Ldlr -/-). These mice were fed a western type diet and atherosclerotic lesions were assessed. The (Mac-RapKO) mice had less macrophage infiltration within the lesions, smaller lesion size, and decreased macrophage chemokine expression (CCL2 and CXCL2). Treatment of macrophages with minimally modified low-density lipoprotein resulted in an increase in chemokine expression levels and STAT3 phosphorylation for WT mice as compared to Mac-RapKO, which showed reductions in both chemokine expression and STAT3 phosphorylation, suggesting an antiatherogenic role of mTORC1 inhibition [94].

These overall findings outline the importance of mTOR in macrophage differentiation, regulation and polarization (Figure 1.6). These results also propose a potential role in targeting mTORC1 in macrophages for various treatment approaches.

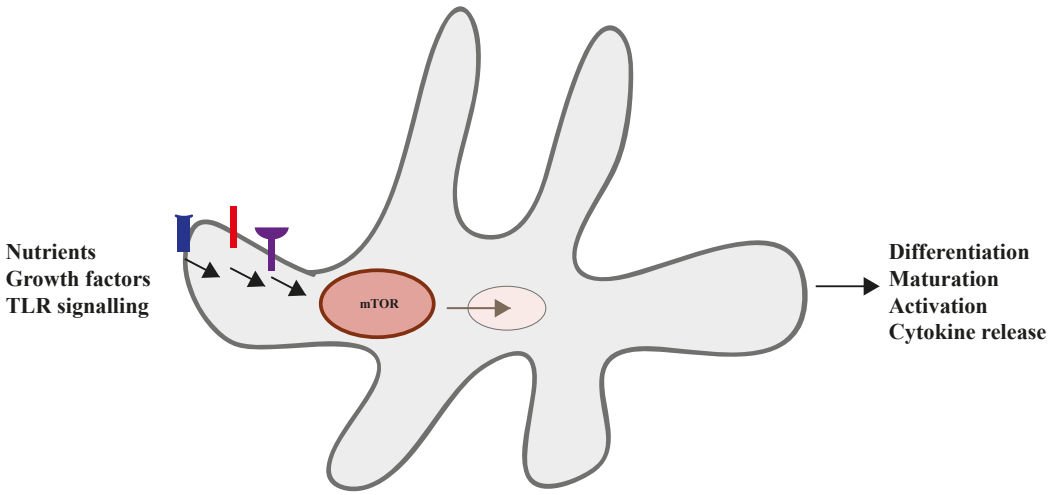

Figure 1.6 mTOR and macrophage differentiation, regulation and metabolism

mTOR plays a vital role in macrophage differentiation, regulation and metabolism by receiving signals through nutrients and / or growth factors and through TLR signalling leading to macrophage activation and subsequently downstream effects on their differentiation, maturation, activation and polarization.

1.2.4 mTOR and T cells

Immunosuppressive effects of rapamycin were thought to originate from its ability to halt T cell proliferation as mTOR activity degrades the cell cycle inhibitor p27 while

activating cyclin D3. Rapamycin's inhibition was hypothesized to lead to T cell anergy (T cell inactivation after antigen encounter) [28]. However further studies showed that there was a difference between rapamycin's ability to inhibit cell cycle progression and its ability to promote T cell anergy. Blocking the cell cycle at G1 without addition of rapamycin did not promote T cell anergy [95]. Furthermore, inducing T cell proliferation in the presence of rapamycin did not prevent T cell anergy. These findings demonstrate that rapamycin does not promote anergy by reducing T cell proliferation but by inhibiting the mTOR pathway, thereby highlighting the capability of mTOR to regulate T cells [96]. Unlike other differentiated cells, which utilize mitochondrial respiration and the TCA cycle in presence of oxygen for energy generation in the form of adenosine triphosphate (ATP), T cells employ oxidative glycolysis in their clonal expansion. This is when quiescence naïve T cells are interrupted by engagement of their TCR by specific antigen and MHCII, activating T cells to become effector T cells [97]. The use of oxidative glycolysis is known as the Warburg effect [98]. Once T cells are activated, biosynthesis of nucleotides, proteins and lipids commences. Since mTOR actively plays a role in metabolism it also promotes immune metabolic functions [99]. Activated T cells upregulate metabolic functions that in turn prompts the PI3K signalling pathway, thereby increasing Akt phosphorylation and subsequently mTORC1 activation. mTORC1 activation promotes expression of proteins needed for glycolysis through HIF-1α [100]. Inhibiting mTORC1 through activation of AMPK, inhibits IL-12 production and leads to T cell anergy [101]. Depleting amino acids as another form of mTORC1 inhibition has also been investigated and was shown to impede T cell functions [102]. Therefore, mTOR has been shown to play a major role in T cell regulation through metabolism and activation of the PI3K/Akt pathway, as inhibition of mTORC1 has led to T cell deregulation.

1.2.5 mTOR and B cells

There is less information on mTOR regulation of B cells. Early stages of B cell development were impaired when an mTOR hypomorph (a mutation causing partial loss of gene function) mouse was used as a model [103]. Furthermore these B cells were unable to proliferate properly in response to B cell antigen receptor (BCR) and CD40 stimulation [104]. In order to assess maturational regulation of mTOR on B cells, a conditional deletion of TSC1 (TSC1 KO) on murine B cells was achieved. This lead to increased mTOR activation, herein B cell maturation was impaired as the amount of marginal zone B cells

was reduced. In a follow up to the previous experiment an *in vivo* experiment in which rapamycin was administered intraperitoneally to mice every other day for 16 days to inhibit mTOR signalling was performed. B cell marginal zones were partially increased and thereby part of the maturational axis was restored. Surprisingly, both hyper-activation of mTOR and mTOR inhibition reduced antibody production [104].

To evaluate the role of mTOR on B cell survival and function, the PI3K-mTOR axis was investigated using inhibitors to the mTOR pathway. B cell activation through the BCR enhances mTOR activation leading to B cell clonal proliferation and survival depending on antigen exposure [105]. B cell stimulation with TLR and CD40 also activates the PI3K-mTOR pathway. Rapamycin inhibits CD40-dependent proliferation and induces apoptosis that otherwise would be inhibited by CD40 activation [106]. Rapamycin also has been shown to inhibit LPS mediated B cell proliferation [107]. Little is known about B cell metabolism, like T B cells upregulate the glycolysis pathway and increase glucose uptake, depending on the PI3K pathway. Metabolism of B cells depends also on the pentose phosphate shunt and HIF-1α, which implies a role of mTOR in B cell metabolism [108].

From the findings above it is possible to speculate an important role of mTOR in macrophage, T cell, and B cell differentiation and maturation. This central role joins two aspects of cell survival and growth, metabolism and immune cell function. However, it should be pointed out that there are many parts in regards to the mTOR pathway and the role it plays in these cell types that have not yet been elucidated. Further extending our knowledge of mTOR regulation, is a key step required to clarify these unanswered questions, which will enable us to understand effectively mechanisms of the cell types within the scope of mTOR.

1.3 Pancreatic cancer

The pancreas is a glandular organ that is composed of the head of the pancreas, neck, body and tail. The pancreas is responsible for both endocrine and exocrine functions in the body. It functions as an endocrine gland as it secretes hormones such as insulin, glucagon, and somatostatin. This secretion occurs through clusters of cells known as pancreatic islets or more precisely the islets of Langerhans. The main role of the pancreas as an endocrine gland is to control blood sugar levels. However, the pancreas also

assumes a vital role in the digestive system, as it is also an exocrine gland maintaining balance of metabolic levels. This occurs within cells known as the acini, where they secrete pancreatic juice that contain digestive enzymes feeding into the duodenum [109 110]

Pancreatic cancer has one of the worst survival rates. It is the 9th most common cancer found in the United Kingdom with a 5% average survival rate of 5 years [111]. There are some risk factors that have been assessed in pancreatic cancer including smoking, chronic pancreatitis, diabetes, and family history. The likely reason for such a low survival rate may relate to the poor early stage detection this cancer receives. Patients typically present with symptoms when the disease has already become too advanced for surgical intervention [112 113].

More than 95% of pancreatic cancers are exocrine tumours since they originate from exocrine pancreatic cells, and about 90% of these are pancreatic ductal adenocarcinomas (PDACs). The most common precursor lesions of the PDACs are non-invasive epithelial neoplasms known as pancreatic intraepithelial neoplasias (PanINs). These are divided into 4 grades according to the increasing degree of architectural and cytological atypia observed [114]; PanIN-1A, PanIN-1B, PanIN-2 and PanIN-3 [115]. These early stage alterations may open a window of opportunity for early diagnosis, before a full-blown transformation to invasive PDACs occurs. PDAC development is a result of accumulation of mutations in tumour suppressor genes and/or oncogenes. Activating point mutations in the *KRAS* gene occurs in the early stages of the precursor lesions, PanIN-1. Inactivating mutations in *INK2A (p16/CDKN2A)* arise in the intermediate stages of PanIN-2, while inactivating mutations of *TP53*, *SMAD4* and *BRCA1* have been found in late lesions of PanIN-3 [116] (Figure 1.7).

The malignant pancreatic cells do not develop in isolation and a complex desmoplastic stroma has been described [117]. The tumour microenvironment contains cellular and acellular components such as immune cells, pancreatic stellate cells, fibroblasts, blood vessels, extracellular matrix proteins, cytokines and growth factors. The stroma itself differs in composition as the cancer advances, and may occupy a larger fraction of the tumour than cancer cells. This microenvironment plays a deleterious role by suppressing immune responses that may be attempting to eradicate tumour cells [118 119].

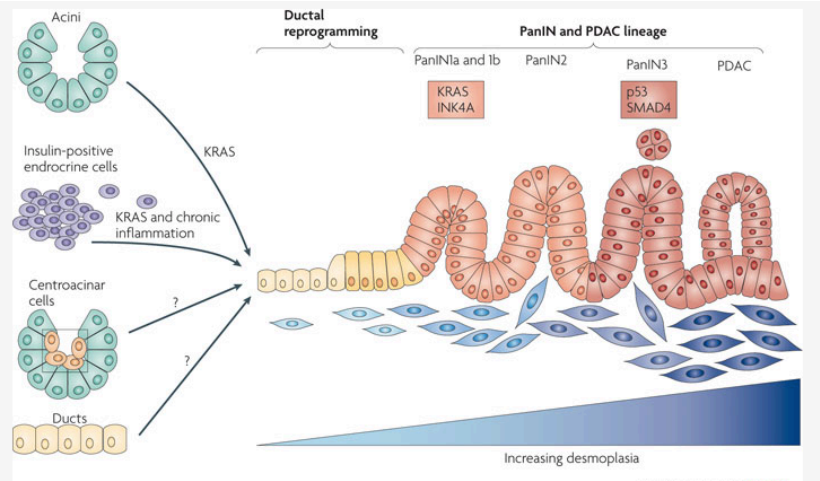

Figure 1.7 Development of pancreatic ductal adenocarcinomas

Pancreatic cancer may develop from acinar, endocrine, centroacinar or ductal cells. Pancreatic cancer gradually gains more desmoplasia as it develops and mainly originates from ductal cells. There are many precursor lesions known as pancreatic intraepithelial neoplasias (PanINs) that are divided into 4 grades (PanIN-1A, PanIN-1B, PanIN-2 and PanIN-3). Each grade is known to gain specific mutations such as KRAS, INK4A (p16/CDKN2A), TP53, and SMAD4. As these lesions gain mutations, progression to pancreatic ductal adenocarcinomas ensues. (Figure taken from Morris et al, 2010 [117])

1.4 Pancreatic cancer and the surrounding tumour microenvironment

As mentioned above, pancreatic cancers usually begin as precursor lesions and develop into PDACs. In recent years it has been established that inflammation can have cancer-promoting activity [120].The inflammatory components not only promote cancer but also increase incidence of metastasis and contribute to the high mortality rate [121]. The presence of inflammatory cells accompanied by secretion of pro-inflammatory cytokines (for example TNF-α), chemokines, growth and angiogenic factors (for example VEFG and insulin-like growth factor) support the switch to a pro-tumourigenic environment [122] [123]. This microenvironment leads tumour cells to become refractory to immune surveillance. It contains cytokines such as TNF-α and IFN-γ, as well as reactive oxygen species, generated by tumour-associated macrophages and neutrophils, which all cause cellular damage. Consequently, tumour cells respond with an increase in signals that support wound healing and restoration of normal cellular function. These heightened signals for wound healing and cell proliferation leads to the development of tumour cells [124] [125]. It has been shown that the main immunosuppressive cells found within the pancreatic tumour microenvironments are T regulatory cells (T regs), myeloid derived suppressor cells (MDSCs), tumour associated macrophages (TAMs), and cancer associated fibroblasts (CAFs). They account for about 50% of the tumour stromal population [126] (Figure 1.8) .

1.4.1 T regulatory cells (T regs)

T regs are known for their immunosuppressive features as they suppress T cytotoxic cells. It has been shown that in pancreatic cancers there are more T regs found in the stroma as compared to T cytotoxic cells, thereby enhancing tumour progression [127].

1.4.2 Myeloid derived suppressor cells (MDSCs)

MDSCs are a heterogeneous group of myeloid cells. They have been attributed with high expression levels of CD11b and Gr1 and are considered monocytic and granulocytic, making it difficult to distinguish them from other myeloid cells (neutrophils, macrophages and dendritic cells) [80]. Moreover as MDSCs are believed to populate the tumour stroma at different stages of myeloid cell differentiation there is no general consensus on how to identify these cells with specific cell markers [128]. Their main role is immunosuppression, and this has been observed in their suppression of T and NK cell activity and proliferation [129]. Tumour cells release specific cytokines (G-CSF and/ GM-CSF) into the tumour microenvironment recruiting MDSCs to the site, where they expand in quantity [130]. These MDSCs release additional cytokines and chemokines into the tumour microenvironment promoting angiogenesis that is needed to support tumour progression, which in time may lead to metastasis [131].

1.4.3 Tumour associated macrophages (TAMs)

Macrophages constitute a large component of the tumour microenvironment [132] and these are referred to as tumour associated macrophages (TAMs) [133]. TAMs are considered 'double-edged swords' for their involvement either in tumour progression or tumour inhibition. This depends on the type of signals they receive from either the tumour cells or their surroundings. These signals may skew these TAMs into a particular phenotype that may be pro or anti-tumour progressive [134 135].

Nevertheless, most TAMs express a predominantly M2 tumour-promoting phenotype[136]. TAMs produce cytokines and chemokines that play a major role in tumour development by increasing angiogenesis, upregulating VEGF leading to an angiogenic switch. Novel angiogenic markers made by granulocytes have also been observed to cause refractoriness to immune surveillance [137]. At the first stages of pancreatic tumour formation, these tumour cells need oxygen and nutrients to help them grow. In order for these cells to

continue to survive and proliferate while gaining more mutations, they send out signals to recruit macrophages and neutrophils to the tumour surroundings [138]. This inflammatory tumour microenvironment with infiltrating immune cells promotes tumour formation and extends the survival and proliferation tumour cells [139]. Cancer cells are able to circumvent immune surveillance as they release signals and interact with myeloid cells leading to an upregulation of IL-10 secretion while down regulating TNF-α and IFN-γ secretions [140]. Tumour cells release chemotactic factors that increase influx of macrophages, forming niches within the tumour microenvironment [141]. TAMs take part in remodelling the tumour microenvironment by increasing expression of matrix metalloproteinases (MMPs) and other matrix remodelling enzymes [142]. This remodelling supports tumour motility and therefore leads to tumour invasion and metastasis [143]. The amount of TAM infiltration is often inversely proportional to overall survival, meaning TAM infiltration is a sign of poor prognosis [134].

1.4.4 Cancer-associated fibroblasts (CAFS)

Fibroblasts are major components of the cancer stroma and are known as cancer associated fibroblasts. In a tumour setting CAFs are said to be constantly activated and do not revert back to an inactivated state, nor do they go through apoptosis like normal fibroblasts [144]. Resident fibroblasts are an important source of cancer-associated fibroblasts (CAFs) and contribute to tumour progression in many ways. They become activated as they receive signals from cancer cells and the surrounding stroma where they organise the extracellular matrix and help cancer cells proliferate and migrate by increasing β-catenin expression and decreasing E-cadherin on cancer cells, thereby increasing invasiveness of cancer cells [145]. Reactive oxygen species also promote conversion of resident fibroblasts into CAFs by accumulation of chemokine CXCL12 and HIF1α [146]. CAFs also originate from bone marrow derived mesenchymal stem cells, hematopoietic stem cells, epithelial and endothelial cells [147]. CAFs originating from bone marrow mesenchymal stem cells were shown to convert resident fibroblasts into CAFs by secretion of TGFβ [148]. CAFs are a source of IL-6 which in turn leads to an increase in angiogenesis and tumour progression [149].

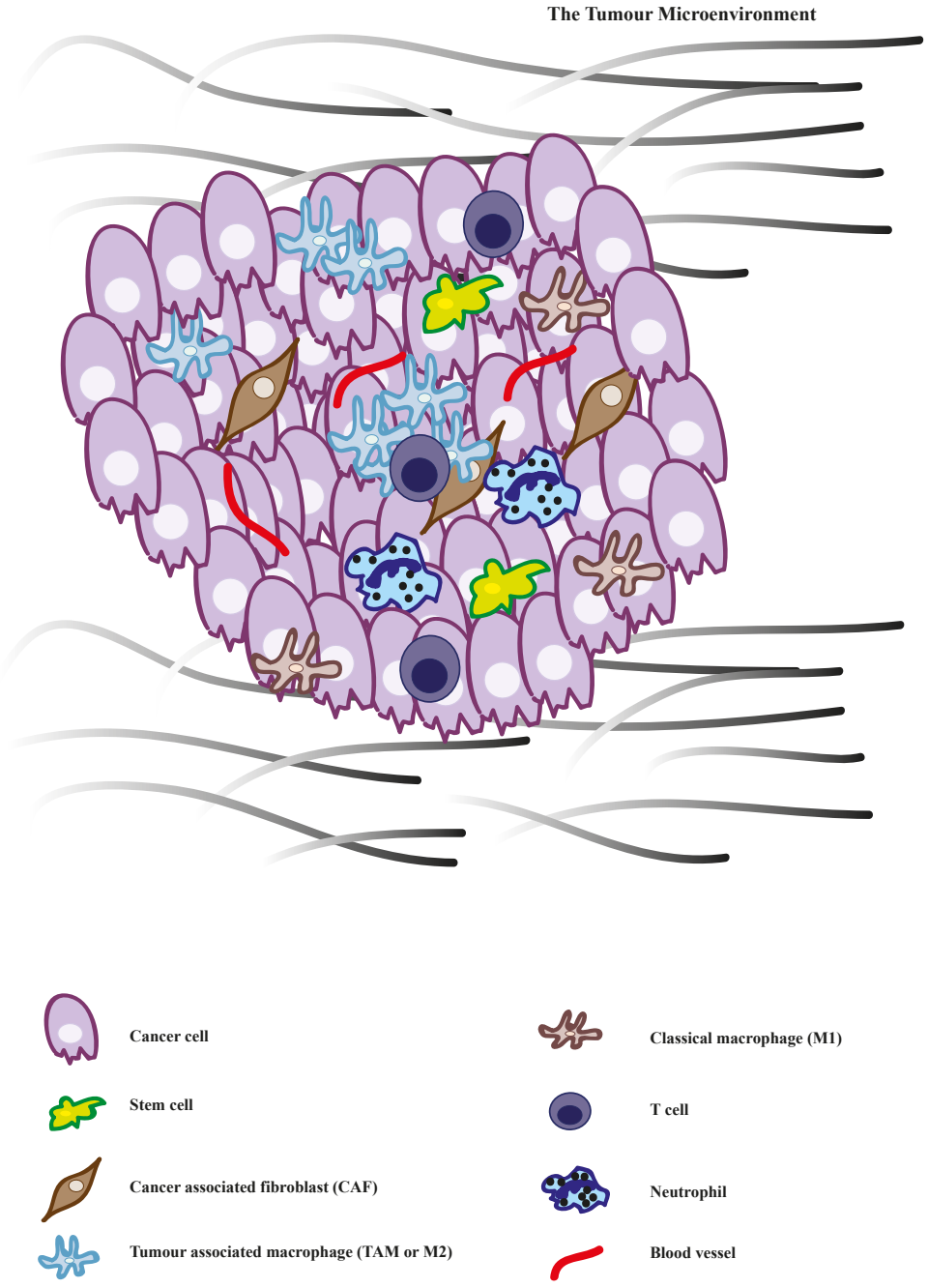

Figure 1.8 The tumour microenvironment

The pancreatic tumour microenvironment is made up of many components, apart from the malignant cells; they are made up of macrophages infiltrating the niche known as TAMs which release cytokines promoting immunomodulation. CAFs also play an important role where they are needed for subsequent metastasis by changing the extracellular matrix. They activate VEGF by their secretion of IL-6 leading to blood vessel formation and therefore a supply of oxygen to the cancer cells. Classical macrophages and neutrophils only add on to the inflammatory state observed in tumour microenvironments. T cells are found but many are of the regulatory type known as T regs, which promote tumour progression. Stem cells are present and effect the tumour environment by continuously replenishing the surrounding with new cancer cells.

1.5 The mTOR pathway and pancreatic cancer

One of the early genetic alterations observed in PDAC development is a mutation in the KRAS oncogene [150]. This mutation is observed in the earliest stages of PanIN progression, being present in approximately 20% of lesions of the PanIN-1A stage [151 152]. This KRAS oncogene plays a major role in signalling as it activates the PI3K/Akt pathway in 60% of PDACs [153]. As mentioned previously PI3K/Akt signalling is also involved in mTOR activation and further signalling and activation of its substrates. mTOR is activated in 75% of PDACs [154]. Emphasis must be placed on developing more inhibitors against the mTOR-signalling pathway as this pathway reduces apoptosis occurrence in cells and may be used as a survival advantage by tumour cells. Many inhibitors to this pathway have been developed showing promising results. These results are further amplified once gemcitabine is used in combinatorial therapy [155 156].

A research group highlighted the need of selective targeted therapies based on individual pancreatic cancer phenotypes. They found that PDACs that had both KRAS and PTEN mutations were highly dependent on mTOR signalling. Inhibition of the mTOR pathway yielded better outcome by observing a halt in tumour cell proliferation leading to tumour regression [157].

These results emphasise the importance of having selective patient therapies in order to promote effective treatment against pancreatic tumours.

1.6 Hypothesis

Given the current literature on mTOR, I hypothesize that targeting mTORC1 pathways via deletion of Raptor in myeloid cells will polarize macrophages to a more inflammatory phenotype and this will have an impact on pancreatic tumour progression and the tumour microenvironment.

In order to test my hypothesis, I aim to:

1.7 Aims

1. Characterise the role of Raptor of the mTORC1 complex in macrophage maturation, differentiation, and function.

2. Explore the effect of Raptor KO on macrophage polarisation.
3. Explore the effect of Raptor KO on macrophage signalling.
4. Explore the role that myeloid cells lacking Raptor have on the pancreatic tumour microenvironment.

2 Materials and Methods

2.1 Mice

All procedures performed on animals were carried out in accordance with the U.K. Home Office Animal and Scientific Procedures Act 1986, under the project licence 70/7411. The licence holder is Professor Frances Balkwill. Original breeding pairs were a generous gift from Professor Markus Rüegg. The mouse lines were generated and kept at the Biological support unit (BSU) within Charterhouse Square (at a given time they were also transferred to the BSU at St. Georges Hospital). They are C57BL/6 mice, genetically modified to delete Raptor within myeloid compartments using a *Cre/LoxP* recombination system (*Raptor f/f; Csf1r Cre-ERT* (KO)). It is an inducible model that requires administration of tamoxifen (Sigma Aldrich, cat- T5648-1G lot- WXBB5732V), via an intraperitoneal (I.P) injection on 3 consecutive days. As controls C57BL/6 mice containing *Cre* without *LoxP* bind to the *Csf1r* promoter region were used for comparisons (*Raptor WT/WT; Csf1r Cre-ERT* (WT)). In order to be certain of the genotypes, mice ear clips were given to Transnetyx, Inc, USA.

Experiments were performed on *Raptor WT/WT; Csf1r Cre-ERT* (WT) and *Raptor f/f; Csf1r Cre-ERT* (KO) mice, I.P injections were given once every 3 consecutive days. On the 4th day mice were culled and collection of bone, spleen and blood was made (unless otherwise specified).

*****I.P injections, oral gavages, and tissue collection were performed with help from ATS staff members (Mrs. Julie Cleaver, Mrs. Tracey Chaplin Perkins, and Mr. Hagen Schmidt) and Mr. Colin Pegrum (an animal technician working in the Centre for Cancer and Inflammation.

2.1.1 Subcutaneous tumour experiments

Mice from *Raptor WT/WT; Csf1r Cre-ERT* (WT) and *Raptor f/f; Csf1r Cre-ERT* (KO) mice, were given I.P injections once for 3 consecutive days. On the 4th day a KPC pancreatic tumour cell line (TB32048) (derived from a PDAC tumour in a female/C57BL/6 mouse) was injected into one flank of the shaven mice. This cell line was generated from a female C57BL/6 KPC mouse and was given to the lab as a

generous gift from Professor David Tuveson. Injections with the pancreatic cell line TB32048 were used to induce tumour formation (precautions were taken to make sure the cell line was mycoplasma free). These cells were cultured in a T175 flask (Corning, 175cm^2 cell culture flask, ref- 431080) using Dulbecco's Modified Eagle Media (DMEM) (Sigma Aldrich, cat- D5796 lot- RNBF3517) with 10% heat inactivated Hyclone Fetal Bovine Serum (FBS) (Sigma Aldrich, cat- SV30160.03 lot- RXL35906), 100units/ml penicillin and 100μg/ml streptomycin (Sigma Aldrich, cat- P4333, lot- 115M4795V). The cells were placed in a 5% CO_2 incubator (Galaxy 170S New Brunswick eppendorf company) at 37°C. Cells were used at passage number 2 and were dissociated from the flask using 2X trypsin-EDTA solution (10X Sigma Aldrich, cat- SLBP3635 lot- 59418C) diluted in phosphate buffer saline (PBS) (Sigma Life Sciences cat- D8537, lot- RNBF3793). Media and trypsin were kept at 37°C for optimal conditions using a water bath. Cells were centrifuged at 211 rcf for 5 min at 4°C. Cells were counted using Beckman Coulter vi-cell XR (cell viability analyser, AH06019). 100,000 cells were injected per mouse. Mice wellbeing was monitored twice per week, observing any changes in weight, tumour growth, visible ulcerations, piloerection, loss of appetite or difficulty in movement. Oral gavages of tamoxifen followed every week for 3 consecutive days to sustain Raptor knockout status until tumours were palpable and have reached 1.2cm in diameter. Once tumours had grown to 1.2cm in diameter all mice were culled, spleen, blood, and tumour were collected. FACS staining and analysis was performed.

2.1.2 Orthotopic tumour experiments

Mice from *Raptor WT/WT; Csf1r Cre-ERT* (WT) and *Raptor f/f; Csf1r Cre-ERT* (KO) mice, were given I.P injections once a day for 3 consecutive days. Mice were shaved and injected with Vetergesic (Buprenorphine) (0.3 mg/ml stock concentration that was diluted 1:10 with sterile H_20) subcutaneously (s.c). This was given two hrs before the start of the operation. On the day of the surgery a KPC pancreatic tumour cell line (TB32048) was injected orthotopically into the pancreas of each mouse. This cell line was generated from a female C57BL/6 KPC mouse and was given to the lab as a generous gift from Professor David Tuveson. Injections with the pancreatic cell line TB32048 was used to induce tumour formation (precautions were taken to make sure the cell line was mycoplasma free). These cells were cultured in a T175 flask (Corning, 175cm^2 cell culture flask, ref-

431080) using Dulbecco's Modified Eagle Media (DMEM) (Sigma Aldrich, cat- D5796 lot- RNBF3517) with 10% heat inactivated Hyclone Fetal Bovine Serum (FBS) (Sigma Aldrich, cat- SV30160.03 lot- RXL35906), 100units/ml penicillin and 100µg/ml streptomycin (Sigma Aldrich, cat- P4333, lot- 115M4795V). They were placed in a 5% CO_2 incubator (Galaxy 170S New Brunswick eppendorf company) at 37°C. Cells were used at passage number 2 and were dissociated from the flask using 2X trypsin-EDTA solution (10X Sigma Aldrich, cat- SLBP3635 lot- 59418C) diluted in phosphate buffer saline (PBS) (Sigma Life Sciences cat- D8537, lot- RNBF3793). Media and trypsin were kept at 37°C for optimal conditions using a water bath. Cells were centrifuged at 211 rcf for 5 min at 4°C. Cells were counted using Beckman Coulter vi-cell XR (cell viability analyser, AH06019). Following this step cells were resuspended in BD Matrigel Basement Membrane Matrix High Concentration (BD Biosciences, ref- 354248). The matrigel was left to thaw overnight and was made up on the day of the surgery from 300µl PBS and 500µl of matrigel (concentrate), which was then resuspended slowly 30-40 times to make sure no clumps or bubbles were formed. Pancreatic tumour cells were suspended at a concentration of 1,000 cells in 5µl and from this mix 5µl was injected per mouse. Dr. Sarah Spear, a postdoc working in the Centre for Cancer and Inflammation performed the surgery. Mice were sprayed with iodine solution to attain maximum sterile conditions; thereafter with a scalpel (Swann-Morton, ref- 0501) an incision was made above the pancreas. The pancreas and spleen were removed gently from the interior cavity and as it was out of the body, cells were injected into the pancreas. Injections into the pancreas were made using a Hamilton syringe 700 series, disposable needles of 25µl volume and 22s gauge (bevel tip) (Fisher Scientific, ref-10100332) were used. Pancreas was not touched until signs of matrigel solidification were observed. Following solidification both pancreas and spleen were placed back into the interior cavity. One or two interrupted sutures using a 6/0 gauge coated vicryl sutures (Ethicon, ref- W9500T) were made on the peritoneal wall. Then two 9mm Clay Adams Clips (VetTech solutions, ref- IN015A) with an Autoclip applier (VetTech solutions, ref- IN015B) were used to shut the wound. Mice were again injected with 30µl of Vetergesic s.c. Mice went through a recovery period of approximately 45 min, on heat boxes at 37°C. Surgical clips were removed one week after surgery. Mice wellbeing was monitored twice per week, observing any changes in weight, tumour growth (by palpating pancreas area), visible ulcerations, piloerection, loss of appetite or difficulty in movement. Oral gavages of tamoxifen followed every week for 3 consecutive days to sustain Raptor knockout status

until tumours were palpable and have reached 1.2cm in diameter. Mr. Colin Pegrum and Dr. Sarah Spear were needed for their experience in approximating tumour size by palpation. Once tumours have grown to 1.2cm in diameter all mice were culled, spleen, blood, and tumour were collected. FACS staining and analysis was performed.

2.1.3 Tamoxifen preparation

1.0G tamoxifen vial was mixed with 25ml corn oil (Sigma Aldrich, ref- C8267) (40mg/ml^{-1}) and left shaking at 55°C. Aliquots were made and placed into eppendorf tubes stored at -20°C.

2.2 Tissue collection and processing

2.2.1 Bones

To isolate bone marrow derived macrophages (BMDMs), mice were sacrificed and both femur and tibia were collected in PBS on ice. The muscle and skin were removed using a disposable scalpel (Swann-Morton, ref- 0501 lot- 6521603). A syringe (1ml soft-ject syringe, lot- 16B29C8) (BD, microlance 3 27G ¾ 0.4x19mm ref- 302200 lot- 1507 16) filled with DMEM with 10% heat inactivated FBS, penicillin and streptomycin was used to flush bone marrow cells from the bones through a cell strainer (Falcon, sterile cell strainer 70µm nylon mesh ref- 352350) and collected in a 50ml falcon tube. After centrifugation at 211 rcf for 5 min at 4°C the cell pellet was resuspended in fresh DMEM and plated in non-treated petri dishes (Falcon, untreated cat- 351058 lot- 4210803). Addition of 20ng/ml of Macrophage Colony Stimulating Factor (MCSF) (eBioscience, cat- 34-8983-85) was used to assist in BMDM differentiation. The bone marrow cells isolated from bones were allowed to differentiate for 7 days and then were harvested. To harvest the cells, Cell Dissociation buffer (Life Technologies, enzyme free PBS based cat- 13151-014 lot- 1736823) was added and cell scrapers (Falcon, 18cm handle/1.8cm blade ref- 353085) were used to remove the cells from the petri dishes (Figure 2.1).

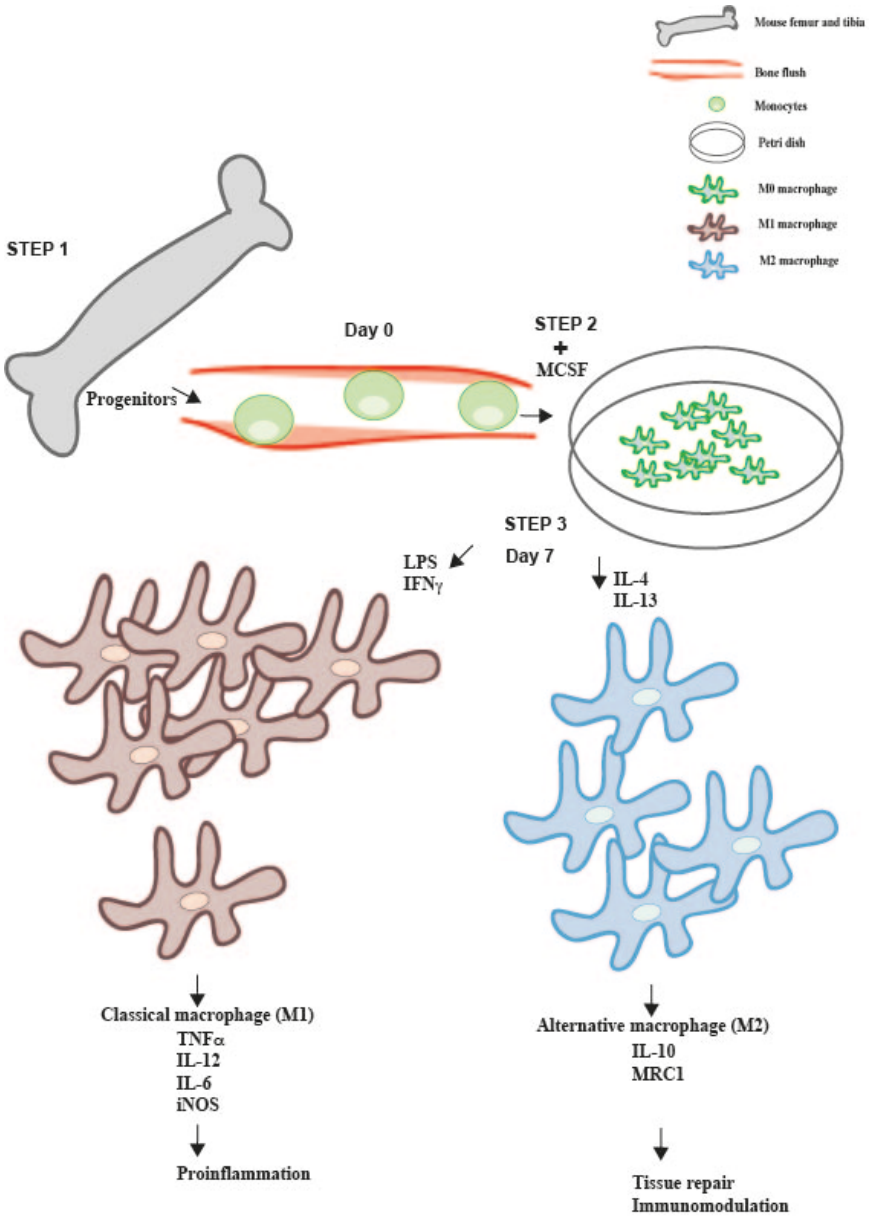

Figure 2.1 Macrophage development *in vitro*

Murine bone of femur and tibia are flushed (STEP 1), and myeloid progenitors along with other cells are placed into a petri dish (day 0). MCSF is added (STEP 2) in order to skew development and maturation of macrophages only from myeloid progenitors while other cells die off. On day 7 (STEP 3) M0 macrophages have matured, they are replated and stimulated with either LPS/IFNγ becoming what is known as classical or M1 macrophages. These release proinflammatory cytokines, for example TNFα and IL-12 and help fight against foreign bodies. They may also be stimulated with IL-4/IL-13 and become alternative or M2 macrophages. These macrophages are needed for tissue repair and immunomodulation leading to balance and homeostasis. Macrophages stimulated with either LPS/IFNγ or IL-4/IL-13 are then used for experiments accordingly.

2.2.2 Spleen

Spleen was removed from mice and placed in ice cold PBS. Spleen was meshed up using a 3ml plunger and kept wet by addition of cold FACS buffer (PBS, 1% FBS and (2mM) EDTA (Ambion, 0.5M pH 8.0 lot- 1512003 P/N: AM9262)). Cells were passed through a 70μm cell strainer and collected using a 50ml falcon tube. The tube was centrifuged at 211 rcf for 5 min at 4°C. Cell pellet was resuspended in 10ml of RBC lysis buffer (cat-555899, BD Biosciences) diluted in water (1:10) and tube was inverted 5 times. It was incubated at room temp (RT) for 10 min. Addition of 10ml cold FACS buffer to stop the lysis process and a further centrifugation was performed. The cell pellet was resuspended in cold FACS buffer and further passed into a 70μm cell strainer. The mixture was centrifuged and supernatant was removed. Cells were resuspended in cold FACS buffer. Cell count was performed and cells were resuspended in an appropriate volume of cold FACS buffer for FACS staining.

2.2.3 Blood

Mice were placed in a tank containing 3% isofluorane / O_2 for anaesthesia. During anaesthesia mice were kept warm by placing tissues underneath their bodies. Using a 1ml syringe (27 gauge needle) a cardiac puncture was performed into the heart. About 1.0ml fresh blood was obtained and placed immediately into EDTA-coated eppendorf tubes and placed on ice. To collect plasma, the blood was centrifuged at 0.2 rcf for 10 min. Supernatant was removed and centrifuged two more times at 2.3 rcf for 5 min and then again at 16.1 rcf for 3 min. Plasma was obtained from the final centrifugation, and stored at -80°C. The whole blood found on the bottom of the tube was resuspended in 5ml of RBC lysis buffer diluted in water (1:10) for 10 min at RT, tube was inverted 5 times. An addition of 10ml cold FACS buffer was used to stop the lysis process. The mixture was centrifuged at 211 rcf for 5 min at 4°C and supernatant was removed. Cells were washed by resuspending in cold FACS buffer then were centrifuged. This procedure was performed twice. Cell count was performed and cells were resuspended in an appropriate volume of cold FACS buffer for FACS staining.

2.2.4 Tumour

2.2.4.1 Subcutaneous tumour

The subcutaneous tumour was removed from the mice and was cut in half longitudinally using a scalpel. One half was placed immediately in dry ice and stored at -80°C. The other half was placed in cold PBS. The tumour was cut into tiny pieces and was placed in a 50ml falcon with Dnase I (50mg/ml) (Roche, cat- 10104159001) and collagenase D (1mg/ml) (Sigma Aldrich, cat- 11088858001) for digestion. The falcon tube was placed in a shaker at 200 rcf for 20 min at 37°C. To stop the digestion process EDTA (5mM) was added. After digestion, tumour cells were passed through a 70µm cell strainer with further meshing using a 3ml syringe plunger. To keep cells from drying cold FACS buffer was added. Cell suspension was centrifuged at 211 rcf for 5 min at 4°C. The cell pellet was resuspended in cold FACS buffer and further passed into a 70µm cell strainer. The mixture was centrifuged and supernatant was removed. Cell count was performed and cells were resuspended in an appropriate volume of cold FACS buffer for FACS staining.

2.2.4.2 Orthotopic tumour

The orthotopic pancreatic tumour was removed from the mice and was cut in half longitudinally using a scalpel. One half was placed immediately in dry ice and stored at -80°C. The other half was place in cold PBS. The tumour was cut into tiny pieces and was placed in a 50ml falcon with a 5ml mix of Dnase I (10mg/ml) (Sigma Aldrich, cat- D4513) and collagenase (2mg/ml) (Sigma Aldrich, cat- C9263) for digestion. The falcon tube was placed in a shaker at 200 rcf for 20 min at 37°C. To stop the digestion process 50µl of EDTA (5mM) was added. After digestion, tumour cells were passed through a 70µm cell strainer with further meshing using a 3ml syringe plunger. To keep cells from drying cold FACS buffer was added. Cell suspension was centrifuged at 211 rcf for 5 min at 4°C. The cell pellet was resuspended in cold FACS buffer and further passed into a 70µm cell strainer. The mixture was centrifuged and supernatant was removed. Cell count was performed and cells were resuspended in an appropriate volume of cold FACS buffer for FACS staining.

2.3 Flow cytometric analysis

Harvested cells (refer to 2.2.1: 2.2.2: 2.2.3: 2.2.4) were stained at $1.0x10^6$ cells/well for FACS analysis. They were plated onto a 96 well v-bottom microtiter plate (lot- 2774065). The plate was centrifuged at 244 rcf for 5 min at 4°C in a Thermo Scientific centrifuge (Sorvall, -ST16R). Supernatant was removed and the pellet found on bottom of the well was resuspended in 50µl of anti CD16/32, Fc block (BD Biosciences, -553142,) diluted with cold FACS buffer (1:200). Cells and Fc block were incubated for 15 min at 4°C. Another 50µl of antibody master mix (2X) (Table. 2.1 and 2.2) was added to the well. Cells and antibodies were incubated for 30 min at 4°C in the dark. The plate was centrifuged at 244 rcf for 5 min at 4°C, supernatant was removed and well was washed with cold FACS buffer, followed by another centrifugation at 244 rcf for 5 min at 4°C. Fixable viability dye was also added at a volume of 50µl to differentiate between live and dead cells. It was diluted in FACS buffer (1:200), kept at 4°C for 20 min in the dark. Plate was centrifuged at 244 rcf for 5 min at 4°C. Cells were washed twice in FACS buffers with centrifugation in between each wash. A 1:1 dilution of PBS and 4% PFA was added to the cells in a volume of 100µl for 30 min at RT to fix the cells. Cells were washed twice with FACS buffer and centrifugation was performed between each wash at 244 rcf for 5 min at 4°C. Cells were resuspended into 200µl of FACS buffer and kept at 4°C in darkness until time of acquisition.

Compensation was performed using 1 drop of Ultracomp ebeads (full spectrum cell analysis) (eBioscience, cat- 01-2222-42) in FACS buffer. Single cell suspensions were analysed using flow cytometry by the BD LSR FORTESSA machine. The machine uses FACS DIVA software (BD Biosciences), analysis and interpretation was done by FlowJo software (Tree Star 9.4.7). Experimental data was analysed using Excel for Mac. Graphs were prepared using GraphPad Prism 5 Mac OS X version 5.0b (121908).

Antibody	Fluorochrome	Company	Clone	Reference/ Catalogue Number	Lot number
CD45	BV785	Biolegend	145-2C11	100320	B207976
CD3	PE-Cy7	Biolegend	30-F11	103149	B208623
CD4	BV605	Biolegend	RM4-5	100548	B209228
CD8	APC	eBioscience	53-6.7	17-0081-82	E07056-1635
CD11b	BV650	Biolegend	M1/70	101239	B197319
F4/80	PE	eBioscience	BM8	12-4801-80	E01704-1642
MHCII	APC/Cy7	Biolegend	M5/114.15.2	107628	B198298
Ly6G	Alexafluor700	eBioscience	RB6-8C5	56-5931-82	E09029-1632
Ly6C	E450	eBioscience	HK1.4	485932-82	E14323-103
CD19	Percp5.5	Biolegend	6D5	115534	B183173
CD11C	FITC	eBioscience	N418	11-0114-82	F001541630

Table 2.1 List of antibodies used for subcutaneous and orthotopic staining of blood, spleen, and tumour

Antibody	Fluorochrome	Company	Clone	Reference/ Catalogue Number	Lot number
Flt3/CD135	PE	eBioscience	A2F10	12-1351-81	E01493-1634
CD34	FITC	eBioscience	RAM34	11-0341-82	E00264-1631
CD127	APC/efluor 780	eBioscience	A7R34	47-1271-80	E10810-1636
c-Kit/CD117	APC	eBioscience	2B8	17-1171-82	E07203-1634
Lin	efluor 450	eBioscience	17A2	88-7772-72	E10650-1632
Sca1	PerCP/Cy5.5	eBioscience	D7	45-5981-82	E08412-1633
CD16/32	PE/Cy7	eBioscience	93	25-0161-82	-
CD45	BV785	Biolegend	30-F11	103149	B208623
CD45	APC	eBioscience	30-F11	17-0451-82	E07148-1631
CD11b	BV650	Biolegend	M1/70	101239	B214270
CD11b	PE/Cy7	eBioscience	M1/70	25-0112-81	-
F4/80	PE	eBioscience	BM8	12-4801-82	E01705-1638
CD3	PE/Cy7	Biolegend	145-2C11	100320	B207976
CD4	BV605	Biolegend	RM4-5	100548	B195962
CD8	APC	eBioscience	53-6.7	17-0081-82	E07056-1633
MHCII	APC/Cy7	Biolegend	M5/114.15.2	107628	B198298
CD19	PerCP/Cy5.5	Biolegend	6D5	115534	B183173
Ly6G	Alexafluor 700	eBioscience	RB6-8C5	56-5931-82	E09029-1632
Ly6C	efluor 450	eBioscience	HK1.4	48-5932-82	E14323-103
CD11C	FITC	Biolegend	N418	117306	B191236
FVD	efluor 506	eBioscience	-	65-0866-14	E15162-128

Table 2.2 List of antibodies used for macrophage lineage and maturation staining

2.4 BMDM gene expression analysis

2.4.1 BMDM stimulation

BMDMs that have been harvested (refer to section 2.2.1) were replated in a 6 well plate (CoStar, Cell culture plate ref- 3506), at $1x10^6$ cells/well and were left approximately 16 hrs for cells to settle. BMDMs were stimulated either with 100 ng/ml of LPS (Sigma Aldrich, cat- L2630) and 20 ng/ml of IFNγ (Peprotech, cat- 315-05) or were stimulated with 10ng/ml of IL-4 (Peprotech, cat- 214-14) and 10ng/ml of IL-13 (Peprotech, cat- 210-13) (Table 2.3). Stimulation was performed at differing time points 2, 4, 6, 12, 22, and 30 hrs. Plate was placed in a 5% CO_2 incubator at 37° C.

Ligand	Company	Catalogue Number	Working Concentration	Stock Concentration
LPS	Sigma Aldrich	L2630	100ng/ml	1mg/ml
IFNγ	Peprotech	315-05	20ng/ml	100µg/ml
IL-4	Peprotech	214-14	10ng/ml	100µg/ml
IL-13	Peprotech	210-13	10ng/ml	50µg/ml

Table 2.3 List of ligands used for BMDM stimulation

2.4.2 RNA extraction

Media was removed from cells in petri dishes and washed twice in PBS. Cell lysates were obtained by adding 350µl of RLT buffer (Qiagen, cat- 79216). Cells were scraped using cell scrapers and lysates were placed in eppendorf tubes. These tubes were snap-frozen immediately in dry ice and were stored at -80° C.

2.4.3 RNA isolation

Cell lysates were thawed on ice. The Qiagen RNeasy mini kit (250) (Qiagen, cat- 74106) was used for RNA isolation and purification. Extreme caution was taken to clean area before following RNA isolation procedure. RNAZap (Ambion, cat- AM9780) was sprayed onto surfaces, pipettes, vortex, and centrifuge. Addition of 350µl of 70% ethanol was used (Sigma, cat- E7023). Cell lysate and ethanol were mixed gently by pipetting a few times. The mixture was added onto RNeasy spin columns. The columns were

centrifuged for 20 sec at 9.3 rcf. To the columns 350µl of RW1 buffer was added. Again a centrifugation of 9.3 rcf for 20 sec was done. A master mix of DNase solution was prepared by making up 70µl of RDD buffer plus 10µl of DNase stock (Qiagen, Rnase free Dnase set (50) cat- 79254), 80µl of this master mix was added onto each column, and was left to incubate for 10 min, then spun for 20 sec at 9.3 rcf. 500µl of RPE buffer was added onto the column then spun for 20 sec at 9.3 rcf. An addition of 500µl of 80% ethanol was added to the column, and then centrifuged for 2 min at 9.3 rcf. To make sure no ethanol was left on the column, a new 2ml tube was used with a centrifugation step for 5 min at maximum speed. The column was transferred to a new 1.5ml tube and an elution process to isolate RNA was performed by adding 15µl of nuclease free H_2O (Ambion, P/N: AM9938 lot- 1311047). The tubes were centrifuged for 1 min at 16.1 rcf. Apart from the elution step, discarding the filtrate followed all centrifugation steps. Tubes were stored in -20°C. Measurement of RNA concentration was achieved using the nanodrop (ND-1000 Spectophotometer).

2.4.4 cDNA synthesis

The high capacity cDNA reverse transcription kit (Applied Biosystems, cat- 4368813) was used for cDNA synthesis. A 2X Reverse Transcription master mix (MM) was prepared for one reaction (Table 2.4).

Reagent	Volume (µl) / reaction
10X RT Buffer	2
25X dNTP Mix (100mM)	0.8
10X RT Random Primers	2
MultiScribe Reverse Transcriptase	1
Nuclease Free H_2O	4.2
Total per Reaction	10

Table 2.4 List of reagents and volumes used for cDNA synthesis / reaction

To prepare the cDNA reverse transcription reaction, 10µl of the 2X Reverse Transcription master mix was added onto PCR strip tubes (Axygen, cat- PCR-0208-C) on ice. 10µl of RNA was added (after normalization) onto the tubes and mixed by pipetting. The tubes were sealed and a vortex was used to ensure proper mixing. A brief centrifugation was performed to make sure all contents were on the bottom of the tube. The tubes were kept on ice until they were ready to load on the thermal cycler (Bio-Rad, T100) (Table 2.5). cDNA was placed in -20°C until ready for qPCR.

	Step 1	**Step 2**	**Step 3**	**Step 4**
Temperature	25°C	37°C	85°C	4°C
Time	10 min	120 min	5 min	∞

Table 2.5 Cycling conditions for cDNA synthesis / reaction

2.4.5 qPCR

Using the cDNA produced in section 2.4.4, a dilution of the cDNA in nuclease free water was achieved (1:10) and a qPCR MM was made using iTaq universal probe system (Bio-Rad, Universal probe supermix cat- 172-5131) (Table 2.6). Expression levels of different genes were analysed (Table 2.8).

Reagent	**Volume (µl) / reaction**
iTaq	5
Primer	0.5
cDNA	4.5
Nuclease free water	-

Table 2.6 Master mix using iTaq universal probe system

The qPCR was performed using the step one plus real time PCR system (Applied biosystems). Mixture was added onto a 96 well plate (Applied biosystems, microAmpfast optical 96-well reaction plate, 0.1ml PCR compatible, DNA/RNA/ Rnase free ref-4346906). Plates were sealed with adhesive film (Applied biosystems, microAmp optical adhesive film, PCR compatible, DNA/RNA/ Rnase free lot- 201310207 P/N: 4311971) and centrifuged for approximately 1 min at maximum speed. Cycling Conditions are found in (Table 2.7).

Cycles	Time	Temperature (°C)
1	2 min	50
1	10 min	95
40	15 sec	95
	1 min	60

Table 2.7 Cycling conditions for qPCR

2.4.5.1 Gene Expression Analysis

Analysis was performed subsequently by exporting the raw C_T values of the 40 cycles produced for each gene. In order to calculate the ΔC_T, the C_T value of the housekeeping gene B2M was subtracted from the C_T value of the gene of interest.

$$\Delta C_T = C_T \text{ (gene of interest)} - C_T \text{ (housekeeping gene)}$$

To obtain the final result $2 \wedge (-\Delta C_T)$ was used to achieve relative expression against the house keeping gene. Experimental data was analysed using Excel for Mac. Graphs were prepared using GraphPad Prism 5 Mac OS X version 5.0b (121908).

Gene	Primer code	Company	Lot number
RAPTOR	Mm00712698_m1	Applied Biosciences	P150703-005 102
TNFα	Mm00443258_m1	Applied Biosciences	1457792
IL-12b	Mm00434174_m1	Applied Biosciences	1406055
IL-6	Mm00446190_m1	Applied Biosciences	1453207
iNOS	Mm01309898_m1	Applied Biosciences	1081296
IL-10	Mm00439614_m1	Applied Biosciences	1415579
MRC1	Mm00485148_m1	Applied Biosciences	1423400
B2M	Mm00437762_m1	Applied Biosciences	1464053

Table 2.8 List of genes used for TaqMan gene expression

2.5 Protein analysis

2.5.1 BMDM stimulation

BMDMs that had been harvested (refer to section 2.2.1) were replated in a 6 well plate. Replating was at $1x10^6$ cells/well and was left approximately 16 hrs for cells to settle. BMDMs were stimulated with 100 ng/ml of LPS and 20 ng/ml of IFNγ (refer to Table 2.2). Stimulation was performed at differing time points 15, 30, 60, 120, and 180 min. Plate was placed in a 5% CO_2 incubator at 37°C.

2.5.2 Protein lysis

Radio Immunoprecipitation Assay Buffer (RIPA) (Sigma Aldrich, cat- R0278 SLBD5707) in combination with a protease inhibitor cocktail I (one tablet/ 10ml RIPA buffer) (Roche, cat- 11836153001 lot- 14015000) was made prior BMDM protein lysis.

BMDMs were lysed by first washing wells twice in cold PBS, making sure that no PBS is left on the well after suctioning. 80µl of RIPA buffer with phosphatase inhibitor cocktail II (Sigma Aldrich, cat- P5726) and phosphatase inhibitor cocktail III (Sigma Aldrich, cat- P0044) in a 1:100 dilution was added for 30 min on ice. BMDM lysates were harvested using cell scrapers and placed in individual eppendorf tubes that have been centrifuged for 15 min at 15.7 rcf at 4°C. Lysates were kept at -20°C.

2.5.3 Protein quantification

Bicinchoninic Acid Assay (BCA Assay)

BMDM protein concentration was measured using 200µl of 4% w/v copper II sulphate solution (Sigma Aldrich, cat- C2284) that was diluted 1:50 in bicinchoninic acid (Sigma Aldrich, cat - B9643). This BCA reagent was added to 10µl of either BMDM samples or 10µl of Bovine Serum Albumin (BSA) standards (Sigma Aldrich, cat- A4503) which were diluted in PBS in a 96 well plate (CoStar, Cell culture plate ref- 3599). The plate was incubated for 30 min at 37°C, then the optical density was measured using a plate reader spectrophotometer at 595 nm (OpSys MR Dynex technologies). BMDM protein concentrations were then calculated using the standard curve.

2.5.4 Western blot

Prior to loading on gel, samples were prepared by adding 5µl (4X) of NuPAGE LDS sample buffer (Life Sciences Solutions, cat- NP0008) along with 2µl (10X) of NuPAGE sample reducing agent (Life Sciences Solutions, cat- NP0009) into eppendorf tubes. To this mix 13µl of protein was added making sure equal amounts of protein is placed into each well within the gel (may add H_2O if necessary). This mixture was vortexed and placed on a heat block for 10 min at 70°C.

2.5.4.1 Gel Eectrophoresis

Preparation of running buffer:

25ml of NuPAGE tris-acetate (TA) SDS running buffer (20X) (Life Sciences Solutions, cat- LA0041) was added to 475ml of deionized H_20.

Running buffer was added into a chamber that had a gel already placed into it. Samples were loaded onto NuPAGE Novex 3-8% tris-acetate protein gel (Life Sciences Solutions, cat- EA03785BOX). A HiMArk pre-stained protein standard ladder (Life Sciences Solutions, cat- LC5699) was also loaded onto the gel well. 500µl of NuPAGE antioxidant (Life Sciences Solutions, cat- NP0005) was added on to cover the gel area. The gel was run at 150V for approximately 90 min, separating the protein based on its molecular weight.

25ml of NuPAGE transfer buffer (20X) (Life Sciences Solutions, cat- NP0006) was added to 425ml of deionized H_2O. 50ml of methanol (Fisher Scientific, cat- 11976961) was added including 500µl of NuPAGE antioxidant.

Polyvinylidene fluoride (PVDF) (Novex Life Technologies, cat- LC2005) Invitrolon filter paper sandwich 0.45µm pore size was used. Transfer was at 30V for approximately 1h 15 min.

2.5.4.2 Immunoblotting

Preparing TBS (10X)

10X TBS buffer was prepared from 1.5M NaCl (Sigma Aldrich, cat- 71380) and 200mM of Trizma base (Sigma Aldrich, cat- T1503) in deionized H_2O (bringing pH to 7.6 using

HCL and a pH meter). A 1:10 dilution of 10X TBS in deionized H_2O was prepared to make 1X TBS. The addition of 0.1% v/v Tween20 (Sigma Aldrich, cat- P7949) was done to make TBST. Blocking Buffer was prepared by adding 1X TBST to dissolve 5% w/v of dried skimmed milk powder (Marvel), membrane was blocked for 1 hr at room temperature on a rocker.

Primary antibody for staining the membrane was used at a 1:1000 dilution with blocking buffer (Table 2.9). It was kept overnight at 4°C on a rocker. Membrane was washed 3 times in 1X TBST for 5 min each on a rocker. Then was stained with HRP-linked secondary donkey anti-rabbit IgG (GE Healthcare, cat- NA9340) at a 1:2000 dilution using blocking buffer for 1 hr at room temperature on a rocker. Membrane was washed 3 times in 1X TBST for 5 min each on a rocker. Addition of 750µl of Amersham ECL western blot detection reagent (GE Healthcare, cat- RPN2106) was used on the membrane and incubated for 1 min. Developing of the membrane was done using Super Rx X-ray film (Fujifilm, cat- 4741019236). The machine was a medical film processor (Konica Minolta, Model- SRX-101A). Developing of membrane was also done using the Amersham Imager 600 (Chemidoc system ref-R188609).

Reblotting the membrane was achieved by adding Reblot plus strong (10X) (Millipore, cat- 2504) at a dilution of 1:10 in deionized H_20 and applied onto the membrane for 5 min at room temperature on a rocker.

Housekeeping protein detection was done by using β- actin, (a mouse anti-β-actin) used at a dilution of 1:5000 (Sigma Aldrich, cat- A1978 clone-AC15) and the secondary to that was a sheep anti-mouse IgG also used at a dilution of 1:5000 (GE Healthcare, cat- NXA931).

Antibody	Company	Clone	Reference/ Catalogue Number	Lot number
RAPTOR	Cell Signalling	24C12	Jan-16	11 2280S
p-AKT	Cell Signalling	S473	Sep-15	14 9271L
AKT (Pan)	Cell Signalling	1.10E+08	Feb-16	3 4685S
p-S6 Ribosomal protein S23S/236	Cell Signalling	D57.2.2E	Apr-15	11 4858S
S6	Cell Signalling	5G10	2217	5
p-P44/42 MAPK	Cell Signalling	T202/Y206	Dec-14	28 91015
P44/42 MAPK	Cell Signalling	ERK1/2	Aug-15	26 9102S
p-IKBα (S32)	Cell Signalling	14D4	Oct-15	14 2859S
IKBα	Cell Signalling	-	Jul-11	9 9242S
p-STAT3 (Y705)	Cell Signalling	D3A7	Mar-16	26 9145S
STAT3	Cell Signalling	79D7	Jul-12	3 4904S

Table 2.9 List of antibodies used for Western blot staining (all antibodies were anti-rabbit antibodies)

2.6 Detection and quantification of secreted cytokines by enzyme linked immunosorbent assay (ELISA)

Media was collected from plated BMDMs that were harvested and used for gene expression assays (refer to section 2.4). BMDMs were stimulated with 100 ng/ml of LPS and 20 ng/ml of IFNγ or stimulated with 10ng/ml of IL-4 and 10ng/ml of IL-13 (refer to Table 2.2). The stimulation was performed at differing time points 2, 4, 6, 12, 22, and 30 hrs. Plate was placed in a 5% CO_2 incubator at 37°C (refer to section 2.4). The media was collected in a 5ml falcon tube and was centrifuged at 211 rcf for 5 min at 4°C. Supernatant was carefully removed and placed in eppendorf tubes at -80°C. ELISA kits (Table 2.10) were used to detect secretion of cytokines in BMDM media.

Previous day 96 well plate (CoStar, EIA/RIA half area flat bottom lot- 16213005) was coated with 50µl of capture antibody (refer to Table 2.10) diluted in PBS (1:250), covered and kept at 4°C.

The following day the plate was washed 3 times with wash buffer (PBS + 0.05% tween). 100µl of assay diluent (PBS + 10% FBS) was added as a blocking solution for 1 hr at room temperature. After blocking, the plate was washed a further 3 times with washing buffer. An addition of 50µl of either standard (serial dilution) or sample (1:250) diluted in assay diluent was added to each well (in triplicates). Plate was incubated at room temperature for 2 hrs. Next the plate was washed 5 more times with wash buffer. 50µl of HRP and 50µl of working detection were added to the plate for 1 hr (1:250) in assay diluent. Plate was washed 7 times in wash buffer with 1 min soaks each. 50µl of substrate solution TMB-peroxidase (KBL Insight biotechnology, P/C 50-76-00 [TMB peroxidase substrate 130522 P/C 50-76-01; peroxidase substrate solution B 130611 P/C 50-65-00]) was added for approximately 30 min in the dark (until wells turned blue). 25µl of stop solution (1M phosphoric acid) was then added to stop the reaction (wells turned yellow). Plate was read within 30 min using plate reader at 570nm. Experimental data was analysed using Excel for Mac. Graphs were prepared using GraphPad Prism 5 Mac OS X version 5.0b (121908).

Cytokine	Company	Catalogue Number	Lot Number
TNFα	BD optEIA	558534	5204766
IL12b (p40)	BD optEIA	555165	3135570
IL-6	BD optEIA	555240	4357560
IL-10	BD optEIA	555252	5323643

Table 2.10 ELISA kits used for cytokine detection and quantification

2.7 Migration assay

2.7.1 Migration towards fibroblasts

BMDMs that have been harvested (refer to section 2.2.1) were replated in a 24 well plate (CoStar, Cell culture plate ref- 3527) on transwells (permeable supports 6.5mm inserts 5.0µm polycarbonate membrane tissue culture treated lot- 29915004). Replating was done at $1x10^5$ cells/transwell and were left approximately 4 hrs for cells to settle. BMDMs were stimulated either with 100 ng/ml of LPS and 20 ng/ml of IFNγ or were stimulated with 10ng/ml of IL-4 and 10ng/ml of IL-13 (refer to Table 2.3). Stimulation was performed for 4 hrs. Plate was placed in a 5% CO_2 incubator at 37°C. At the same time on separate wells mouse embryonic fibroblasts (MEFs) were also replated at $1x10^5$ cells/well. Once the BMDMs were stimulated DMEM was removed and replaced with fresh media and transwells were moved on top of wells with fibroblasts (making the ratio of BMDMs to Fibroblasts 1:1). Plate was placed in a 5% CO_2 incubator at 37°C for 24 hrs. Onto a new 24 well plate 500µl of crystal violet (0.2% in 0.5% ethanol) was added, DMEM was removed from the transwells then inserts were placed into the crystal violet for 10 min. The inserts were removed from the crystal violet and washed in water. The inserts were left to dry approximately 30 min. 300µl of acetic acid (10%) was added into fresh wells, dry inserts were placed into the acetic acid. 100µl of acetic acid were placed into 96 well plates (in triplicates) and read using a plate reader at 595nm. Experimental data was analysed using Excel for Mac. Graphs were prepared using GraphPad Prism 5 Mac OS X version 5.0b (121908).

2.7.2 Migration towards pancreatic cancer cells (TB32047)

BMDMs that have been harvested (refer to section 2.2.1) were replated in a 24 well plate (CoStar, Cell culture plate ref- 3527) on transwells (permeable supports 6.5mm inserts 5.0µm polycarbonate membrane tissue culture treated lot- 29915004). Replating was done at $1x10^5$ cells/transwell and were left approximately 4 hrs for cells to settle. BMDMs were stimulated either with 100 ng/ml of LPS and 20 ng/ml of IFNγ or were stimulated with 10ng/ml of IL-4 and 10ng/ml of IL-13 (refer to Table 2.3). Stimulation was performed for 4 hrs. Plate was placed in a 5% CO_2 incubator at 37°C. At the same time on separate wells a KPC pancreatic tumour cell line pancreatic cancer cells (TB32047) (derived from a PDAC tumour in a male/C57BL/6 mouse) were also replated at $1x10^5$

cells/well. Once the BMDMs were stimulated DMEM was removed and replaced with fresh media and transwells were moved on top of wells with cancer cells (making the ratio of BMDMs to cancer cells 1:1). Plate was placed in a 5% CO_2 incubator at 37°C for 24 hrs. Onto a new 24 well plate 500µl of crystal violet (0.2% in 0.5% ethanol) was added, DMEM was removed from the transwells then inserts were placed into the crystal violet for 10 min. The inserts were removed from the crystal violet and washed in water. The inserts were left to dry approximately 30 min. 300µl of acetic acid (10%) was added into fresh wells dry inserts were placed into the acetic acid. 100µl of acetic acid were placed into 96 well plates (in triplicates) and read using a plate reader at 595nm. Experimental data was analysed using Excel for Mac. Graphs were prepared using GraphPad Prism 5 Mac OS X version 5.0b (121908).

2.8 Phagocytosis assay

2.8.1 Phagocytosis with fluorescent beads

BMDMs that have been harvested (refer to section 2.2.1) were resuspended in 1% FBS DMEM media. BMDMs were replated in a 6 well plate for 5 conditions (Media only, 15, 30, 60, and 90 min). Another 6 well plate was used to replate BMDMs for one condition (ice control). Re-plating was at $1x10^6$ cells/well and was left approximately 4 hrs for cells to settle in a 5% CO_2 incubator at 37°C. Media was removed and replaced with serum free DMEM media for 1 hr in the incubator. BMDMs were stimulated with 100ng/ml LPS overnight in 10% FBS DMEM media. The following day 1ml of the fluorescence beads were added (Life technologies, Fluospheres Carboxylate modified microspheres 1.0µm yellow/green fluorescent 505/515 cat- F-8823) at a concentration of 60 x 10^/well (stock concentration 3.6 x 10^{10}) to the wells according to the time point. The ice control was always on ice. Beads were diluted in FACS buffer. After the last time point was reached wells were washed in cold FACS buffer and then 1ml FACS buffer. Cells were scraped using a cell scraper. Cells were pooled in a separate tube labelled as minus DAPI. Cells were centrifuged at 211 rcf for 5 min at 4°C. They were resuspended in 200µl of FACS buffer. Before cells were acquired on the BD LSR FORTESSA machine DAPI was added to each sample at a 1:5000 dilution. Analysis and interpretation was done by FlowJo software (Tree Star 9.4.7). Experimental data was analysed using Excel for Mac. Graphs were prepared using GraphPad Prism 5 Mac OS X version 5.0b (121908).

2.8.2 Phagocytosis with pancreatic cancer cells (TB32048)

BMDMs were harvested on day 6, they were scraped with cell dissociation buffer. BMDMs were labelled with an orange-red cell tracker (Thermo fisher scientific, ref- V22885 Dil) at a concentration of 5µl / $2x10^6$ cells/ 1ml for 30 min at 37°C in serum free media (DMEM without FBS). During the 30 min incubation, cancer cells (TB32048) were stained with far red cell tracker (Thermo fisher scientific, ref- V22887 Vibrant DiD cell labelling solution) at a concentration of 5µl / $2x10^6$ cells/ 1ml for 30 min at 37°C in serum free media. After the 30 min incubation, cells were washed twice in normal media (DMEM with FBS). BMDMs were replated in a 6 well plate for 6 conditions (Media only, 2, 4, 6, 8, and 16 hrs). Another 6 well plate was used to replate BMDMs for one condition (ice control at 16 hrs). Replating was at $5x10^5$ cells/well. MCSF was added

onto the BMDMs since they were replated at day 6. Cancer cells were plated in regular petri dish plates (Falcon, 100 x15mm ref- 351008) at 8 $x10^6$ / plate. On day 7 BMDMs were stimulated with 100ng/ml of LPS overnight in a 5% CO_2 incubator at 37°C. Cancer cells were treated with 100µM gemcitabine (Hospira, Onco-tain, PL 04515/0224 ; PA 437/6311) overnight in a 5% CO_2 incubator at 37°C. On day 8, cancer cells were scraped and washed in normal media, they were then placed on top of the BMDMs in descending order starting from the 8 hr time point. After the last time point was reached wells were washed in cold FACS buffer and then 1ml FACS buffer. Cells were scraped using a cell scraper. Cells were pooled in a separate tube labelled as minus DAPI. Cells were centrifuged at 211 rcf for 5 min at 4°C. They were resuspended in 200µl of FACS buffer. Before cells were acquired for all the time points on the BD LSR FORTESSA machine, DAPI was added to each sample at a 1:5000 dilution. Cancer cells were added onto the 16 hr plate and left overnight in a 5% CO_2 incubator at 37°C an ice control well was kept overnight at 4°C in the dark. The following day the cells from the 16 hr time point and ice control were scraped in the same way as for the other time points. Cells were centrifuged at 211 rcf for 5 min at 4°C. They were resuspended in 200µl of FACS buffer. Prior to acquisition on the BD LSR FORTESSA machine, DAPI was added to each sample at a 1:5000 dilution. Analysis and interpretation was done by FlowJo software (Tree Star 9.4.7). Experimental data was analysed using Excel for Mac. Graphs were prepared using GraphPad Prism 5 Mac OS X version 5.0b (121908).

2.9 Fc receptor quantification

Harvested cells (refer to 2.2.1) were stained at 1.0x10^6 cells/well for FACS analysis. They were plated onto a 96 well v-bottom microtiter plate (lot- 2774065). The plate was centrifuged at 244 rcf for 5 min at 4°C in a Thermo Scientific centrifuge (Sorvall, -ST16R). Supernatant was removed and the pellet found on bottom of well was resuspended in 100µl of antibody master mix (Table. 2.11). Cells and antibodies were incubated for 30 min at 4°C in the dark. The plate was centrifuged at 244 rcf for 5 min at 4°C, supernatant was removed and well was washed with cold FACS buffer, followed by another centrifugation at 244 rcf for 5 min at 4°C. Fixable viability dye was also added at a volume of 50µl to differentiate between live and dead cells. It was diluted in FACS buffer (1:200), kept at 4°C for 20 min in the dark. Plate was centrifuged at 244 rcf for 5 min at 4°C. Cells were washed twice in FACS buffers with centrifugation in between

each wash. A 1:1 dilution of PBS and 4% PFA was added to the cells in a volume of 100µl for 30 min at RT to fix the cells. Cells were washed twice with FACS buffer and centrifugation was performed between each wash at 244 rcf for 5 min at 4°C. Cells were resuspended into 200µl of FACS buffer and kept at 4°C in darkness until time of acquisition.

Compensation was performed by using 1 drop in FACS buffer of Ultracomp ebeads (full spectrum cell analysis) (eBioscience, cat- 01-2222-42). Single cell suspensions were analysed using flow cytometry by the BD LSR FORTESSA machine. The machine uses FACS DIVA software (BD Biosciences), analysis and interpretation was done by FlowJo software (Tree Star 9.4.7). Experimental data was analysed using Excel for Mac. Graphs were prepared using GraphPad Prism 5 Mac OS X version 5.0b (121908).

Antibody	Fluorochrome	Company	Clone	Reference/ Catalogue Number	Lot number
CD64 (FcγR1)	PE (1:200)	Biolegend	X54-5/7.1	139303	B191539
CD16/32	FITC (1:200)	eBioscience	93	11-0161-81	E00172-1632
CD206 (MMR)	APC (1:400)	eBioscience	MR6F3	17-0261-80	-
CD86	BV605 (1:200)	Biolegend	GL-1	105037	B202374

Table 2.11 List of antibodies used for Fc receptor staining

2.10 iNOS quantification

2.10.1 Intracellular staining

Harvested cells (refer to 2.2.1) were stained at $1.0x10^6$ cells/well for FACS analysis. They were plated onto a 96 well v-bottom microtiter plate (lot- 2774065). The plate was centrifuged at 244 rcf for 5 min at 4°C in a Thermo Scientific centrifuge (Sorvall, - ST16R). Supernatant was removed and the pellet found on the bottom of the well was resuspended in fixable viability dye at a volume of 50µl to differentiate between live and dead cells. It was diluted in FACS buffer (1:200), kept at 4°C for 20 min in the dark. Plate was centrifuged at 244 rcf for 5 min at 4°C. Cells were washed twice in FACS buffers with centrifugation in between each wash. Supernatant was removed and the pellet found on bottom of the well was resuspended in 50µl of anti CD16/32,Fc block (BD

Biosciences, -553142,) diluted with cold PBS (1:200). Cells and Fc block were incubated for 15 min at 4°C. The plate was centrifuged at 244 rcf for 5 min at 4°C, supernatant was removed and well was washed with cold PBS (twice), followed by another centrifugation at 244 rcf for 5 min at 4°C. Supernatant was removed, and plate was pulse vortexed to completely dissociate the pellet. To the plate 100µl of fixation/permeabilization working solution (Fixation/permeabilzation diluent: eBioscience, ref- 00-5222-56; Fixation/permeabilzation concentrate: eBioscience, ref- 00-5123-43) was added in 1:3 dilution, then pulse vortexed once more. The plate was incubated at 4°C for 1 hr in the dark. 1X Permeabilization buffer (eBioscience, ref- 00-8333-56) was added to the plate after incubation in 1:10 dilution using distilled water. The plate was centrifuged at 244 rcf for 5 min at 4°C, supernatant was removed and well was washed with 1X permeabilization buffer. Centrifugation was repeated at same conditions. Supernatant was removed and pellet was reuspended in 100µl of 1X permeabilization buffer. iNOS (eBioscience, PE, clone: CXNFT ref- 12-5520-82 lot-E17914-103 ; 1:400) antibody was added (isotype was also used : rat IgG2aκ). The plate was incubated at 4°C for a minimum of 30 min in the dark. Plate was washed with permeabilization buffer twice with centrifugation at 244 rcf for 5 min at 4°C, each wash. Cells were resuspended into 200µl of FACS buffer and kept at 4°C in darkness until time of acquisition. Single cell suspensions were analysed using flow cytometry by the BD LSR FORTESSA machine. The machine uses FACS DIVA software (BD Biosciences), analysis and interpretation was done by FlowJo software (Tree Star 9.4.7). Experimental data was analysed using Excel for Mac. Graphs were prepared using GraphPad Prism 5 Mac OS X version 5.0b (121908).

2.11 BMDM cytoskeleton analysis (Immunofluorescence staining)

BMDMs that have been harvested (refer to section 2.2.1) were replated in a 24 well plate on coverslips. Replating was at $5x10^5$ cells/well and were left approximately 16 hrs for cells to settle. BMDMs were stimulated either with 100ng/ml of LPS and 20ng/ml IFNγ or were stimulated with 10ng/ml of IL-4 and 10ng/ml of IL-13 (refer to Table 2.3). Stimulation was performed for 4 hrs. The plate was placed in 5% CO_2 incubator at 37°C. Coverslips were washed twice in PBS and were fixed using 4% PFA for 15 min at room temperature. Two more washing steps followed fixation with PBS. Permeablization of cells with 0.1% Triton-X100 (Sigma Aldrich, 066K0089) for 5 min at room temperature

was achieved. Cells were washed once in PBS and blocked in 2.5% BSA (Sigma Life Science, A4503-500G), + 5% goat serum (Sigma Life Science, SLBK7718V) for 1 hr at room temperature in the dark. Cells were stained with phalloidin stain (Life technologies, ref- A22287 lot-1731699 ; Alexa fluor 647) (diluted in blocking solution ; 2.5% BSA plus 1% goat serum in PBS) for 1 hr at room temperature. Cells were washed after staining twice in PBS. Then washed once in water. Coverslips were removed gently from the wells and were mounted on slides using prolong gold antifade reagent with DAPI (Life technologies, ref- P36931 lot-1681269). Slides were kept in the dark up to time of reading. Slides were read using the LSM 710 Confocal microscope (Zeiss Laser Scanning Microscope LSM710). 4-5 fields were captured; analysis was performed using ImageJ software.

2.12 F / G actin ratio assay

BMDMs that have been harvested (refer to section 2.2.1) were resuspended in 1% FBS DMEM media. BMDMs were replated in a 6 well plate for 6 conditions (Media only, 5, 20, 30, 60, and 90 min). Another 6 well plate was used to replate BMDMs for one condition (ice control). Replating was at $1x10^6$ cells/well and was left approximately 4 hrs for cells to settle in a 5% CO_2 incubator at 37°C. Media was removed and replaced with serum free DMEM media for 1 hr in the incubator. BMDMs were stimulated with 100ng/ml LPS overnight. The following day 1ml of the fluorescence beads were added (Life technologies, Fluospheres Carboxylate modified microspheres 1.0µm yellow/green fluorescent 505/515 cat- F-8823) at a concentration of 60 x 10^/well (stock concentration 3.6×10^{10}) to the wells according to the time point. The ice control was always on ice. Beads were diluted in FACS buffer. After the last time point was reached wells were washed in cold FACS buffer and then 1ml FACS buffer. Cells were scraped using a cell scraper. Cells were centrifuged at 211 rcf for 5 min at 4°C. They were resuspended in 100µl of FACS buffer. Cells were plated onto a 96 well v-bottom microtiter plate (lot-2774065). The plate was centrifuged at 244 rcf for 5 min at 4°C in a Thermo Scientific centrifuge (Sorvall, -ST16R). Supernatant was removed and the pellet found on bottom of well was resuspended in fixable viability dye at a volume of 50µl to differentiate between live and dead cells. It was diluted in FACS buffer (1:200), kept at 4°C for 20 min in the dark. Plate was centrifuged at 244 rcf for 5 min at 4°C. Cells were washed twice in FACS buffers with centrifugation in between each wash. A 1:1 dilution of PBS and 4% PFA

was added to the cells in a volume of 100µl for 30 min at RT to fix the cells. Cells were washed twice with FACS buffer and centrifugation was performed between each wash at 244 rcf for 5 min at 4°C. Cells were permeablized with 0.1% triton-X100 (Sigma Aldrich, 066K0089) for 10 min at RT. Plate was centrifuged at 244 rcf for 5 min at 4°C. Supernatant was removed and cells were resuspended in FACS buffer, followed by another spin at 244 rcf for 5 min at 4°C. Cells were stained with F-actin (1:400) and G-actin (1:550) stain (Table 2.12) at a volume of 100µl. Plate was kept at 4°C, for 1 hr. The plate was centrifuged at 244 rcf for 5 min at 4°C. Cells were washed twice with FACS buffer and centrifugation was performed between each wash at 244 rcf for 5 min at 4°C. Cells were resuspended into 200µl of FACS buffer and kept at 4°C in darkness until time of acquisition.

Compensation was performed by using 1 drop in FACS buffer of Ultracomp ebeads (full spectrum cell analysis) (eBioscience, cat- 01-2222-42). Single cell suspensions were analysed using flow cytometry by the BD LSR FORTESSA machine. The machine uses FACS DIVA software (BD Biosciences), analysis and interpretation was done by FlowJo software (Tree Star 9.4.7). Experimental data was analysed using Excel for Mac. Graphs were prepared using GraphPad Prism 5 Mac OS X version 5.0b (121908).

Stain/dye	Fluorochrome	Company	Reference/ Catalogue Number
F-actin	APC	Thermofisher	A22284
G-actin	PE	Thermofisher	D12372

Table 2.12 Stains/Dyes used in F/G actin ratio assay

3 Characterisation of Macrophages Lacking Raptor Protein

3.1 Introduction

Macrophages are highly plastic cells that respond to different environmental cues and are considered to participate in frontline host defence in times of infection and disease. As they are plastic cells they have diverse phenotypes allowing them to adopt different effector states. Macrophages needed for innate and adaptive immune responses are known to assume a classical phenotype and are usually placed in the M1 macrophage category [158] [76]. Those needed for physiological homeostasis, maintenance, and tissue repair are of the alternative phenotype, and are categorized as M2 macrophages [158]. Nevertheless it should be noted that this description of two extreme phenotypes is an oversimplification of macrophage phenotypes *in situ* where a spectrum of phenotypes is observed [142]. Stimulating with either LPS/IFNγ [159] [63] [160] [161], or IL-4/IL-13 [162] [163] [64] is a commonly used method of polarizing these macrophages into either of the two extremes. Addition of LPS along with IFNγ generates classical macrophages whereas addition of IL-4/IL-13 leads to alternative macrophages.

Since macrophages are important cells of the immune system and contribute to host survival and homeostasis [164], it is important to try and understand how the mTOR pathway affects macrophage differentiation, maturation and activation. There are many groups who have perturbed the pathway by inhibiting upstream negative (TSC1/2 complex) or positive regulators (RHEB) [89] [87] [88] [165] but little research has been done on specific proteins of the mTOR complexes in macrophages. It would be interesting to observe how mTORC1 regulates macrophages and how this regulation may affect their surroundings in regards to their polarisation. The main focus of the experiments in this chapter was to inhibit the mTOR pathway by removing the Raptor protein, part of mTORC1, which is known to assemble the complex together and promote downstream signalling required for cell growth and persistence, and observe effects on macrophage differentiation, maturation and activation.

3.2 Model

In order to understand mTORC1 and the influence of Raptor protein on differentiation, growth, and maturation of macrophages, an inducible *Cre/LoxP* mouse model was used under the *Csf1r* promoter on the C57Bl/6 genetic background. This allowed conditional knockout of the *Raptor* gene within myeloid compartments (Figure 3.1). *LoxP* sites flanked either side of exon 6 of the *Raptor* gene. Once tamoxifen was injected into the mice via the intraperitoneal route (I.P), *Cre*, under the control of the *Csf1r* promoter region, removed exon 6 from cells in the myeloid compartment. Components of the mTOR pathway are essential for embryonic survival therefore, constitutive *Raptor* KO mice are not viable and could not have been used [166].

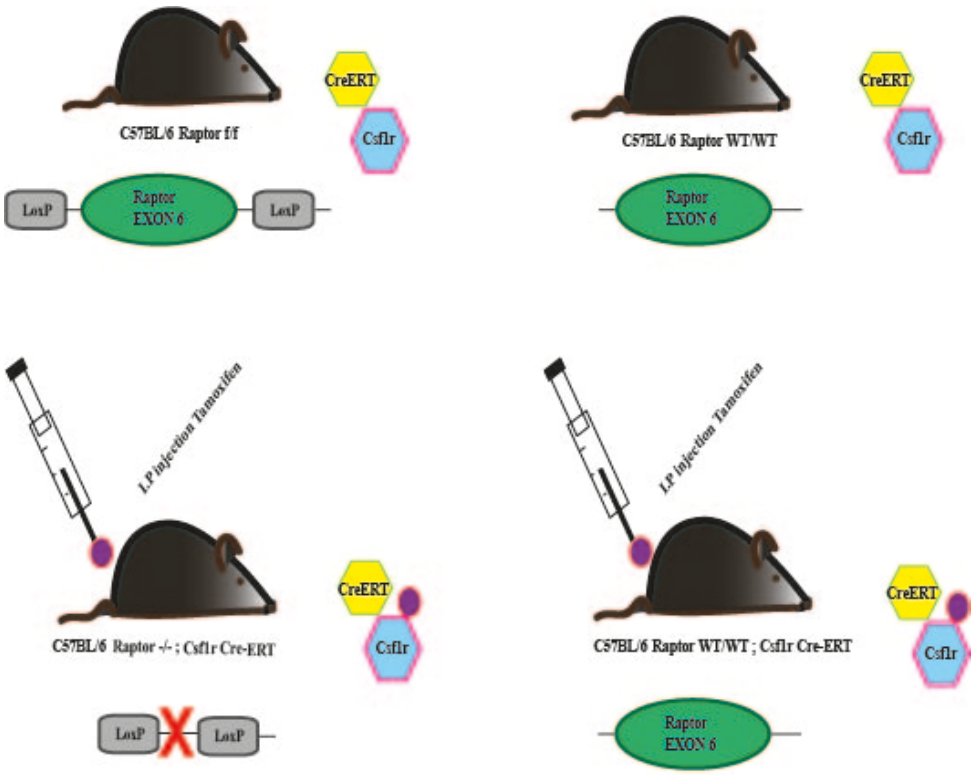

Figure 3.1 Mouse model for Raptor gene KO

An inducible model using the Cre/LoxP system that is under the control of the Csf1r promotor region. As tamoxifen is added exon 6 is removed within myeloid cell compartments.

3.3 Confirming Raptor KO in macrophages

It was essential to confirm that knockout, KO, of Raptor expression was achieved in myeloid cells before beginning any experiments. To test this inducible model I decided to assay for *Raptor* mRNA by qPCR. BMDMs from *Raptor WT/WT; Csf1r Cre-ERT* (WT) and *Raptor f/f; Csf1r Cre-ERT* (KO) were either left unstimulated (NS) or stimulated by either LPS/IFNγ or IL-4/IL-13 for 4 hrs (Figure 3.2A). Expression of *Raptor* from the KOs was markedly reduced in comparison to the WTs in all of the conditions. This shows that the inducible model accomplished a decrease in *Raptor* transcription and therefore lowers RNA levels of *Raptor* in the KOs. Results were taken as relative expression to the housekeeping gene *B2m,* a constitutive gene expressed in myeloid cells during normal or pathophysiological conditions (Figure 3.2A).

In order to validate this result, it was important to look at Raptor protein levels. I used WT and KO BMDMs; they were either left unstimulated (NS) or stimulated with LPS/IFNγ for 15, 30, 60, 120, and 180 minutes. Protein lysates were prepared, and immunoblotting was performed. A reduction in intensity of the bands appeared in the KO protein lysates signifying a decrease in expression of Raptor protein levels as compared to WT lysates, which showed stronger band intensities. Protein levels were compared to the loading control β-actin that had equal band intensities associated with equal protein loading (Figure 3.2B).

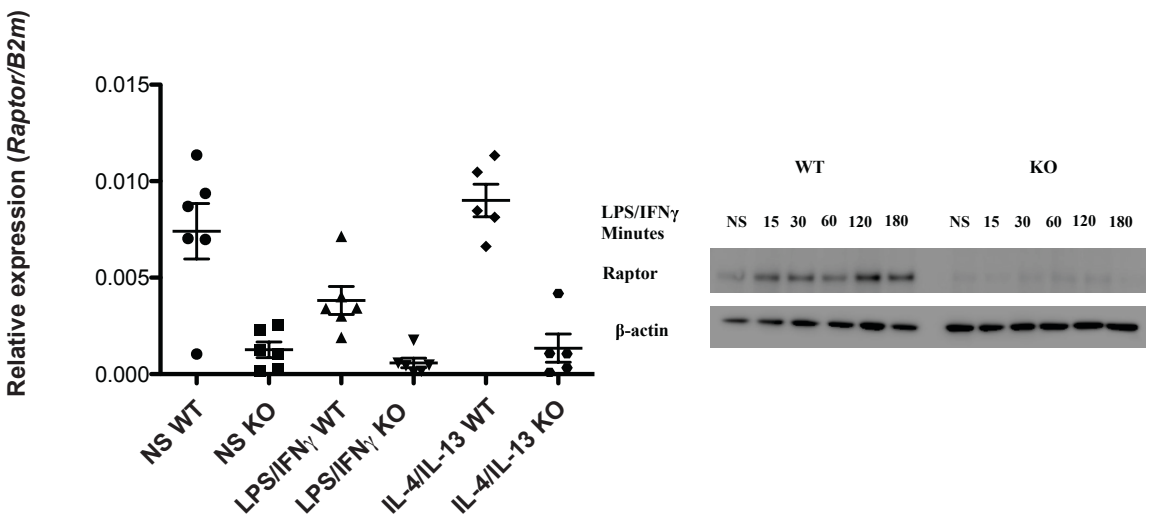

Figure 3.2 Confirmation of Raptor KO

qPCR was performed on BMDMs that were left unstimulated (NS) or stimulated either with LPS/IFNγ or IL-4/IL-13 for 4 hrs. Expression levels of Raptor were low in the KO as compared to WT (n=6), β2m was used as a house keeping gene (A). Western blot performed on BMDM lysates (NS, or LPS/IFNγ stimulated either for 15, 30, 60, 120 and 180 minutes). Immunoblot stained for Raptor showing diminished bands on BMDMs from KO, as compared to WT controls. Blot was also stained for β-actin a house keeping protein, showing protein level and loading on to gel was equal. This immunoblot in the Figure is representative of 3 independent experiments (BMDM lysates from 3 different mice) (B).

3.4 Does the absence of Raptor affect the common myeloid progenitor population?

The way macrophages develop is very important for their function. In order to answer the question of whether Raptor is important for macrophage differentiation and development I investigated the levels of common myeloid progenitors in the Raptor KO BMDMs. Hematopoietic stem cells (HSC) are self-renewing, multipotent progenitor cells from which differentiated cells in the bone marrow arise. Common progenitors are bone marrow stem cells that continually populate the niche with cells that give rise to either myeloid or lymphoid lineages [167] [168] [169]. Within the two lineages they separate into diverse cell types. Macrophages are produced from the myeloid lineage. HSCs and their differentiated progeny may be distinguished from one another through their expression of various cell surface lineage markers. To be able to distinguish between stem cells and differentiated cells I performed experiments using fluorescence activated cell sorting (FACS), on bone marrow cells (BM) at day 0 (cells taken directly after bone flushing)

and BMDMs from day 3 and day 7 maturation *in vitro* of WT and Raptor KOs (cultured in DMEM media). I incorporated a cell specific lineage marker cocktail of antibodies to identify the two populations. This cocktail (LIN; lineage), includes markers that are expressed on stem cells and will not be expressed on differentiated cells. Stem cells that express these surface markers were labelled LIN^+ while differentiated cells that do not express these markers were labelled LIN^-. Cells were gated on live cells and from that gate all the LIN^- cells were gated. From the LIN^- cell gate, it was important to focus on markers that were specific to the common myeloid progenitors hence combinations of these markers were used to gate on the referred cell types. These markers were: stem cells antigen 1 (Sca1) a common biological marker used to identify hematopoietic stem cells; CD117 (c-Kit), a cell surface marker used to identify hematopoietic cells in bone marrow; hematopoietic progenitor cell antigen (CD34), an adhesion molecule needed for progenitor cell migration, and Fc receptor (CD16/32) found on myeloid cells. (LIN^- Kit^+ Sca^- $CD34^+$ $CD16/32^{mid}$). The results show no significant differences within the common myeloid progenitor population in absence of Raptor either when harvested or during culture (Figure 3.3).

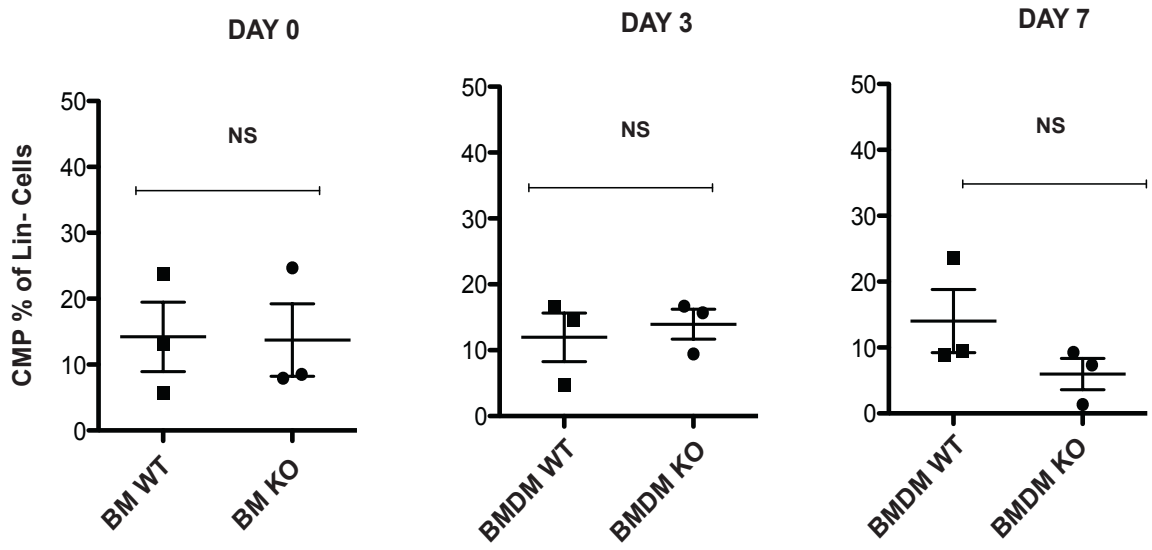

Figure 3.3 Percentage of common myeloid progenitor (CMP) populations based on LIN- cells.

No difference observed in common myeloid progenitor populations of KOs on day 0 (BM), day 3 and day 7 BMDMs as compared to WTs (n=3). Student's t-test was used to check for statistical significance: NS= non- significant.

3.5 Does the absence of Raptor affect macrophage phenotype?

Macrophages from bone marrow (BM) day 0, and BMDMs from day 3 and day 7 culture of Raptor WT and Raptor KO, were quantified using FACS to look for any differences in their survival and maturation [170] [171] [172]. There was no significant difference between the KO and WT macrophages. The markers used were: $CD45^{+}CD11b^{+}$ $F480^{+}$ (Figure 3.4). CD45 is a cell surface marker expressed on all lymphoid and myeloid cells, while CD11b is expressed on cell surfaces of myeloid cells and F480 is a specific marker for macrophages.

It was reassuring to observe that as the quantity of the common myeloid progenitors decreased with time (as shown in Figure 3.4), the amount of macrophages ($F480^{+}$) increased. This means that as these myeloid progenitors are maturing with time; they are losing a progenitor phenotype while gaining a mature one instead.

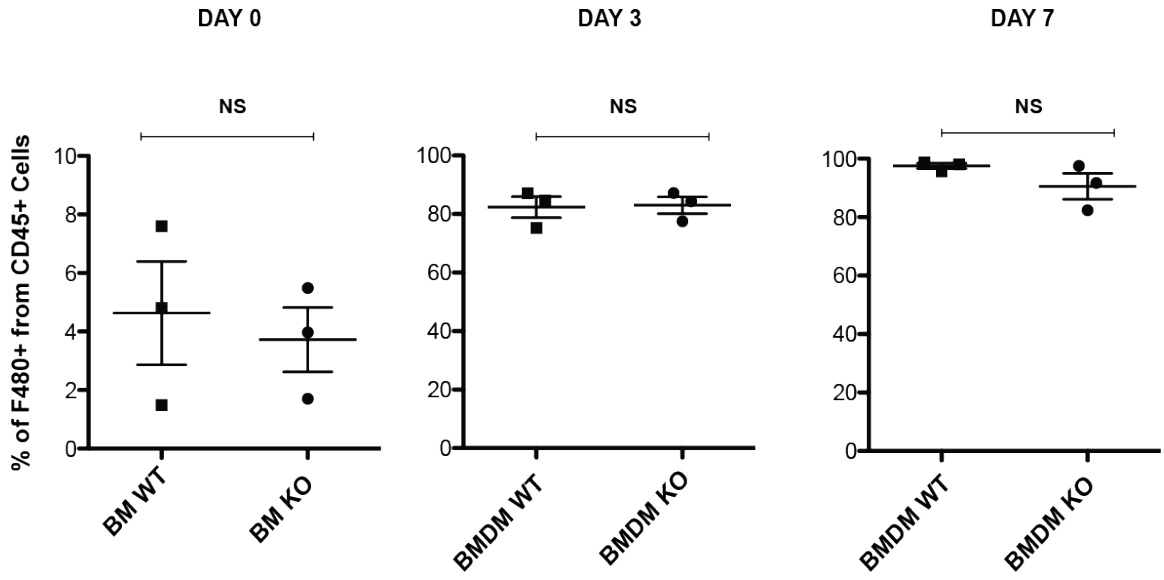

Figure 3.4 Macrophage populations in BM and harvested BMDMs

There is no significant difference between the macrophage populations in Raptor KO as compared to Raptor WT controls in BM or on day 3 and day 7 of BMDM maturation (n=3). Student's t-test was used to check for statistical significance: NS= non-significant.

3.6 Does the absence of Raptor generate a more proinflammatory macrophage phenotype?

It is reported that a disruption or loss of mTORC1 signalling leads to an overall increase in inflammation [89]. In order to study this with RAPTOR KO in myeloid cells, the levels of mRNA expression of genes associated with inflammation were studied by qPCR. I stimulated WT and KO BMDMs with either LPS/IFNγ or IL-4/IL-13 and assessed at six time points (2, 4, 6, 12, 22, and 30 hrs). Time points I chose for these experiments were based on different optimization trials that I tried in order to obtain a full scope of gene transcription patterns. The genes that were chosen to represent inflammatory or immunomodulatory genes have all been well established in literature. They are used when investigating inflammation and cellular homeostasis and are usually categorized as being either M1 or M2 genes. The M1 genes used were *TNFα*, *Il-12b*, *NOS2, Il-6* [173]. The M2 genes were *Il-10 and Mrc1* [174] [175].

As well as mRNA assays I used ELISAs to measure protein levels for most of the cytokines, TNFα, IL-12b, IL-6, IL-10, and FACS for iNOS, and Mrc1 (CD206), to quantify protein levels of inflammatory modulators.

3.6.1 TNFα

Relative expression of *TNFα* for KO BMDMs was significantly higher than WT BMDMs at 2, 12 and 30 hrs of stimulation with LPS/IFNγ. For the rest of the time points (4, 6, and 22 hrs) *TNFα* expression showed no difference. *B2m* was used as a house keeping gene (Figure 3.5). Moreover, levels of secreted protein showed a similar trend, there was no difference in secretion apart from 30 hrs of LPS/IFNγ stimulation where it was more in the KOs as compared to the WTs. Unstimulated BMDMs were used to assess basal levels and showed no expression. (Figure 3.6).

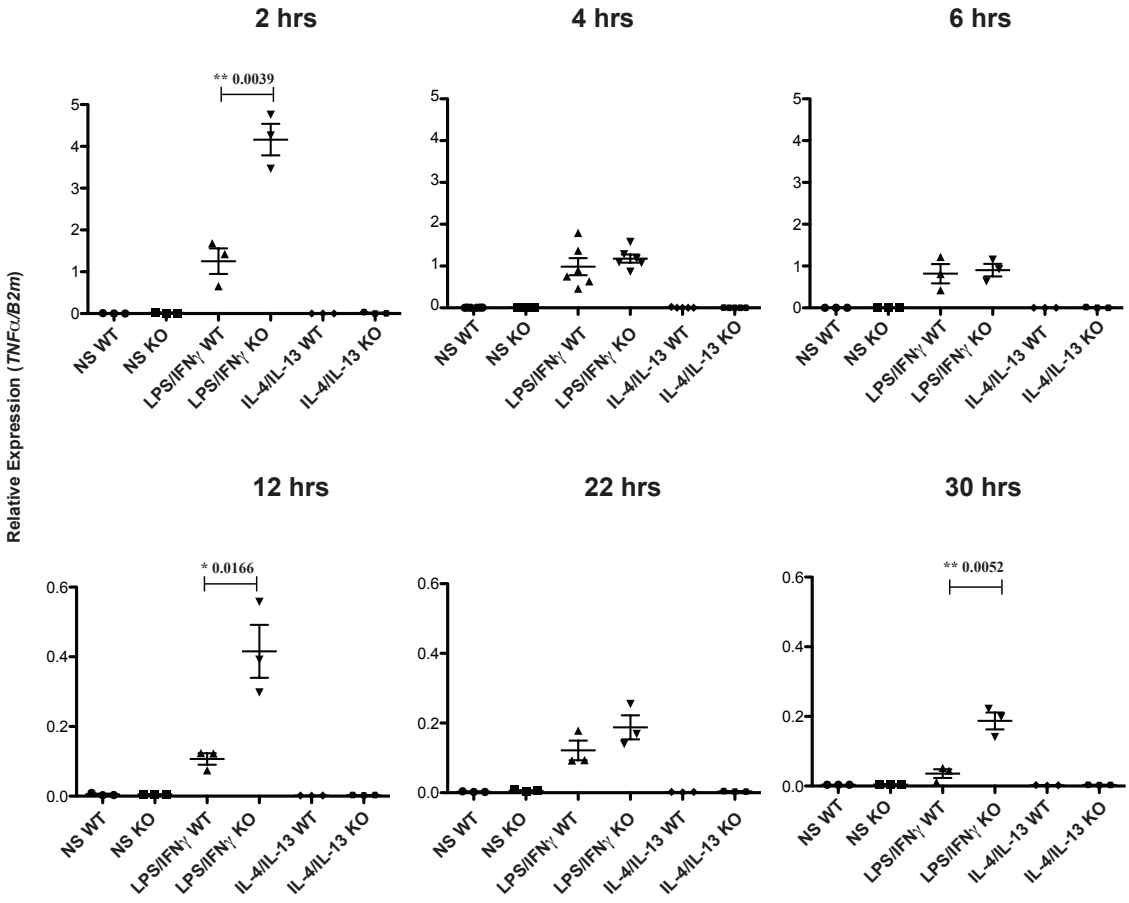

Figure 3.5 Relative expression of TNFα

qPCR analysis of TNFα mRNA levels from WT and Raptor KO BMDMs stimulated with 100ng/ml of LPS and 20ng/ml of IFNγ, showing a significantly higher expression in KO BMDMs stimulated with LPS/IFNγ for 2, 12 and 30 hrs. BMDMs were also stimulated with 10ng/ml of both IL-4 and IL-13 but no TNFα was induced in this group or the NS group. Relative expression was taken as expression against β2m (a house keeping gene). Time points 2, 6, 12, 22, and 30 hrs (n=3) ; time point 4hrs (n=6). Student's t-test was used for statistical significance: p-value of <0.05 is statistically significant (*) or <0.005(**).

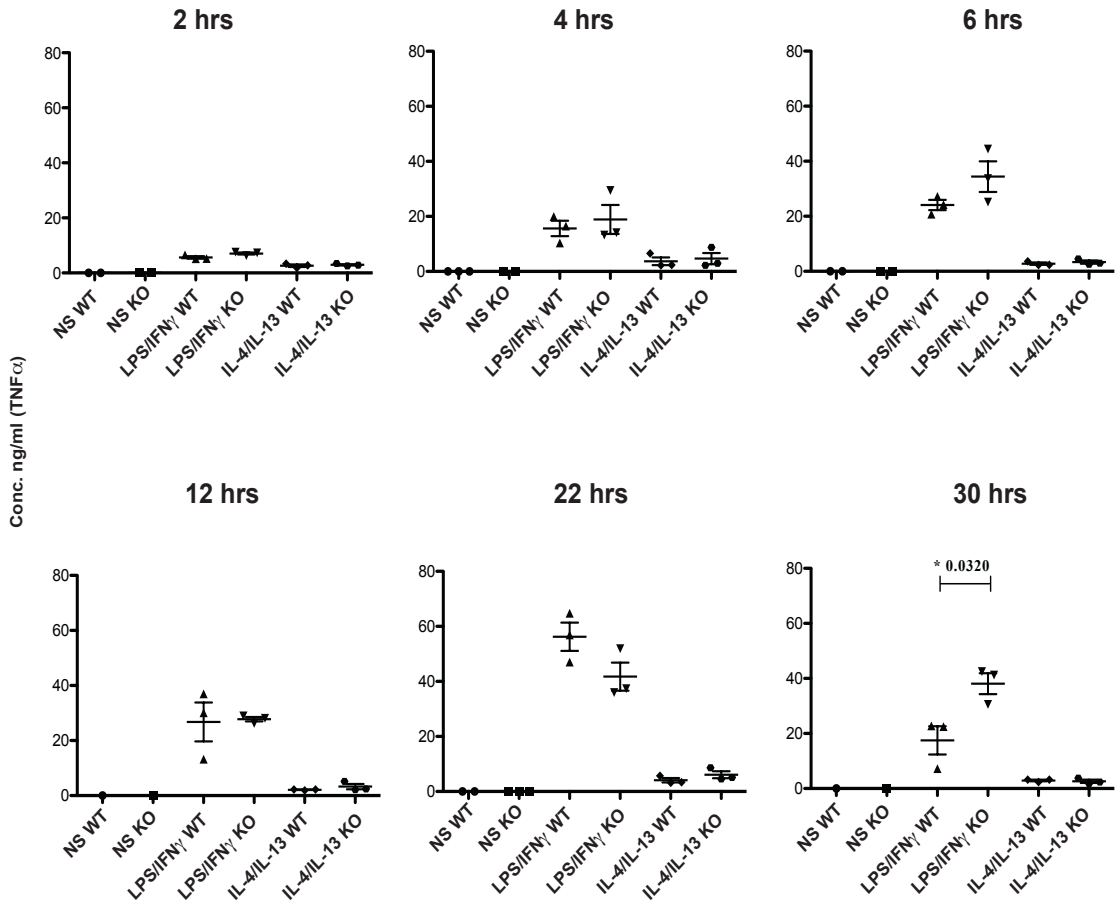

Figure 3.5 TNFα cytokine secretion

Protein level analysis was performed on supernatant of BMDMs from WT and Raptor KO BMDMs stimulated with 100ng/ml of LPS and 20ng/ml of IFNγ, showing a significant increase in secretion of TNFα in KOs stimulated with LPS/IFNγ at 30 hrs compared to WT. LPS/IFNγ stimulation at other time points shows no difference in TNFα protein secretion for either WT or KOs. BMDMs were also stimulated with 10ng/ml of both IL-4 and IL-13 but minimal levels of TNFα were induced. All time points n=3. Student's t-test was used to check for statistical significance: p-value of <0.05 is statistically significant (*).

3.6.2 IL-12β

There was a significantly higher relative expression of *Il-12*β mRNA in Raptor KO BMDMs compared with WT BMDMs after 4, 12 and 30 hrs stimulation with LPS/IFNγ. While at 2 and 6 hrs there was no difference in expression of *Il-12*β mRNA in Raptor KO BMDMs stimulated with LPS/IFNγ compared with WT BMDMs (Figure 3.7). However, protein levels show different results than those seen on mRNA levels. During 4 and 12 hrs stimulation with LPS/IFNγ there is a significant increase in IL-12 (p40) secretion in WT BMDMs as compared to the Raptor KOs. The rest of the time points show no difference once BMDMs were stimulated with LPS/IFNγ between WT BMDMs compared to KO BMDMs (Figure 3.8).

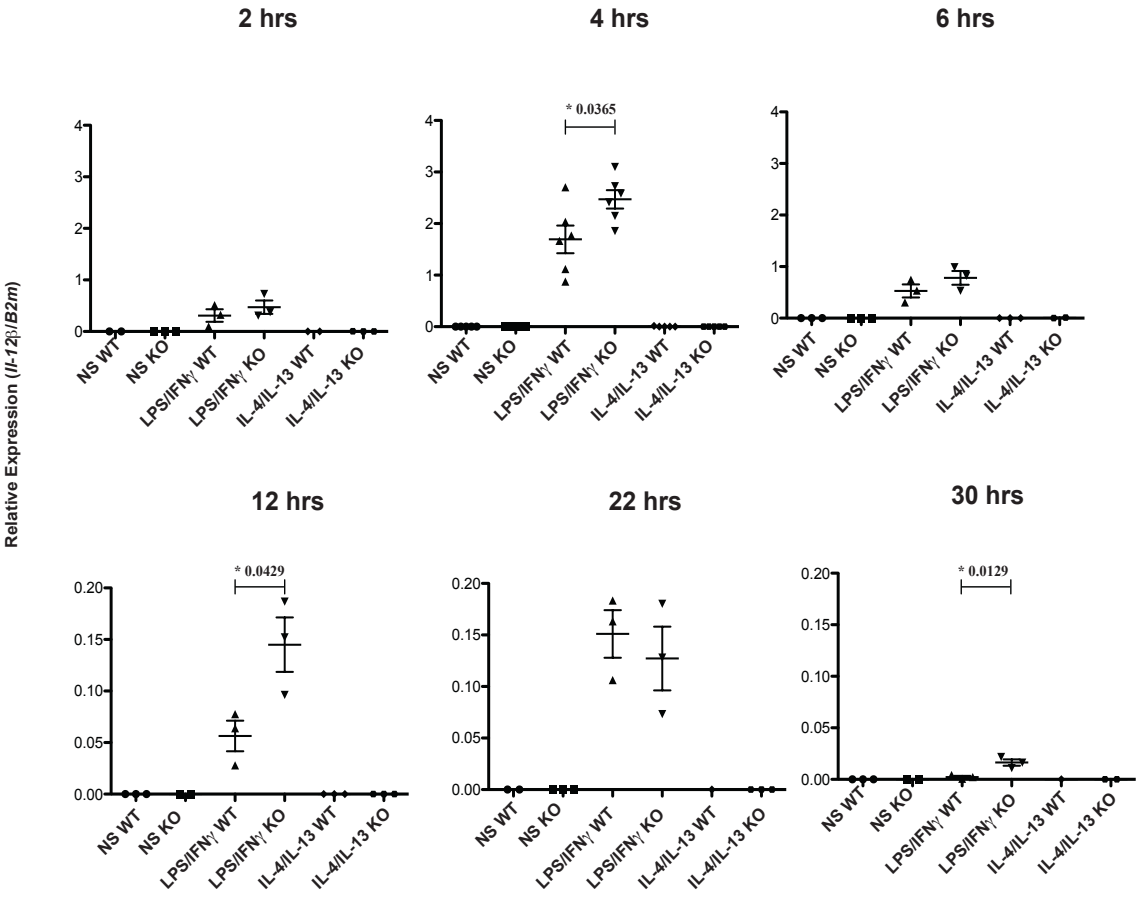

Figure 3.6 Relative expression of IL-12β

qPCR analysis of mRNA levels for IL-12β from WT or Raptor KO BMDMs stimulated with 100ng/ml of LPS and 20ng/ml of IFNγ, showing a significantly higher expression of IL-12β in KOs stimulated with LPS/IFNγ for 4, 12 and 30 hrs. LPS/IFNγ stimulation for rest of the time points shows no difference in expression of IL-12β in KOs compared to WT BMDMs. BMDMs were also stimulated with 10ng/ml of both IL-4 and IL-13 but no IL-12β mRNA could be detected. Relative expression was taken as expression against β2m (a house keeping gene). Time points 2, 6, 12, 22, and 30 hrs (n=3 ; time point 4hrs (n=6). Student's t-test was used to check for statistical significance: p-value of <0.05 is statistically significant (*).

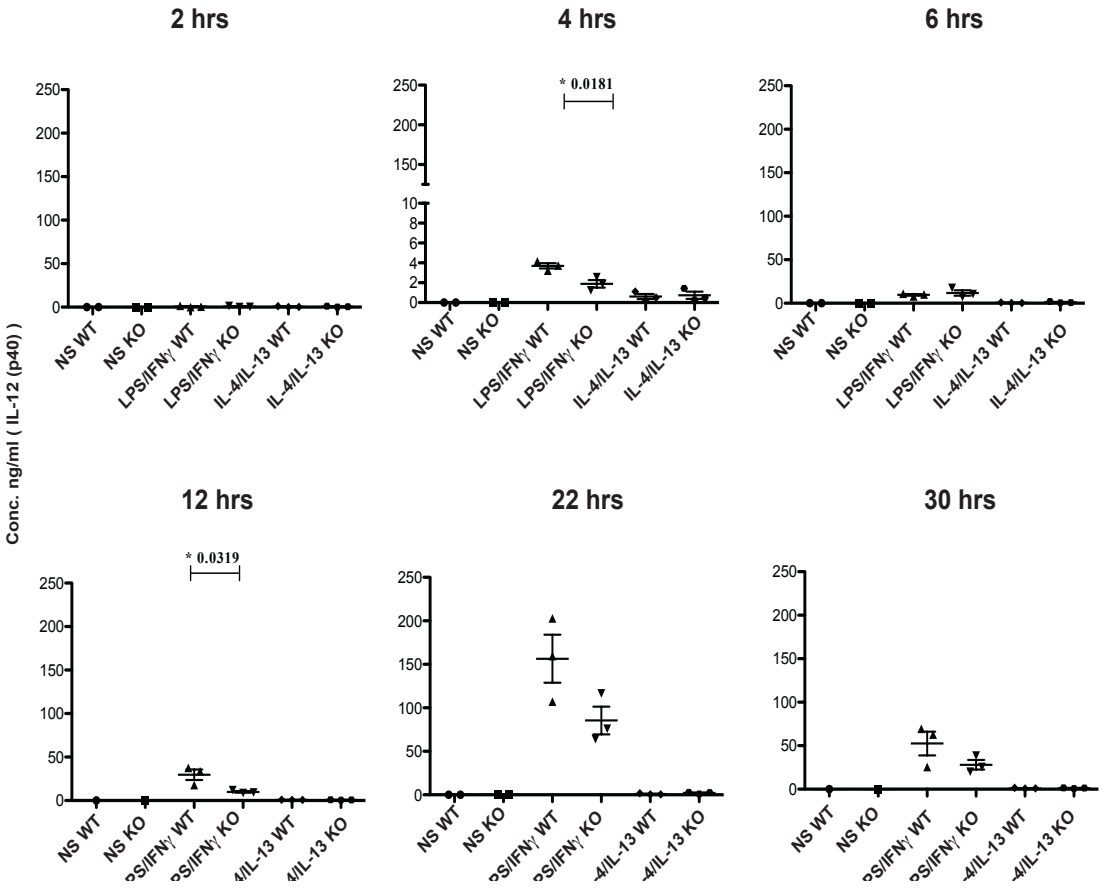

Figure 3.7 IL-12(p40) cytokine secretion

Protein level analysis was performed using supernatants from WT or Raptor KO BMDMs stimulated with 100ng/ml of LPS and 20ng/ml of IFNγ, showing a significant increase in secretion of WTs at 4, and 12 hrs. LPS/IFNγ stimulation at other time points shows no difference of protein secretion for WTs compared to KOs. BMDMs were also stimulated with 10ng/ml of both IL-4 and IL-13, which showed no secretion. All time points (n=3). Student's t-test was used to check for statistical significance: p-value of <0.05 is statistically significant (*).

3.6.3 IL-6

There was significantly higher expression of *Il-6* in Raptor KO BMDMs at 12 and 30 hrs stimulation with LPS/IFNγ as compared to WTs. The increase was evident at later time points as compared to other cytokines studied, which may be due to the fact that it takes *Il-6* longer time to be transcribed. At the rest of the time points there was no difference in *Il-6* expression in the Raptor KOs as compared to the WT controls (Figure 3.9). IL-6 protein secretion was also significantly different after LPS/IFNγ stimulation at 6 and 22 hrs, but it increases for WTs as opposed to the KOs (Figure 3.10).

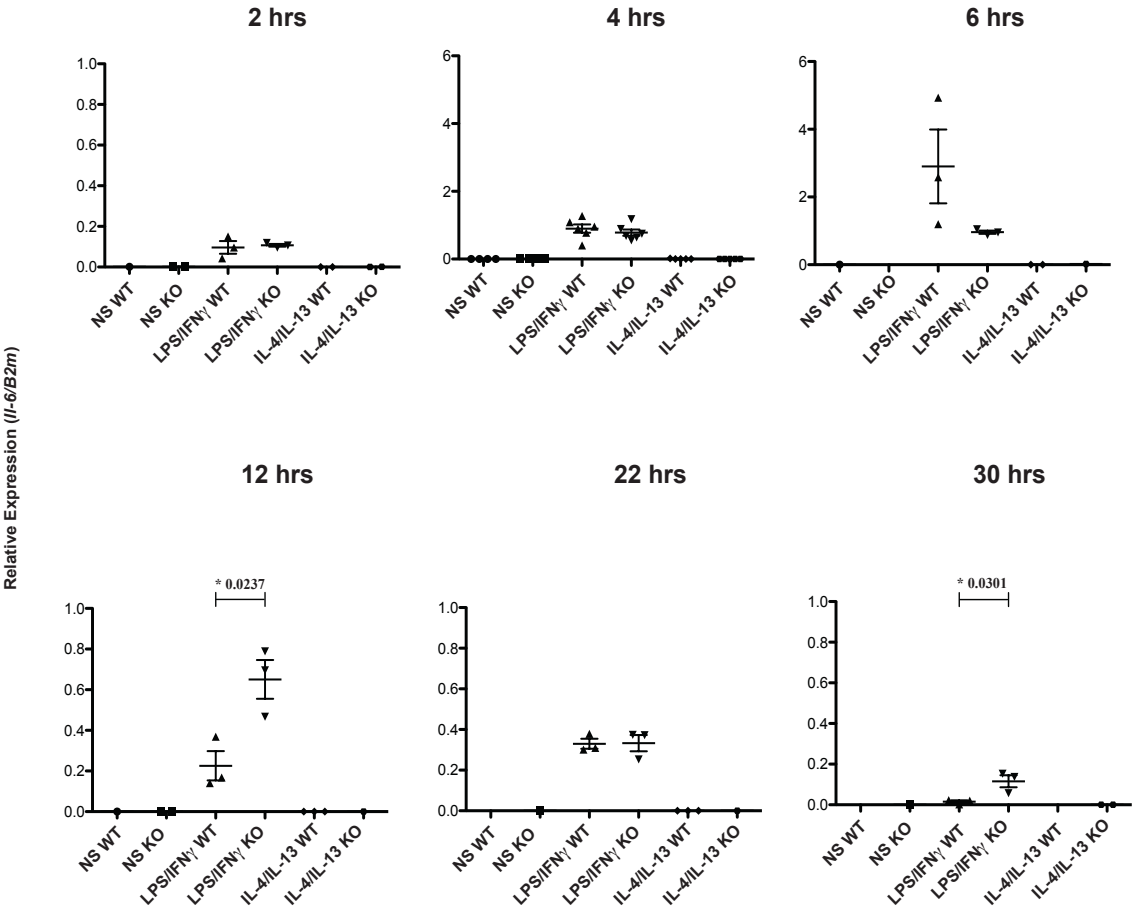

Figure 3.8 Relative expression of Il-6

qPCR analysis of mRNA levels from BMDMs of WT and Raptor KOs stimulated with 100ng/ml of LPS and 20ng/ml of IFNγ, showing a significant increase in expression of KOs stimulated at 12 and 30 hrs. LPS/IFNγ stimulation at other time points shows no difference in expression of KOs compared to WTs. BMDMs were also stimulated with 10ng/ml of both IL-4 and IL-13, which showed no expression. Relative expression was taken as expression against β2m (a housekeeping gene). Time point 2, 6, 12, 22, and 30 hrs (n=3) ; time point 4 hrs (n=6). Student's t-test was used to check for statistical significance p-value of <0.05 is statistically significant (*).

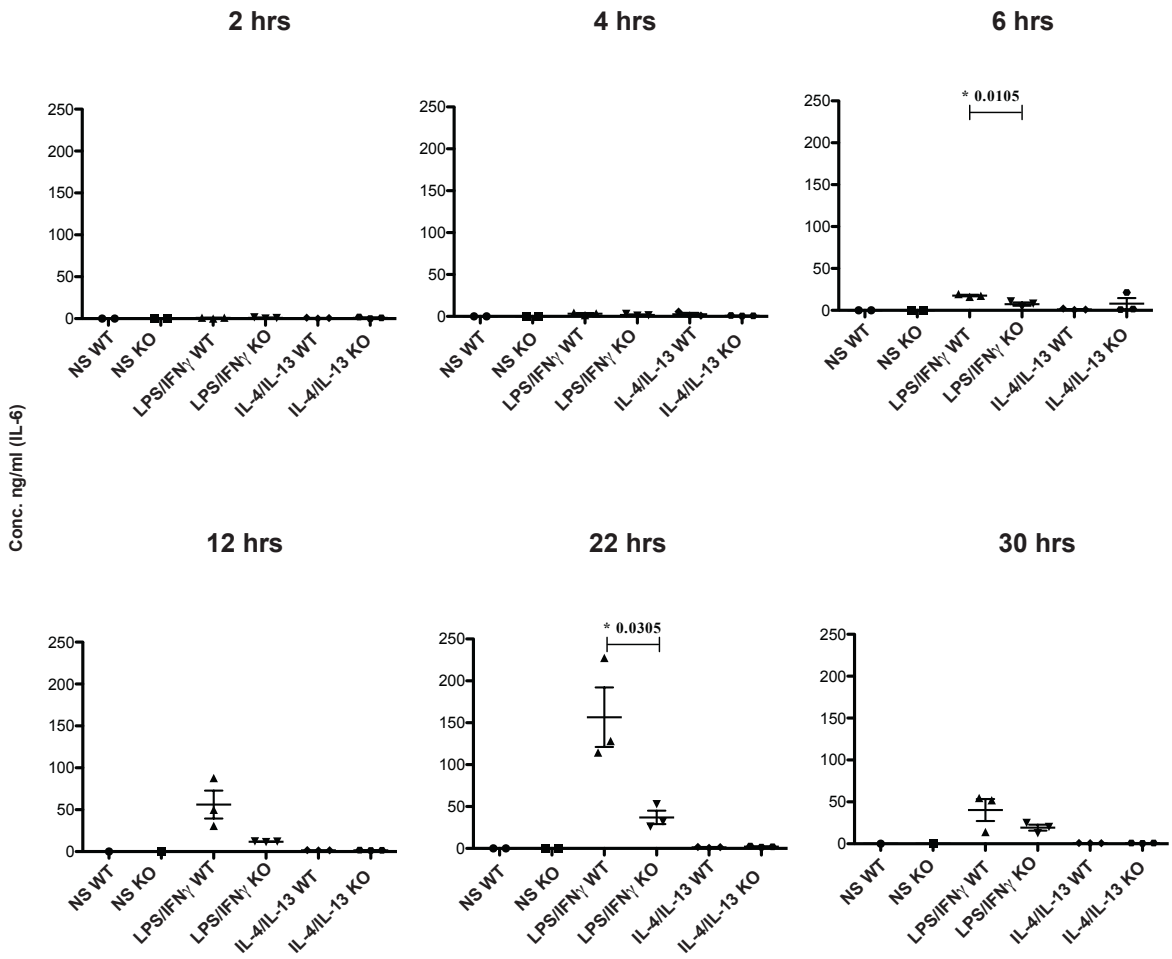

Figure 3.9 IL-6 cytokine secretion

Protein level analysis was performed on supernatants from BMDMs of WT and Raptor KOs stimulated with 100ng/ml of LPS and 20ng/ml of IFNγ, showing a significant increase in secretion of IL-6 in WTs stimulated at 6 and 22 hrs. LPS/IFNγ stimulation at other time points shows no difference in secretion for WTs as compared to KOs. BMDMs were also stimulated with 10ng/ml of both IL-4 and IL-13, which showed no secretion. All time points (n=3). Student's t-test was used to check for statistical significance p-value of <0.05 is statistically significant (*).

3.6.4 iNOS

There was no significant difference in the relative expression of *Nos2* between WT and Raptor KO BMDMs (Figure 3.11). Protein analysis was also performed using FACS. BMDMs were stimulated with LPS/IFNγ for 6 hrs, iNOS protein expression shows no difference in BMDMs stimulated with LPS/IFNγ either from WTs or Kos. Unstimulated BMDMs show expression of iNOS at basal levels. Isotype was used as a negative control, confirming minimal expression in BMDMs of both WT and KO (Figure 3.12).

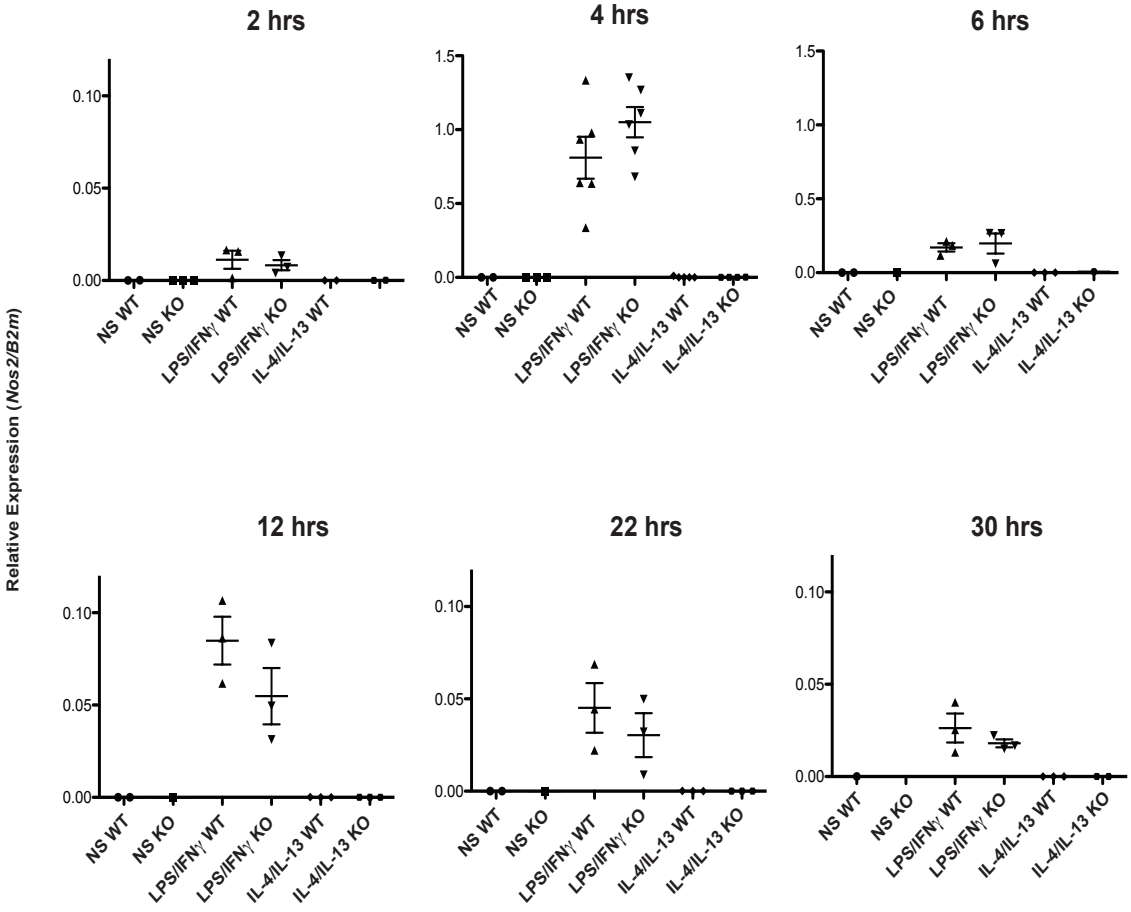

Figure 3.10 Relative expression of Nos2

qPCR analysis of mRNA levels from BMDMs of WT and Raptor KOs stimulated with 100ng/ml of LPS and 20ng/ml of IFNγ, showing no significant difference in expression of WTs compared to KOs. BMDMs were also stimulated with 10ng/ml of both IL-4 and IL-13, which showed no expression. Relative expression was taken as expression against β2m (a house keeping gene). Time points 2, 6, 12, 22, and 30 hrs (n=3); time point 4 hrs (n=6). Student's t-test was used to check for statistical significance.

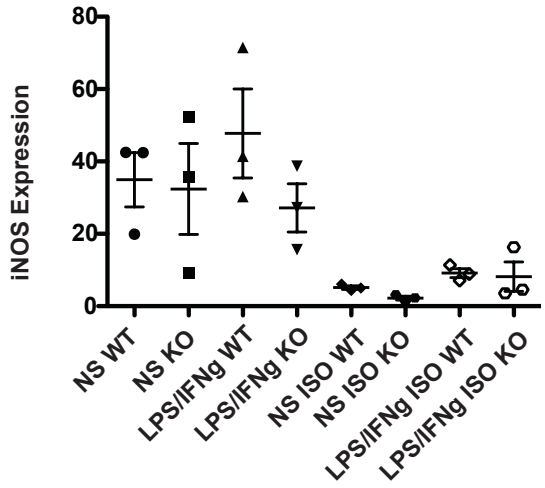

Figure 3.11 Expression of iNOS

Protein level analysis was performed using FACS on BMDMs of WT and Raptor KOs stimulated with 100ng/ml of LPS and 20ng/ml of IFNγ, showing no significant difference between WT and KO stimulated with LPS/IFNγ. Non stimulated levels had basal expression of iNos without having statistical significance. Isotype was used as a negative control (n=3). Student's t-test was used to check for statistical significance.

3.6.5 IL-10

There was a significantly higher expression shown for WT BMDMs at 4 hrs of stimulation with LPS/IFNγ. IL-10 is known as an anti-inflammatory cytokine; its expression increases once stimulated with IL-4/IL-13. In view of the results observed it opposes what has been established in literature since it increases once stimulated with LPS/IFNγ [89] [87]. Later time points show no *Il-10* expression; this is comparable to the NS BMDMs (Figure 3.13). At the protein level IL-10 is produced and secreted at differing levels in WTs and KO BMDMs but showed no difference between BMDMs from WT or KO once stimulated with LPS/IFNγ or IL-4/IL-13 (Figure 3.14).

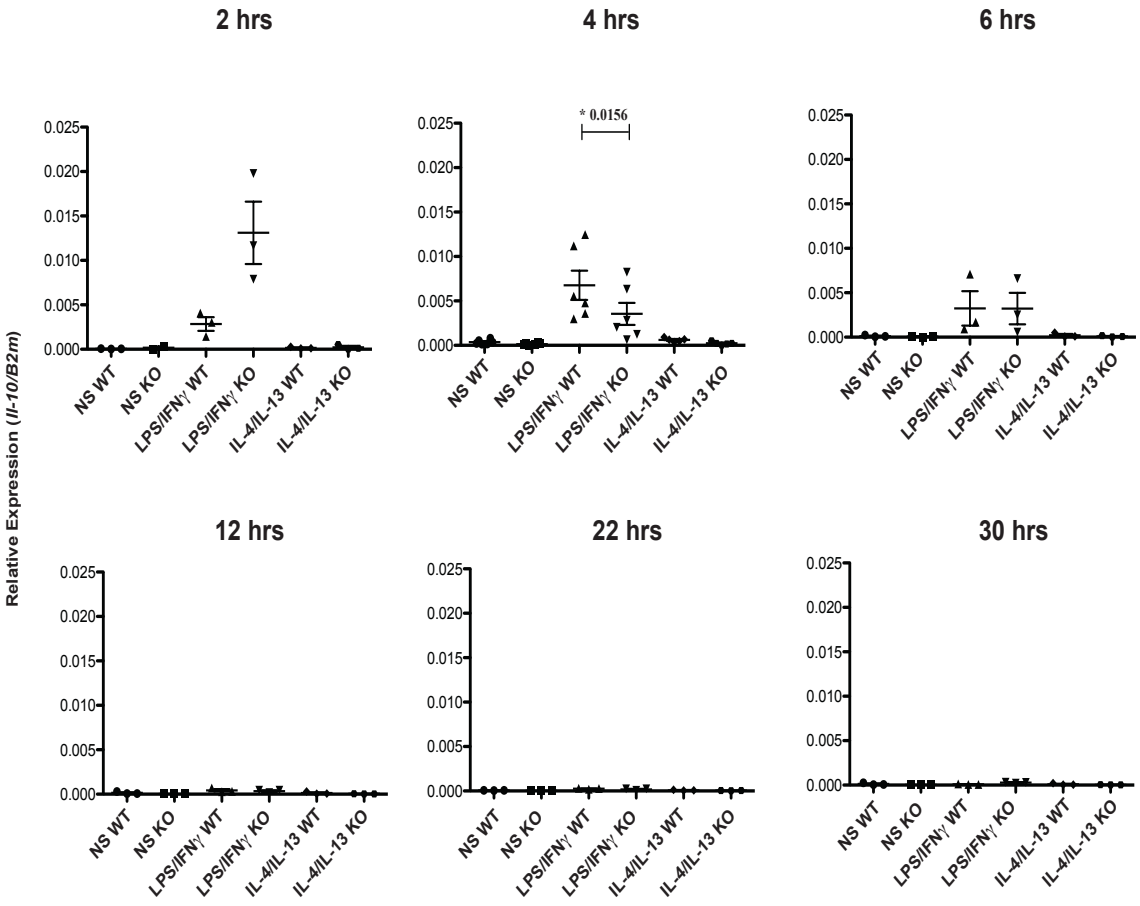

Figure 3.12 Relative expression of Il-10

qPCR analysis of mRNA levels from BMDMs of WT and Raptor KOs stimulated with 100ng/ml of LPS and 20ng/ml of IFNγ,showing a significant increase in expression of WTs stimulated at 4 hrs. BMDMs were also stimulated with 10ng/ml of both IL-4 and IL-13, which showed no expression. Relative expression was taken as expression against β2m (a housekeeping gene). Time point 2, 6, 12, 22, and 30 hrs (n=3) and time point 4 hrs (n=6). Student's t-test was used to check for statistical significance: p-value of <0.05 is statistically significant (*).

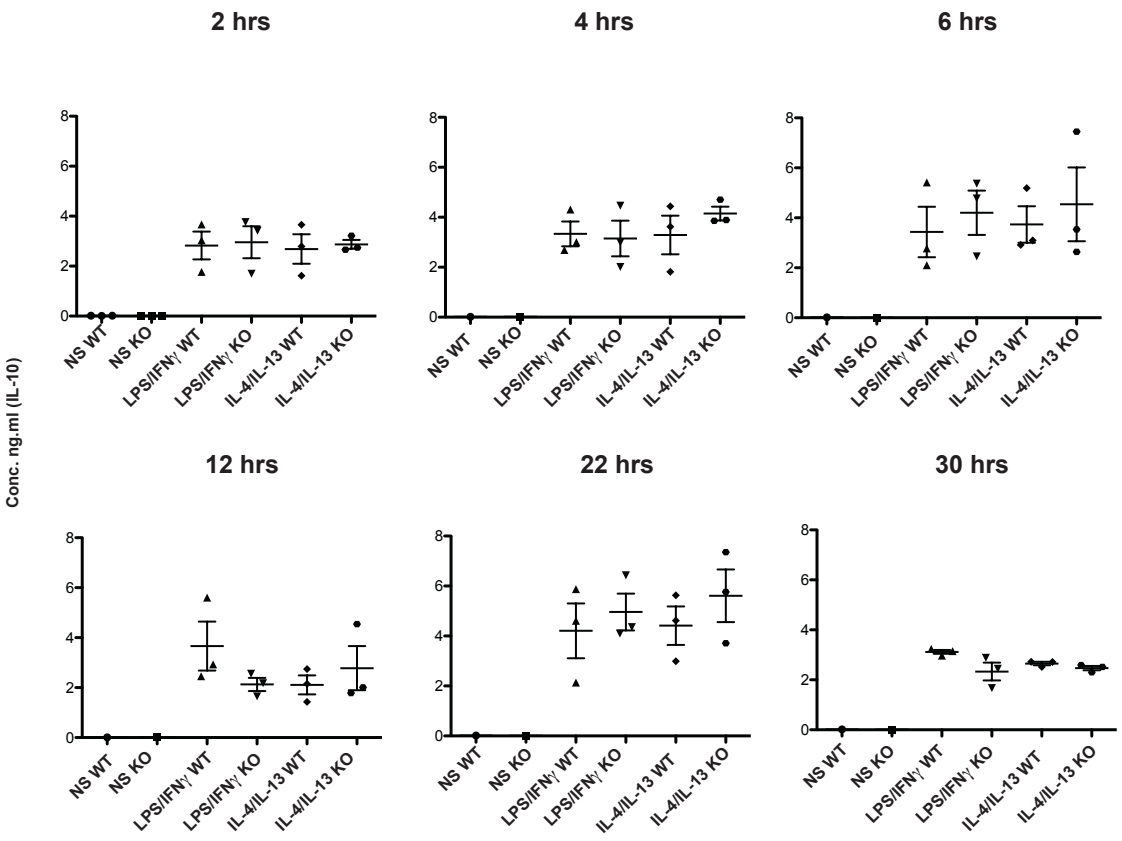

Figure 3.13 IL-10 cytokine secretion

Protein level analysis was performed from supernatant of BMDMs of WT and Raptor KOs stimulated with 100ng/ml of LPS and 20ng/ml of IFNγ, showing no significant increases in secretion of either WTs or KOs stimulated with LPS/IFNγ. BMDMs were also stimulated with 10ng/ml of both IL-4 and IL-13, which showed no significant cytokine secretion at differing time pointss. N=3 for all time points. Student's t-test was used to check for statistical significance.

3.6.6 MRC1

There was no significant difference in relative expression of *MRC1* in either WT or Raptor KO BMDMs at 4, 12, 22, and 30 hrs upon stimulation with IL-4/IL-13. At 2 and 6 hrs the *MRC1* levels were below detection. *MRC1* mRNA expression was observed at basal levels in both WT and KO BMDMs at 4, 12, 22, and 30 hrs (Figure 3.15). Data for protein levels shows, there is a significant decrease in MRC1 levels of Raptor KOs in comparison to WT, during basal levels (Figure 3.16).

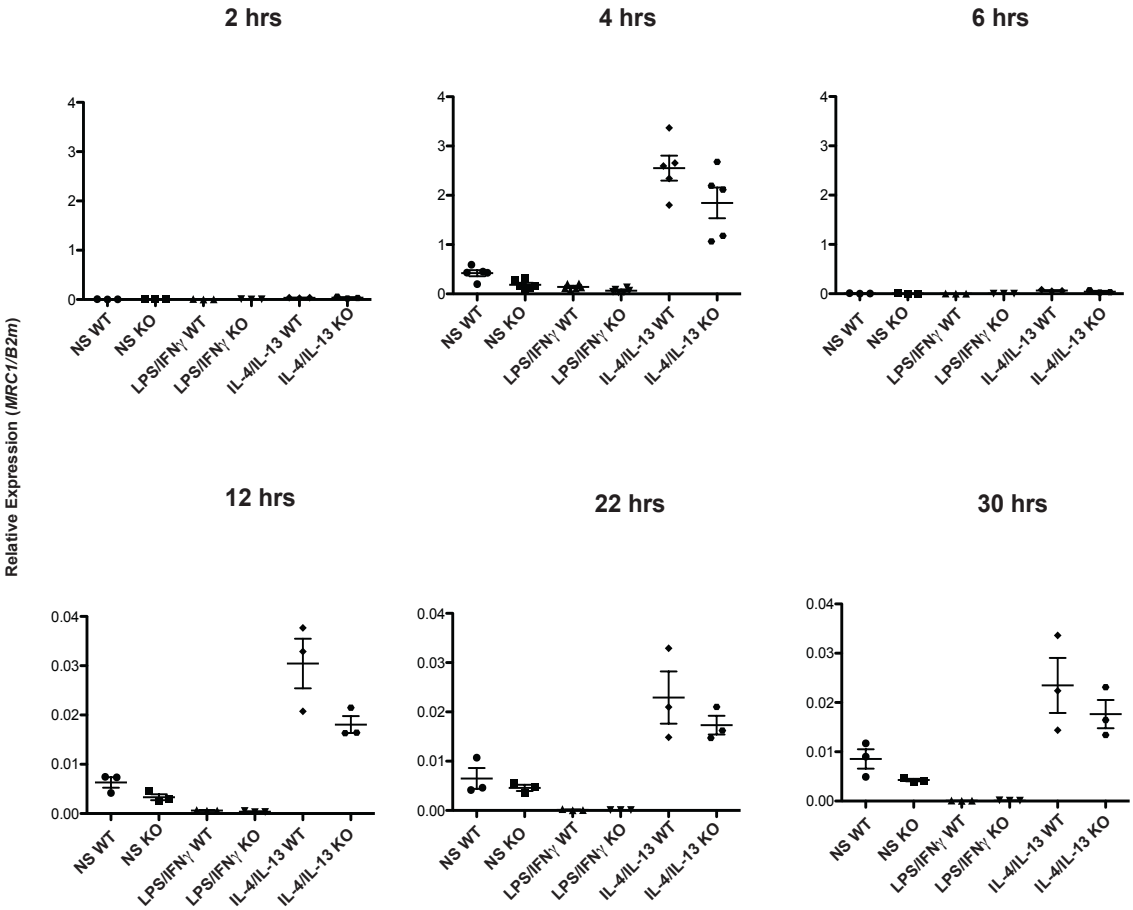

Figure 3.14 Relative expression of MRC1

qPCR analysis of mRNA levels from BMDMs of WT and Raptor KO stimulated with 100ng/ml of LPS and 20ng/ml of IFNγ, showing minimal expression levels. BMDMs stimulated with 10ng/ml of both IL-4 and IL-13 showed no difference in expression with WTs as compared to KOs at all time points. Non stimulated BMDMs also showed minimal expression at 4, 12, 22, and 30 hrs for both WT and KOs. Relative expression was taken as expression against β2m (a house keeping gene). Time point 2, 6, 12, 22, and 30 hrs (n=3) and time point 4 hrs (n=6). Student's t-test was used to check for statistical significance.

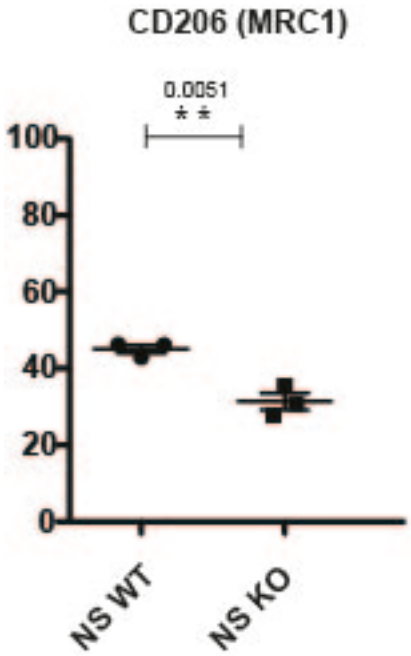

Figure 3.15 Expression of MRC1 (CD206)

Protein level analysis was performed using FACS on BMDMs of WT and Raptor KOs showed a significant decrease in secretion at basal levels of KO BMDMs as compared to WTs (n=3). Student's t-test was used to check for statistical significance: p-value of <0.005 (**) is statistically significant.

3.7 Summary of results from this chapter.

In the Tables below I have summarized the significant differences between WT and Raptor KO BMDMs in terms of inflammatory mediator expression after LPS/IFNγ or IL-4/IL13 stimulation *in vitro*.

RNA	2 hrs	4 hrs	6 hrs	12 hrs	22 hrs	30 hrs
WT		*Il-10*				
KO	*TNFα*	*Il-12β*		*TNFα*		*TNFα*
				Il-12β		*Il-12β*
				Il-6		*Il-6*

Table 3.1 Summary of significant differences between WT and Raptor KO BMDMs in terms of cytokine mRNA expressions after LPS/IFNγ stimulation (qPCR analysis).

PROTEIN	2 hrs	4 hrs	6 hrs	12 hrs	22 hrs	30 hrs
WT		IL-12β	IL-6 MRC1	IL-12β	IL-6	
KO						TNFα

Table 3.2 Summary of significant differences between WT and Raptor KO BMDMs in terms of cytokine protein secretion after LPS/IFNγ stimulation (ELISA and FACS analysis)

The Tables above show significant increases in either cytokine mRNA expressions or secretions which are comparisons obtained between the WT and KO BMDMs.

3.8 Discussion

The mTOR pathway is a major regulator of cell metabolism, growth, proliferation and survival. It also regulates critical processes such as cytoskeletal organization, ribosomal biogenesis, transcription, and protein synthesis [176] [177] [178]. In this chapter I have investigated the influence that mTORC1 has on macrophage maturation, growth and differentiation using BMDMs in which Raptor, a major component of the mTORC1 complex was deleted. The *Raptor* gene was removed using an inducible genetic mouse model. I found that deletion of Raptor did not have any significant effect in macrophage differentiation or maturation *in vitro*; the common myeloid progenitor populations of both WT and KOs had similar percentages on varying days of differentiation and growth. This also is evident for macrophage maturation in both WT and KOs as the frequency of F480 positive cells on different maturational stages was comparable. It was shown in literature that when RHEB, a protein upstream of mTORC1 and a positive regulator, is removed, macrophage differentiation is impaired when a conditional deletion mouse model was used in which *Rheb* was deleted [179]. The monocyte-macrophage differentiation was examined showing a decrease in the amount of differentiated cells in the KO as compared to WT controls. The reason for this discrepancy may be the fact that RHEB is a positive regulator of the mTORC1 pathway, which interacts with Raptor [180], therefore any impairment to this protein might have a more potent effect than deleting a component of the complex itself.

In order to assess the role Raptor has on macrophage polarization, I studied inflammatory gene expression and cytokine secretion after *in vitro* stimulation. Results from *TNFα* are

in line with findings from literature [64], which showed an increase in *TNFα* expression and secretion once stimulated with LPS/IFNγ. It also showed that removal of Raptor increased *TNFα* and was significantly higher in most time points that I investigated for both mRNA and at the longest time point for protein levels. It was reassuring to see that there was no change in expression from either NS or IL-4/IL-13 stimulated BMDMs whether they were KOs or controls. This is due to the fact that TNF*α* is a pro-inflammatory cytokine and is known to increase upon addition of LPS/IFNγ.

Results for *IL-12b* show higher mRNA expression in KOs as compared to WTs that is in agreement with literature [89] [181]. Although IL-12(p40) secretion is inconsistent with literature as I have demonstrated that secretion is more in WT BMDMs in comparison to KOs, while literature showed that KOs secreted more IL-12(p40). This result may be due to Raptor absence affecting protein translation and therefore secretion of IL-12(p40).

Levels of *Nos2* mRNA expression along with protein expression showed no significant differences between WT and Raptor KOs. Literature shows that when rapamycin was used to inhibit the mTORC1 pathway in astrocytes it was found to decrease *Nos2* mRNA levels and stability [182].

My results for *IL-6* showed a significantly higher expression at 12 and 30 hrs LPS/IFNγ stimulation for KOs as compared to WTs on mRNA level, which is in line with literature [89] Weichhart et al, have shown that inhibition of mTORC1 leads to an increase in IL-6 production.

Moreover, in literature it was shown that addition of rapamycin decreased expression of anti -inflammatory cytokines such as IL-10 [183], which I was able to show in RNA levels at 4 hrs of stimulation. I also observed that stimulation with IL-4/IL-13 did not lead to IL-10 mRNA expression of either WT or Raptor KO BMDMs which was unexpected, and it is not clear what is the cause, even though it is observed in secreted levels (the same BMDMs were used to assess mRNA and protein levels). It has been shown that inhibiting mTORC1 leads to a decrease in MRC1 expression in bone marrow derived dendritic cells. My results showed similar mRNA expression between WT and Raptor KO BMDMs, while there was a significant decrease in protein expression at basal levels of KO BMDMs in comparison to the WTs [184].

In regards to the results that I have observed, much of the data is in line with literature when other elements of the mTOR pathway have been inhibited in myeloid cells. Though there are a few contradictions, these contradictions should be considered unique to my model as it was interesting to see that inhibiting mTORC1 either pharmacologically or genetically may have different effects for example when Raptor was absent in comparison to RHEB absence, or usage of mTOR inhibitors such as rapamycin instead of inhibition through Raptor deletion. As it was mentioned earlier it may be due to the different impacts these inhibitions may have on particular components of this complex and thereby the activation of mTORC1. It was also interesting to see that for many of the cytokines there was an oscillating rhythm as to how they were expressed on mRNA levels as some peak at certain hours and lose expression in following hours and peak again at later timepoints. The differences observed between mRNA and protein levels were also unexpected, but again it may be because Raptor plays a major role in protein translation and in its absence, the cell may still have the transcription occurring but translation is impaired. Nevertheless, a more focused investigation on BMDM intracellular signalling in Raptor WT and Raptor KOs may be a useful addition to these studies. Signalling may shed light on the mechanistic effects that differentiate WT BMDMs from KOs.

4 Impact of Raptor Depletion on Intracellular Signalling Pathways

4.1 Introduction

As previously mentioned, the mTOR pathway is known to control cell size, proliferation and regulation of macrophages. Growth factors, nutrients, energy and mitogens are vital constituents needed for mTOR activation. They all stimulate mTOR activity by phosphorylating key kinases including S6K, Akt, and ERK. This means that numerous signalling pathways interconnect and contribute to mTOR activation [88]. mTOR activation leads to S6K phosphorylation, prompting mRNA transcription and protein translation. Akt and ERK work upstream of mTORC1 as they both phosphorylate TSC1/TSC2, the negative regulators of RHEB, which is vital for mTOR activation. Therefore Akt and ERK may contribute to a feedback loop in the absence of mTORC1 activity [185]

Inflammatory cytokines released by macrophages are involved in cell development and differentiation and play critical roles in defending the host against foreign bodies [77 78]. An excess of inflammation may progress with deleterious consequences such as development of autoimmune diseases or diabetes. Furthermore it may also support cancerous cells in evading immune responses, by co-opting mechanisms that assist in tissue repair and homeostasis [186]. Deregulation of the mTORC1 pathway has been suggested to lead to increased pro-inflammatory cytokine production [89]. Although there are data proposing that regulation of the mTOR pathway by many of the kinases and pathways mentioned above is associated with enhancement of cellular growth and proliferation, whether inflammation plays a role in this regulation is yet to be established. It is also not clear whether an inhibition of mTORC1 by deletion of Raptor will affect these signalling pathways. Therefore, the main aim of this chapter was to assess the importance of Raptor on other signalling pathways in macrophages.

4.2 The role of Raptor in intracellular signalling in BMDM

After establishing that Raptor was successfully deleted in the *Raptor f/f; Csf1r Cre-ERT* mice (Figure 3.2), I wanted to investigate whether Raptor KO would have an effect on signalling downstream of mTORC1 in macrophages. In order to answer this question, I stimulated WT and Raptor KO BMDMs with LPS/IFNγ at different time points of 15, 30,

60, 120, and 180 min. WT and KO BMDMs that were left unstimulated were used to determine basal levels. Protein lysates were made and western blot analysis was performed.

The target protein analysed was phosphorylated S6 (p-S6), a ribosomal protein which is a component of the 40S ribosomal subunit. S6 is directly phosphorylated by S6 kinase, which is a direct target of mTORC1. Phosphorylated S6 is routinely used as a read-out for mTORC1 activation, given its abundance and the availability of reliable reagents. The results show that there was a gradual increase of p-S6 (residue S23S/236) from the 30 min time point peaking at 60 min and a slight decrease by 120 and 180 min for WT BMDMs. KO BMDMs show diminished p-S6 levels compared to WT throughout the time course. Hence this result confirmed that downstream signalling was disrupted as mTORC1 activation was inhibited in Raptor KO BMDMs. β-actin was used as a loading control (Figure 4.1).

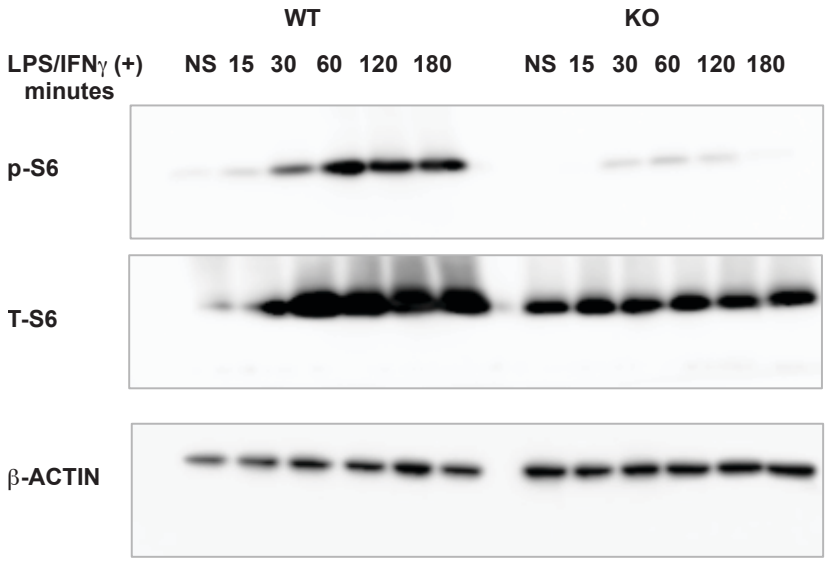

Figure 4.1 BMDM downstream signalling in absence of Raptor

$1x10^6$ BMDMs from WT and Raptor KOs were plated and either left unstimulated (NS) or stimulated with 100ng/ml of LPS and 20ng/ml of IFN γ for different time points of 15, 30, 60, 120, and 180 min. Cells were lysed and 20 μ g of protein was used targeting phosphorylated S6 (p-S6) (top blot) and for total S6 (T-S6) (middle blot) using western blot analysis. β -actin was used as a loading control (bottom blot). This immunoblot in the figure is representative of 3 independent experiments (BMDM lysates from 3 different mice).

4.3 Akt levels in BMDMs in the absence of Raptor

Once I established that there was an mTORC1 downstream signalling defect, I next wanted to investigate whether these Raptor KOs would also have different levels of phosphorylated Akt. Akt feeds into the mTORC1 signalling pathway by inhibiting the negative regulation of TSC1/2 on the RHEB protein, which is upstream of mTORC1. Inhibition of TSC1/2 regulation on RHEB leads to mTORC1 activation. Since Raptor is absent in the KOs, I hypothesised that there would be an effect on Akt which would lead to changes in Akt phosphorylation (p-Akt). As before, I stimulated WT and KO BMDMs with LPS/IFNγ at different time points of 15, 30, 60, 120, and 180 min. WT and KO BMDMs that were left unstimulated were used to determine basal levels. Protein lysates were made and western blot analysis was performed.

Phosphorylation of Akt (residue S473) in KO BMDMs upon stimulation was overall lower compared to WT counterparts, with the exception of the 60 min time point where levels in KO were slightly higher. This result indicates that, there may be an effect on Akt as mTORC1 is impaired. β-actin was used as loading control (Figure 4.2).

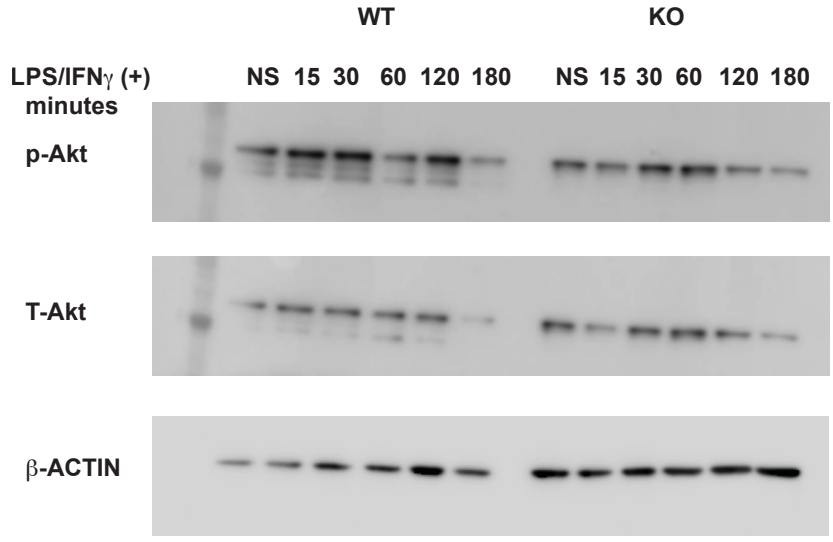

Figure 4.2 Effects on Akt activation in the absence of Raptor

$1x10^6$ BMDMs from WT and Raptor KOs were plated and either left unstimulated (NS) or stimulated with 100ng/ml of LPS and 20ng/ml of IFN γ for different time points of 15, 30, 60, 120, and 180 min. Cells were lysed and 20 μ g of protein was used targeting phosphorylated Akt (p-Akt) (top blot) and for total Akt (T-Akt) (middle blot) using western blot analysis. β -actin was used as a loading control (bottom blot). This is representative of 3 independent experiments (BMDM lysates from 3 different mice).

4.4 Are other signalling pathways affected in the absence of Raptor?

To investigate whether absence of Raptor in BMDMs may affect other signalling pathways I chose to study ERK phosphorylation since activation of the ERK pathway leads to an inhibition of TSC1/2 and therefore instigates active mTORC1 by Rheb activation. In the absence of Raptor, it would be likely to see an induction of phosphorylated ERK (p-ERK) activating the ERK signalling pathway that would enhance mTORC1 activation. In order to address this question, I stimulated WT and Raptor KO BMDMs with LPS/IFNγ at the same time points described above. Protein lysates were made and western blot analysis was performed.

The phosphorylation of ERK increased in the WT BMDMs starting from the 15 min time point and peaking at 30 min. Overall, I observed similar kinetics but weaker induction in p-ERK (residue T202/Y206) levels in KO compared to WT BMDMs. This result suggests that mTORC1 inhibition through Raptor KO results in a less efficient activation of the ERK pathway upon stimulation. β-actin was used as loading control (Figure 4.3).

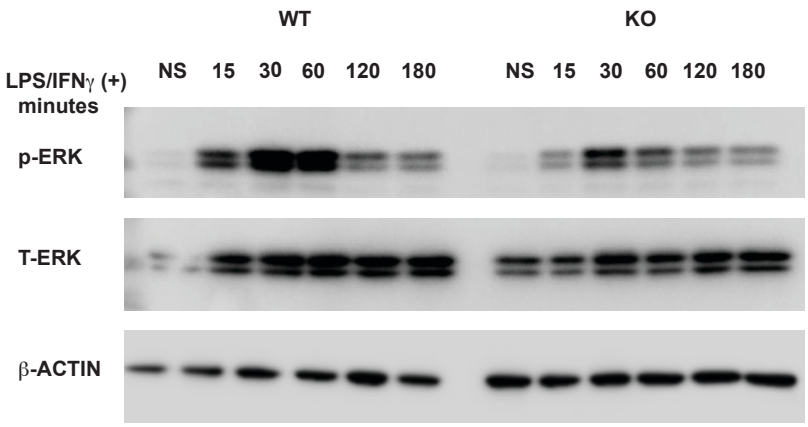

Figure 4.3 Effects on the ERK pathway in absence of Raptor

1x106 BMDMs from WT and Raptor KOs were plated and either left unstimulated (NS) or stimulated with 100ng/ml of LPS and 20ng/ml for IFN γ for different time points of 15, 30, 60, 120, and 180 min. Cells were lysed and 20 μg of protein was used for assaying phosphorylated ERK (p-ERK) (top blot) and for total ERK (T-ERK) (middle blot) using western blot analysis. β-actin was used as a loading control (bottom blot). This is representative of 3 independent experiments (BMDM lysates from 3 different mice).

4.5 Is STAT3 phosphorylation affected by mTORC1 inhibition?

As described in the literature, the mTOR pathway is activated during nutrient abundance, which has also been shown to increase STAT3 translocation to the nucleus mediating the expression of many genes that are needed for cell growth and survival [187]. I was interested in evaluating the phosphorylation level of STAT3 (p-STAT3) and if it would be affected by loss of Raptor. I stimulated WT and Raptor KO BMDMs with LPS/IFNγ as described above. Protein lysates were made and western blot analysis was performed.

Results show a general decrease in phosphorylation levels of STAT3 (residue Y705) in all time points from KO BMDMs as compared to WTs. As mTORC1 activation is inhibited the likelihood of finding a decrease in STAT3 phosphorylation should be evident. It is clear that mTORC1 has an effect on STAT3 expression levels. β-actin was used as loading control (Figure 4.4).

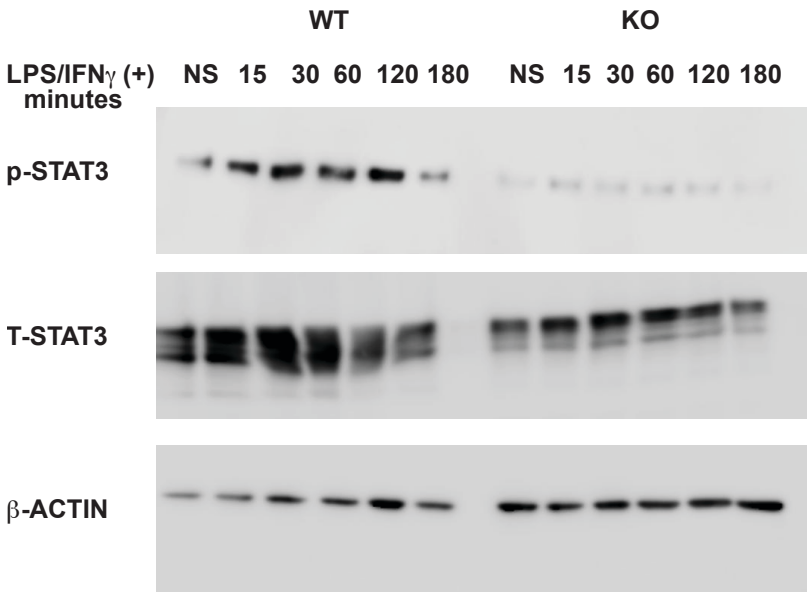

Figure 4.4 Effects on STAT3 phosphorylation in the absence of Raptor

$1x10^6$ BMDMs from WT and Raptor KOs were plated and either left unstimulated (NS) or stimulated with 100ng/ml of LPS and 20ng/ml of IFN γ for different time points of 15, 30, 60, 120, and 180 min. Cells were lysed and 20 μg of protein was used targeting phosphorylated STAT3 (p-STAT3) (top blot) and for total STAT3 (T-STAT3) (middle blot) using western blot analysis. β-actin was used as a loading control (bottom blot). This is representative of 2 independent experiments (BMDM lysates from 2 different mice).

4.6 What happens to the NFκB signalling pathway in absence of Raptor?

There is evidence in the literature suggesting an increase of proinflammatory cytokines released by macrophages as mTORC1 is inhibited [89]. From the data I have shown previously I was able to confirm an upregulation in proinflammatory cytokine at mRNA and to a lesser extent, protein level, within BMDM Raptor KOs (Chapter 3). Though there is a trend of increased inflammatory cytokines, I wanted to investigate further if this was due to an effect on the NFκB pathway, which is a transcription factor that translocates to the nucleus in the event of stress or infection, furthermore inducing the transcription of many inflammatory cytokines. Therefore, to determine whether BMDM Raptor KOs have enhanced NFκB activation, I decided to check phosphorylation levels of IκBα (p-IκBα). IκBα is a negative regulator of NFκB, as it sequesters it within the cytoplasm preventing it from translocating to the nucleus. I stimulated WT and KO BMDMs with LPS/IFNγ as described above. Protein lysates were made and western blot analysis was performed.

Stimulation of WT BMDMs resulted in phosphorylation of IκBα (residue S32) which peaked at the 60 min time point, substantially dropped at 120 min and remained to similar levels at 180 min. Stimulation of KO BMDMs resulted in phosphorylation of IκBα (residue S32) which peaked at the 60 min time point but to lower levels compared to WT. Interestingly, and in contrast to WT, at 120 min phosphorylation of IκBα was not reduced and was found to be at similar levels to the 60 min time point. p- IκBα levels dropped at 180 min following stimulation to similar levels as the WT. Total IκBα (T-IκBα) was also determined; as the phosphorylation levels of IκBα increased there was a general decrease in the total protein which was more profound in the KOs. Notably, although phosphorylation of IκBα was prolonged in KOs at 120 min, the levels of total IκBα had been restored. Together these results indicate an increase in the activation and altered kinetics of the NFκB pathway when Raptor is depleted and thus illustrate a crosstalk between these two pathways. β-actin was used as loading control (Figure 4.5)

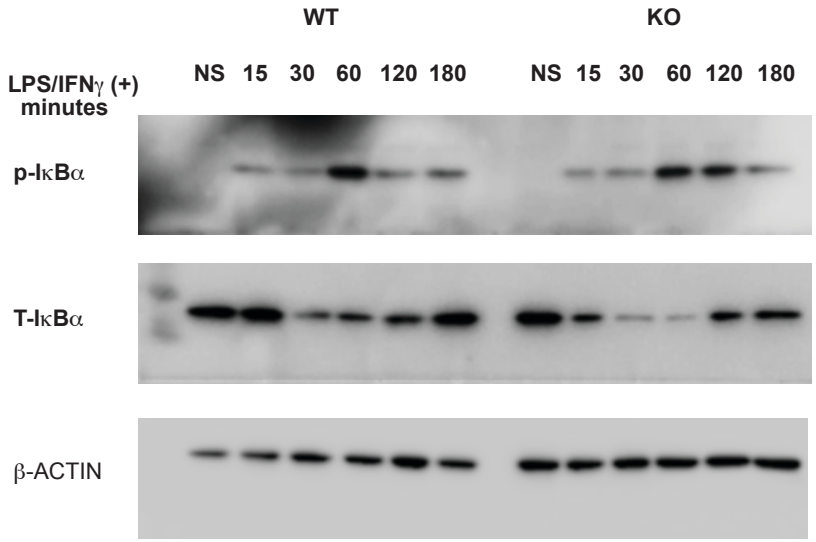

Figure 4.5 Effects on NFκB signalling in absence of Raptor

$1x10^6$ BMDMs from WT and Raptor KOs were plated and either left unstimulated (NS) or stimulated with 100ng/ml of LPS and 20ng/ml of IFN γ for different time points of 15, 30, 60, 120, and 180 min. Cells were lysed and 20 μ g of protein was used targeting phosphorylated I κ B α (p-I κ B α) (top blot) and for total I κ B α (T-I κ B α) (middle blot) using western blot analysis. β -actin was used as a loading control (bottom blot). This is representative of 3 independent experiments (BMDM lysates from 3 different mice).

4.7 Discussion

I was able to establish that disruption of Raptor in KO BMDMs, led to a disruption in the downstream signalling of mTORC1, as indicated by the diminished S6 phosphorylation in the KOs. Interestingly there was no major compensatory induction arising through other signalling pathways such as PI3K/Akt or ERK. These pathways have been shown to feed into the mTOR pathway as they phosphorylate the negative regulator of RHEB, TSC1/2, thereby activating mTORC1 [88]. In fact, I observed a weaker induction of pAkt and pErk in KOs. Carracedo et al, have shown that inhibition of mTORC1 may lead to a feedback activation of MEK/ERK signalling in a tumour setting, although I was not able to observe this with my stimulated Raptor KO BMDMs [188]. In addition, I provided evidence of a decrease in p-STAT3 induction in Raptor KO BMDMs upon stimulation. STAT3 is phosphorylated in presence of cellular stimuli through growth factors and cytokines. My observations are in line with literature of reduced STAT3 phosphorylation when mTORC1 is inhibited [187 189 190]. I also was able to confirm that there is an increase of NFκB activation by the enhanced phosphorylation of IκBα [186 191]. Looking at the total

protein levels of S6, ERK, and STAT3, I repeatedly observed a trend of an increase in WT vs KO BMDMs. This could reflect an effect of Raptor depletion on basal protein levels. A summary figure was made to incorporate the findings of chapter 4 (Figure 4.6).

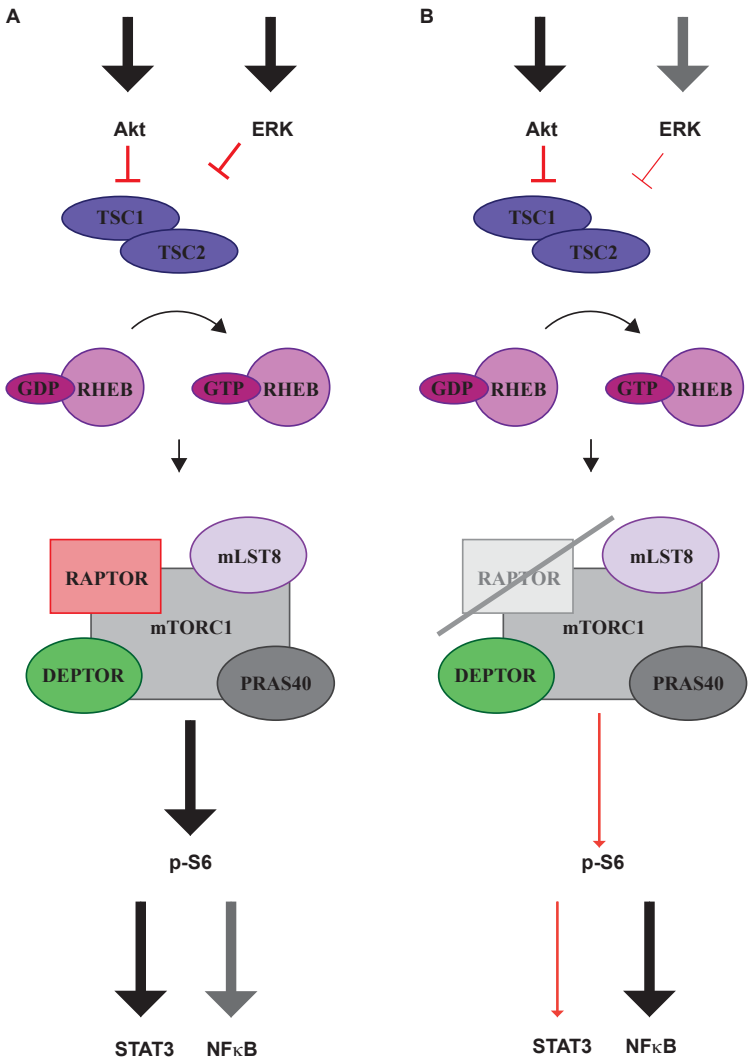

Figure 4.6 Summary of intracellular signalling pathways in presence and absence of Raptor.

In the presence of Raptor, Akt and ERK inhibit the negative regulator of RHEB; the TSC1/2 complex leading to RHEB activation through a GDP to a GTP conversion, which in turn activates mTORC1. Once mTORC1 is activated it leads to downstream signalling through the phosphorylation of S6. Phosphorylation of S6 allows translocation of STAT3 from the cytoplasm into the nucleus where transcription of genes needed for growth and survival commence. To a lesser extent there is NF κ B activation permitting its translocation into the nucleus mediating gene transcription of inflammatory cytokines (A). In the absence of Raptor, Akt and to a lesser extent ERK inhibit TSC1/2 activating RHEB, which activates mTORC1, but phosphorylation of S6 is inhibited due to the absence of Raptor thereby preventing downstream signalling where STAT3 translocation is hindered and activation of NF κ B by its translocation to the nucleus is increased.

I have demonstrated differences in macrophage polarization in the absence of Raptor with a more M1-like phenotype with an increase in transcription of inflammatory genes and to an extent their translation into cytokines. This was confirmed by the increase in the NFκB activation and aberrations in other signalling pathways. Caution must be taken when speaking of an increase in NFκB activation, since this pathway may be activated through canonical and non-canonical means. Further experiments should be performed to confirm that it is indeed activated and it is not just IκBα becoming phosphorylated and degraded without pathway activation [192]. Unravelling the consequences of this macrophage inflammatory phenotype on their basic functionality would be quite interesting. Therefore, I decided that the next step to my experimental analysis would take me to focus on the functional aspect of BMDMs in the absence of Raptor. Hence finding functional differences would open up a window to look into macrophage behaviour in a tumour setting, and whether the absence of Raptor would affect tumour growth and the surrounding tumour microenvironment.

5 Effects of Raptor Protein on Macrophage Function

5.1 Introduction

Macrophages are fundamental to the immune system; they participate in innate immunity by detecting foreign bodies as a first line of defence, doing so through cell surface receptors [193]. Foreign pathogens secrete chemotactic factors attracting macrophages to the area of infection. Once they have detected pathogens, macrophages are able to bind to them through these receptors, thereby initiating cytoskeletal rearrangements involving actin polymerisation and membrane trafficking [194]. This allows macrophages to engulf these foreign bodies in a process known as phagocytosis [195 196]. Phagocytosis is a form of endocytosis, and is specific for the type of pathogen engulfed, as they bind to specific cell receptors on the macrophages. As the pathogen is internalised in a phagosome certain changes occur that allow this phagosome to mature into a phagolysosome. Reactive oxygen and nitrogen species are secreted in the phagolysosome that digest and kill the pathogen. The digested bacterial peptides reach the major histocompatibility complex (MHC class II) through membrane trafficking and move to the cell surface where they interact with the T cell receptor (TCR) in a process known as antigen presentation that is a bridge between innate and adaptive immunity [197]. This presentation subsequently orchestrates a host adaptive immune response.

Phagocytosis is not only important in defence against foreign bodies but is also equally important in cellular homeostasis in removal of apoptotic cells. It is also required for embryonic development and tissue repair [198]. Another form of endocytosis is pinocytosis, which involves uptake of fluids and small particles, it differs from phagocytosis as the uptake is not specific and doesn't involve receptor binding.

The exact nature of the phagocytic process depends on size of the foreign body being engulfed, the type of receptors that recognise the foreign body, and how this foreign body is internalised. Fc receptor (FcR) mediated phagocytosis begins by membrane protrusions that encapsulate the pathogen and is pro-inflammatory in nature, while complement receptor phagocytosis does not involve encapsulation of the foreign particle and is anti-inflammatory [193 197]. Foreign body internalisation involves many signalling pathways and these pathways organize actin rearrangements that are needed to encapsulate the pathogen and allow formation of the phagolysosome. As the pathogens are internalised a series of

gene transcription and protein secretions occur that eventually lead to microbicidal affects.

PKC, a downstream target of mTORC2, plays a major role in particle internalization [199] . Upon activation, PKC is translocated to the membrane of macrophages where it promotes formation of actin filaments below the particle, participating in the early stages of the internalisation. Another pathway involved in internalisation and thereby phagocytosis is the PI3K pathway [200]. PI3K is needed to recruit Akt to the cell membrane and further production of actin filaments. Removal of PI3K is not essential in early particle internalisation but is required for later stages. Another important aspect of macrophage function is their ability to migrate towards certain stimuli while assisting in immune host responses. The PI3K pathway is involved in migration as it regulates actin polymerisation in macrophages [201]. Since PI3K is involved in signalling through the mTORC1 pathway, as Akt inhibits TSC1/2 (the negative regulator of RHEB) therefore activating mTORC1, it is important to look at macrophage function and how absence of Raptor may affect functional abilities. As macrophages are implicated in tumour progression and their involvement in the tumour microenvironment, any functional defects may also have an impact on the tumour microenvironment and tumour development [202] [134] [186] [132]. Therefore, the aim of the work described in this chapter was to investigate functional abilities of macrophages in the absence of Raptor and whether this absence may have an impact on tumour growth and progression within the tumour microenvironment.

5.2 Does absence of Raptor impair BMDM phagocytic activity?

In order to address this question BMDMs from *Raptor WT/WT; Csf1r Cre-ERT* (WT) and *Raptor f/f; Csf1r Cre-ERT* (KO) mice were tested for their phagocytic capabilities. I decided to investigate phagocytosis by using fluorescent beads that were 1.0 um in size [203] [204]. BMDMs were stimulated with LPS overnight prior to incubation with the beads in order to 'prime' them with the aim of enhancing phagocytosis. Fluorescein beads were incubated with the BMDMs at 4 time points: 15, 30, 60, and 90 min. BMDMs without beads were used as controls. Once the beads were added to the BMDM cultures, the macrophages were able to engulf the beads in a timely manner. After the cells were scraped from the tissue culture well, fluorescence intensity was quantified using FACS analysis, the amount of fluorescence was taken to be equivalent to phagocytic activity. The results show a reduction in phagocytic activity in KO BMDMs in comparison to their

WT counterparts. This was found at all the time points, and results were statistically significant at 15, 30, and 60 min after addition of the beads. This observation suggests that in the absence of Raptor these BMDMs have impaired phagocytic abilities (Fig 5.1).

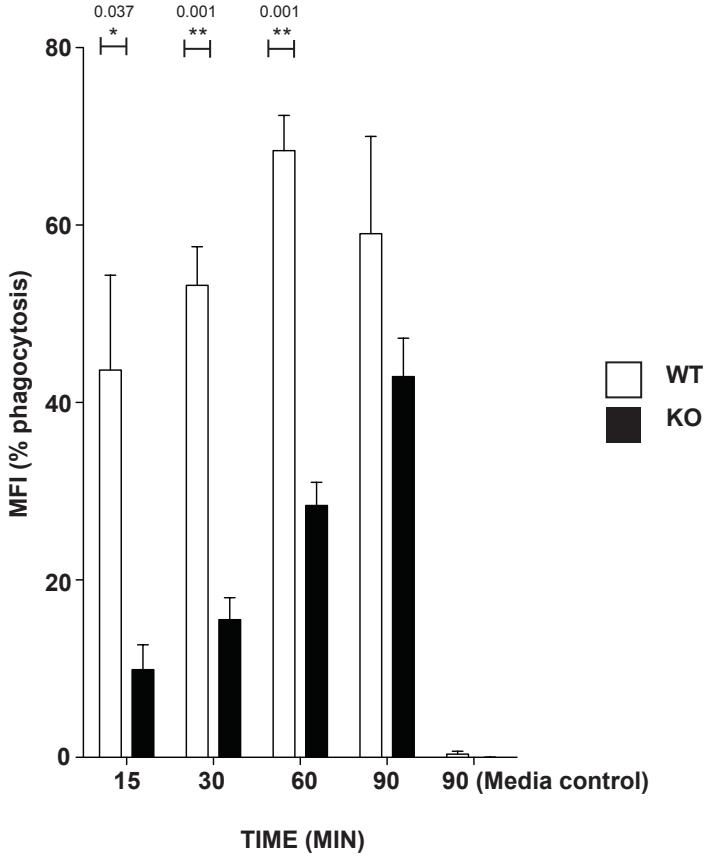

Figure 5.1 Phagocytic capacity of BMDMs to engulf fluorescent beads

WT and KO BMDMs were stimulated with 100ng/ml of LPS overnight prior to addition of fluorescent beads. As fluorescent beads were added at differing time points of 15, 30, 60 and 90 min, BMDMs were able to phagocytose these beads. A significant decrease in the phagocytic capacity was seen in KO BMDMs (black bars) as compared to WT BMDMs (white bars). This significant decrease was observed for the following time points (15, 30, and 60 min). Media control was prepared to demonstrate no phagocytosis. Percentage of phagocytosis was analysed as mean fluorescence intensity (n=3). Student's t-test was used to check for statistical significance: p-value of <0.05 is statistically significant (*) or <0.005 (**).

Many would argue that this result is not a consequence of impaired phagocytosis but pinocytosis due to the size of the fluorescent beads being engulfed, as they are not large enough to activate phagocytosis. Moreover, activation of phagocytosis involves Fc receptors, which is not occurring during the uptake of fluorescent beads. To ensure that absence of Raptor truly impairs phagocytic activity, I performed another experiment using gemcitabine treated cancer cells. For this, I treated a murine pancreatic cancer cell line, TB32048, with a cytotoxic dose of gemcitabine. Gemcitabine is a known chemotherapeutic agent used to treat pancreatic cancer patients. *In vitro* treatment of cancer cells with gemcitabine will initiate apoptosis within these cancer cells, thereby producing signals activating BMDMs, which in turn will begin phagocytosing these cancer cells [205]. WT and KO BMDMs were stained separately using cell tracker fluorescein stains in order to differentiate between apoptotic cancer cells and macrophages. The BMDMs were stimulated with LPS overnight prior to the addition of gemcitabine treated murine pancreatic cancer cells. The apoptotic cancer cells were added on to the BMDMs the following day and were incubated together for 2, 4, 6, 8, and 16 hrs. BMDMs without cancer cells (0 hrs) and 16 hrs ice were used as controls (maximum hours of BMDMs with cancer cells on ice were chosen as a control setting to make sure there is minimal phagocytosis occurring throughout the incubation periods). After the cells were scraped from the wells, fluorescence intensity was quantified using FACS analysis. Both apoptotic cancer cells and macrophages were labelled with different colours of cell trackers and therefore amount of fluorescence of both colours together were taken to be equivalent to phagocytic activity. The results obtained for 4, 6, 8, and 16 hr time points showed a significant reduction in the phagocytic activity of KO BMDMs compared to the WT BMDMs. At the 2 hr time point there was no reduction in the phagocytic activity for KO BMDMs as compared to the WT BMDMs. This confirms that in the absence of Raptor protein, phagocytic activity is impaired (Figure 5.2). The reason for this reduction may be due to a defect in their cytoskeleton as actin polymerisation may be impaired or due to a defect in the Fc receptors in the KO BMDMs.

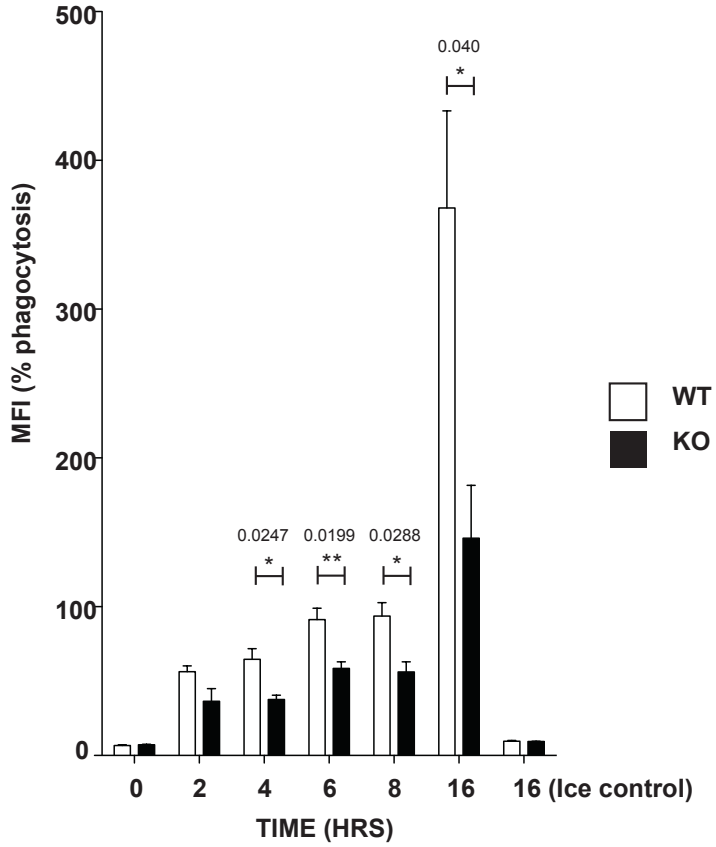

Figure 5.2 Phagocytic activities of BMDMs on apoptotic murine pancreatic cancer cells

WT and KO BMDMs were stimulated with 100ng/ml of LPS overnight prior addition of pancreatic cancer cells, TB32048 treated with 100uM of gemcitabine. A significant decrease in the phagocytic capacity was seen in KO BMDMs (black bars) as compared to WT BMDMs (white bars). This significant decrease was observed for the following time points (4, 6, 8, and 16 hrs). Media and ice control showed minimal phagocytosis. Percentage of phagocytosis was analysed as mean fluorescence intensity (n=3). Student's t-test was used to assess statistical significance: p-value of <0.05 is statistically significant (*) or <0.005 (**).

5.3 Does absence of Raptor affect BMDM cytoskeleton?

5.3.1 BMDM morphology

To assess cytoskeletal impairment in absence of the RAPTOR protein BMDMs from both WT and KO mice were re-plated on coverslips and were either left unstimulated (NS) or stimulated by LPS/IFNγ or IL-4/IL-13 for 4 hrs After stimulation, the cells were stained with phalloidin (F-actin stain) using a fluorescein dye to evaluate the concentration and localisation of F-actin in BMDMs of both WT and KOs. I was also interested in evaluating the size and shape of the BMDMs and whether absence of Raptor would affect these respectively. Images of BMDMs stained with phalloidin without any stimulation,

appeared to show that KO BMDMs are smaller in size in comparison to their WT counterparts. BMDMs in the absence of Raptor also had a more rounded appearance and did not show the typical elongated shape when compared to WT BMDMs. BMDMs stimulated with LPS/IFNγ appeared to show a less pronounced elongated shape in the KOs compared to WT BMDMs. There was however, no apparent difference in morphology between WT and KO BMDMs after stimulation with IL-4/IL-13 (Figure 5.3). As this evaluation was only by observing the images, I needed to quantify cell size and fluorescein intensity in order to investigate whether absence of Raptor affects BMDM cytoskeleton, through F-actin fluorescence staining.

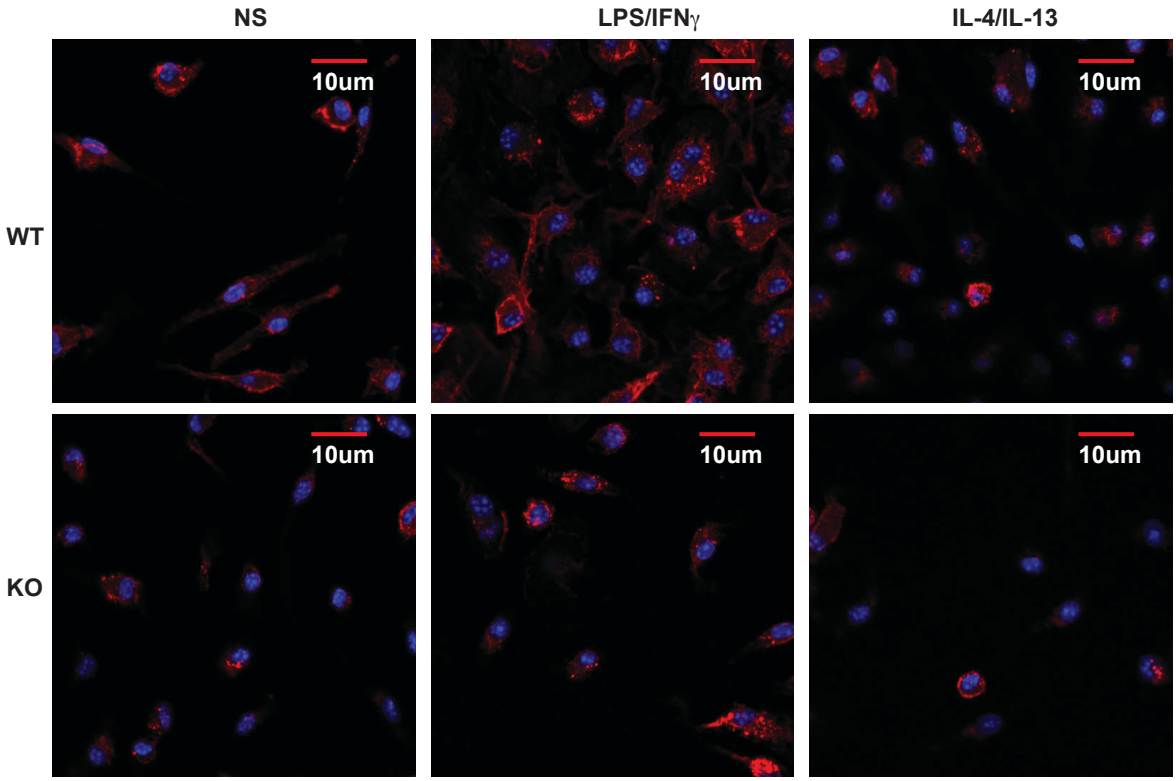

Figure 5.3 BMDM morphology in absence of Raptor protein

Fluorescence staining was performed on WT and KO BMDMs. Phalloidin (F-actin) appears as red, and cell nucleus in blue. Images of non-stimulated (NS) KO BMDMs are smaller in size and more rounded compared to WTs (Left: top and bottom). BMDMs stimulated with 100ng/ml of LPS and 20ng/ml of IFNγ, show a less elongated morphology in KOs as compared to WTs (Middle: top and bottom). BMDMs stimulated with 10ng/ml of both IL-4 and IL-13 show no differences in BMDM morphology for either WT or KOs (Right: top and bottom). Stimulation was for 4 hrs, magnification at 63X using confocal microscopy (n=3).

5.3.2 Quantification of cell size and fluorescence intensity

I began quantification by using images of WT and KO BMDMs from 5 different fields for all of the 3 conditions (NS, LPS/IFNγ and IL-4/IL-13). Using ImageJ I was able to evaluate BMDM cell size. The results show no difference in cell size for KO BMDMs in comparison to their WT counterparts (Figure 5.4). I also evaluated the mean intensity of fluorescence of BMDMs from WT and KO in order to observe whether absence of Raptor may affect the amount of F-actin within the cells. The results show that non-stimulated KO BMDMs had comparable mean intensities of F-actin to WTs. After stimulation with LPS/IFNγ again there was no difference in mean intensity of KO BMDMs compared to WTs, as was also shown when they were stimulated with IL-4/IL-13 revealing no differences (Figure 5.5). I decided to check integrated density, which will evaluate the spread of F-actin within the BMDMs taking into consideration the cell size. The results show that there was no reduction in integrated density in KO BMDMs in comparison to the WTs in non-stimulated conditions. BMDMs stimulated with LPS/IFNγ show a significant decrease in KOs compared to WTs. IL-4/IL-13 stimulation show no differences in integrated density (Figure 5.6). These results suggest cytoskeletal impairment of BMDMs in the absence of Raptor since they appear to be smaller in size and shape, with F-actin integrated density being reduced compared to BMDM WT counterparts.

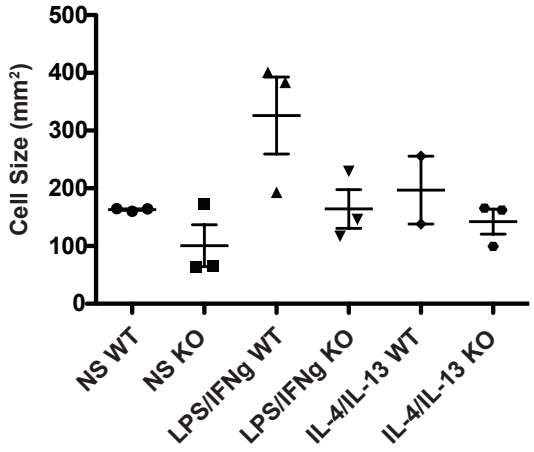

Figure 5.4 Average BMDM size in absence of Raptor protein

Fluorescence staining of phalloidin (F-actin) was performed on BMDMs from WT and Raptor KOs. Quantification was performed to assess cell size (mm^2). Non stimulated (NS) KO BMDMs were no different to WT BMDMs. When WT and KO BMDMs were stimulated with 100ng/ml of LPS and 20ng/ml of IFNγ, there was no difference observed in KOs as compared to WTs. BMDMs were stimulated with 10ng/ml of both IL-4 and IL-13 showing no difference in size between WT and Kos, (NS and LPS/IFNγ n=3; IL-4/IL-13 WT: n=2 KO: n=3). Student's t-test was used to check for statistical significance.

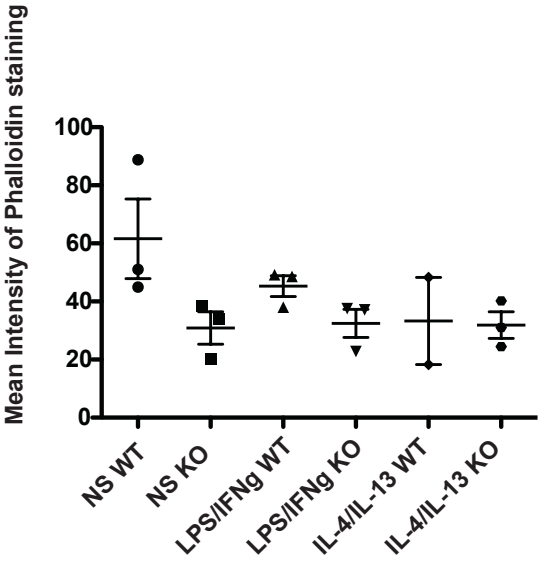

Figure 5.5 Average mean intensity of phalloidin staining on BMDMs in absence of Raptor protein

Fluorescence staining of phalloidin (F-actin) was performed on WT and Raptor KO BMDMs. Quantification was performed to assess F-actin intensity. Non stimulated (NS) KO BMDMs showed no difference in mean intensity as compared to WT BMDMs. BMDMs from WT and KOs were stimulated with 100ng/ml of LPS and 20ng/ml of IFNγ, showing no reduction in mean intensity was observed in KOs as compared to WTs. BMDMs were stimulated with 10ng/ml of both IL-4 and IL-13 showing no difference in mean intensity staining for both WTs and KOs (NS and LPS/IFNγ n=3; IL-4/IL-13 WT: n=2 KO: n=3). Student's t-test was used to check for statistical significance.

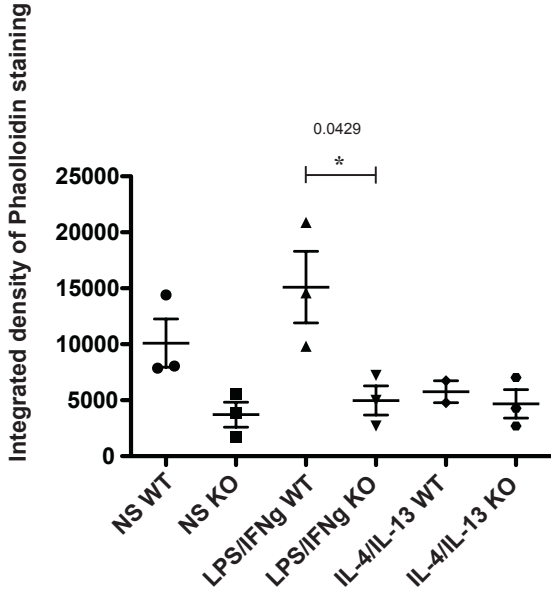

Figure 5.6 Integrated density of phalloidin staining on BMDMs in absence of Raptor protein

Fluorescence staining of phalloidin (F-actin) was performed on BMDMs from WT and Raptor KOs. Quantification was performed to assess F-actin intensity. Non stimulated (NS) BMDMs had no reduction in integrated density for KOs as compared to WTs. WT and KO BMDMs were stimulated with 100ng/ml of LPS and 20ng/ml of IFNγ, showing a significant reduction in integrated density in KOs as compared to their WT counterparts. BMDMs were stimulated with 10ng/ml of both IL-4 and IL-13 showing no difference in integrated density for both WTs and KOs (NS and LPS/IFNγ n=3; IL-4/IL-13 WT: n=2 KO: n=3). Student's t-test was used to check for statistical significance: p-value of <0.05 is statistically significant (*).

5.4 Does absence of Raptor affect BMDM actin polymerisation?

Since I had seen a significant reduction in the integrated density of KO BMDMs stimulated with LPS/IFNγ compared with WT BMDMs, I decided to investigate actin filament polymerisation and see whether this polymerisation is affected in the absence of Raptor. Actin polymerisation occurs when free monomers known as G-actin, polymerise into what is known as active F-actin. It was important for me to assess the amount of F-actin polymerised, as this is the active state needed for essential cytoskeletal functions such as cell motility and phagocytosis in macrophages [206]. BMDMs were stimulated with LPS overnight prior incubation with fluorescent beads (refer to section 5.2) Fluorescein beads were incubated with the BMDMs at 5, 20, 30, 60, and 90 min. BMDMs without beads were used to check basal levels. After the cells were scraped they were fixed, permeabilised, and stained for F-actin and G-actin. Results show no differences in the F/G actin ratio between BMDMs from WTs and KOs (Figure 5.7). These results suggest that in absence of Raptor F-actin polymerisation is not changed and may not be the reason for a cytoskeletal defect in KO BMDMs.

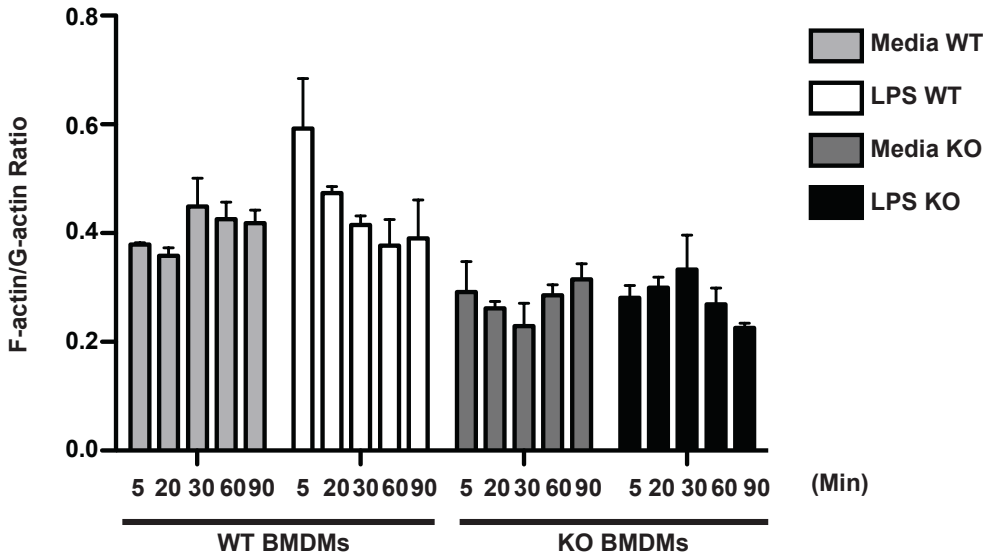

Figure 5.7 F/G actin ratios in absence of Raptor protein

WT and KO BMDMs were stimulated with 100ng/ml of LPS prior to their incubation with fluorescent beads at differing time points of 5, 20, 60, and 90 min. The BMDMs were stained for G-actin and F-actin and the ratios were evaluated. No significant differences were observed (n=3). Student's t-test was used to check for statistical significance.

5.5 Does an absence of Raptor affect Fc receptors?

I wanted to investigate whether absence of Raptor would affect Fc receptors as I have shown above that there is a reduction in phagocytic capabilities of KOs compared to WTs (refer to section 5.2). Therefore, I stimulated both WT and KO BMDMs with LPS/IFNγ and stained the cells with different antibodies targeting different Fc receptors, CD16/32, and CD64. I also looked at other receptors that are needed for macrophage antigen presentation and phagocytosis, CD86, and CD206 respectively. BMDMs left without stimulation were used to check basal levels of receptor expressions. Results show that there is a significant reduction in basal levels of expression of CD16/32 in KO BMDMs compared to WT BMDMs but in stimulated conditions there were no differences in the amount of CD16/32 expression between the two (Figure 5.8 A). CD64 expression also shows a significant reduction in KO BMDM expression as compared to their WT counterparts at basal level, but this reduction is not seen in stimulated conditions (Figure 5.8 B). There were no differences shown in CD86 expression between WT and KO BMDMs (Figure 5.8 C). In regards to CD206 expression there were significant reductions observed at both basal and stimulated conditions for KOs in comparison to WTs (Figure 5.8 D).

Results for the Fc receptors show that in the absence of Raptor, the expressions are affected mainly at basal levels, once stimulated with LPS/IFNγ level of expression are similar suggesting stimulation does not have an effect on either WT or KO BMDMs. Absence of Raptor does not have an effect on CD86 expression suggesting no difference in the way these BMDMs provide costimulatory signals for T cell activation (Figure 5.8 C). On the other hand, the reduction in mannose receptor (CD206) expression seen at both basal and stimulated conditions in KO BMDMs in comparison to WTs suggests a defect in phagocytic function (Figure 5.8 D).

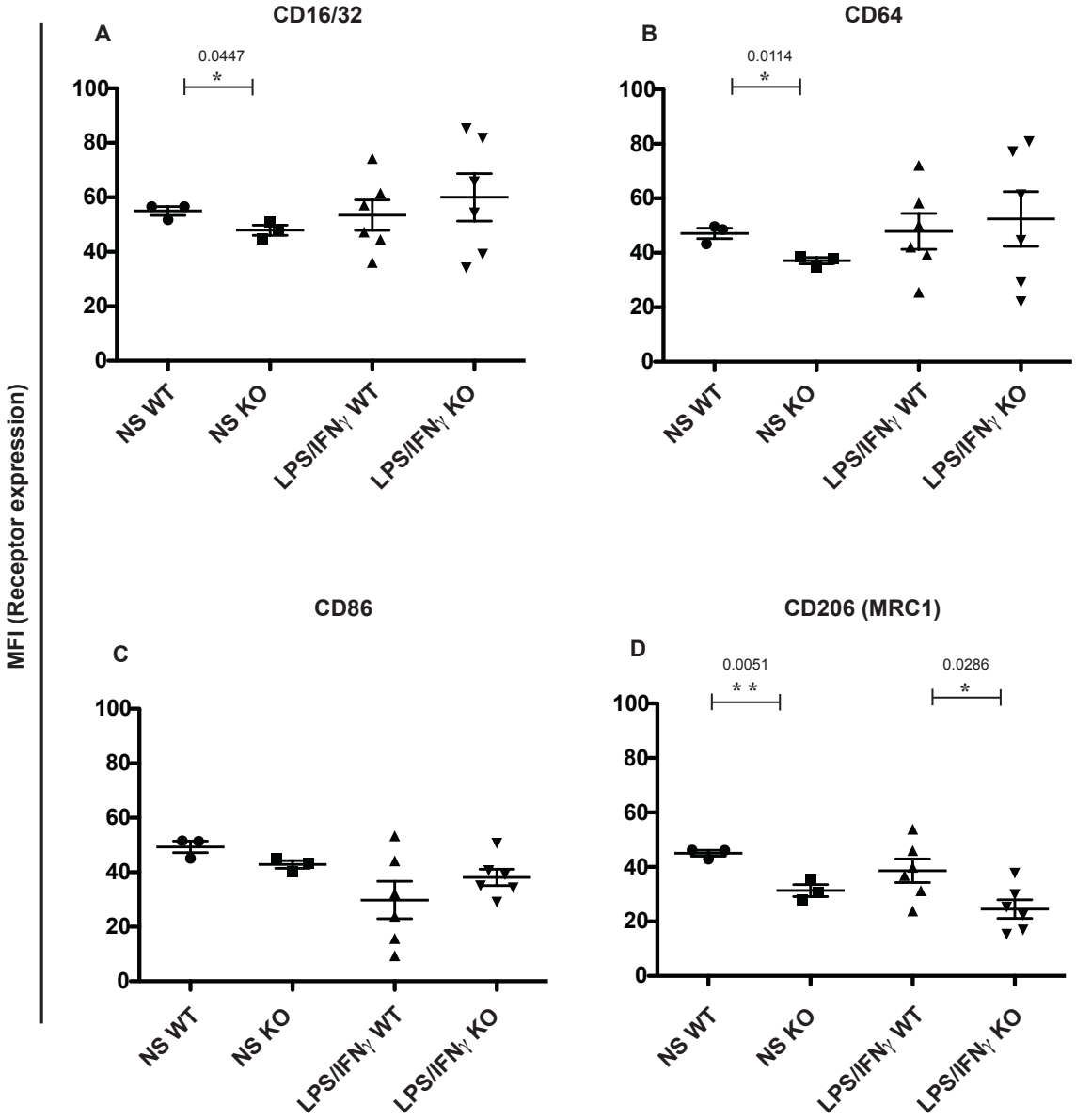

Figure 5.8 Effects on cell surface receptor expression in absence of Raptor

WT and KO BMDMs were stimulated with 100ng/ml of LPS and 20ng/ml of IFNγ. They were stained for different cell receptors and mean fluorescent intensity was evaluated. CD16/32 staining shows a significant reduction in expression in KO BMDMs in comparison to WTs at basal level, but no difference was observed in stimulated conditions (A). CD64 expression was reduced significantly in the KOs as compared to their WT counterparts at basal levels but no difference was shown in stimulated conditions (B). There were no changes observed in CD86 expression either in KOs or WTs at basal levels and stimulated conditions (C). Mannose receptor expression was significantly reduced in KO BMDMs in basal and stimulated conditions (D). NS : (n=3) ; LPS/ IFNγ : (n=6). Student's t-test was used to check for statistical significance: p-value of <0.05 is statistically significant (*) or <0.005 (**).

5.6 Does absence of Raptor affect the migratory ability of BMDMs?

5.6.1 BMDMs migration towards fibroblasts

I also wanted to evaluate BMDM migration capabilities in the absence of Raptor. In order to address this, WT and KO BMDMs were either left un-stimulated (NS) or stimulated with LPS/IFNγ or IL-4/IL-13 for 4 hrs in transwells. After stimulation, transwells were incubated with mouse embryonic fibroblasts (MEFs) in a 24 well plate (1:1 ratio) and left overnight. MEFs were used in these experiments as they secrete insulin growth factor (IGF), hepatocyte growth factor (HGF) and cytokines such as IL-1 along with chemokines such as monocyte chemotactic protein 1 (MCP1/CCL2) needed to activate macrophages and stimulate their migratory properties [207]. The following day these transwells were stained with crystal violet. After washing, the transwells were left to dry and then placed in acetic acid where any purple colour would diffuse into the acid. Migration was assessed by the intensity of the purple colour in acetic acid. The intensity of the colour was taken to be equivalent to the amount of BMDMs that have moved through the transwells towards the fibroblasts. Results show no significant difference in the migratory capability of KO BMDMs as compared to the WT BMDMs, in non stimulated conditions or when stimulated with either LPS/IFNγ or IL-4/IL-13 (Figure 5.9).

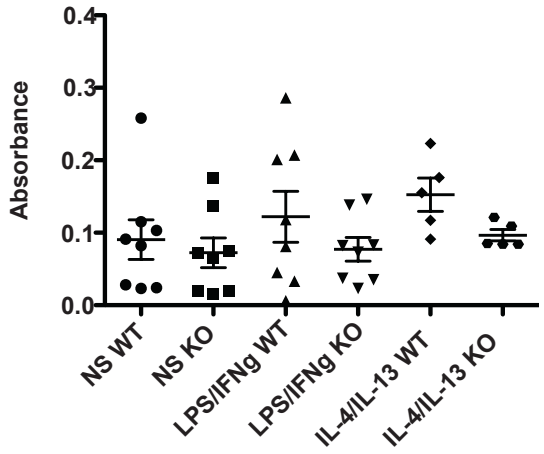

Figure 5.9 Migration of BMDMs towards fibroblasts in absence of Raptor

WT and KO BMDMs were either unstimulated (NS) or stimulated with 100ng/ml of LPS and 20ng/ml of IFNγ or stimulated with 10ng/ml of both IL-4 and IL-13 for 4 hrs. There were no significant differences in BMDM migratory capabilities between WT and KOs left unstimulated or stimulated with either LPS/ IFNγ or IL-4/IL-13. NS and LPS/IFNγ: (n=8) ; IL-4/IL-13 : (n=5). Student's t-test was used to check for statistical significance.

5.6.2 BMDM migration towards cancer cells

I was also interested in evaluating BMDM migration capability towards cancer cells in absence of Raptor. I investigated this by performing the same experiment, as shown previously in section 5.6.1 but using a murine pancreatic cancer cell line, TB32047 (the use of this murine pancreatic cell line instead of the TB32048s was merely due to availability at the given time of the experiments), instead of MEFs. Pancreatic cancer cells were used since they secrete factors that may enhance BMDM migration towards them such as CCL2, CCL5, CCL7, CCL8, CXCL12, VEGF, and CSF-1 [208] [209]. Results show that there was a significant reduction in migration of BMDMs towards the cancer cells from KO BMDMs as compared to the WT BMDMs stimulated with either LPS/IFNγ or IL-4/IL-13 (Figure 5.10). This result suggests that there is a defect in the migratory capability in absence of Raptor. This result is different than what has been shown in BMDM migration towards MEFs, which may be due to the fact that cancer cells release more potent chemoattractants used as homing signals for macrophages strengthening their migratory capabilities towards cancer cells.

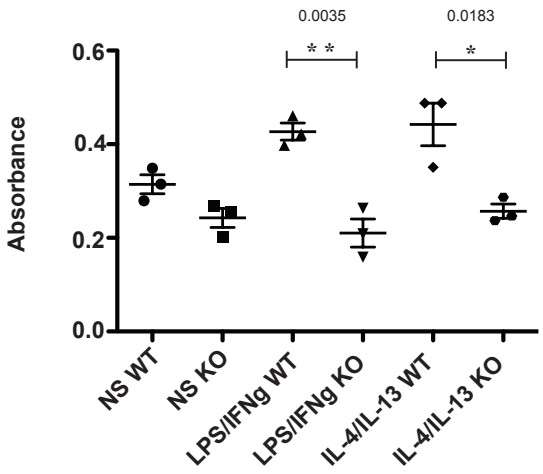

Figure 5.10 Migration of BMDMs towards murine pancreatic cancer cells (TB32047) in absence of Raptor

WT and KO BMDMs were either unstimulated (NS) or stimulated with 100ng/ml of LPS and 20ng/ml of IFNγ or stimulated with 10ng/ml of both IL-4 and IL-13 for 4 hrs. There were no significant differences in BMDM migratory capabilities between WT and KOs left unstimulated. There was a significant reduction in migration towards cancer cells observed in KO BMDMs compared to their WT counterparts once stimulated with either LPS/ IFNγ, or IL-4-IL-13 (n=3). Student's t-test was used to check for statistical significance: p-value of <0.05 is statistically significant (*) or <0.005 (**).

5.7 Does absence of Raptor affect the tumour microenvironment?

5.7.1 Subcutaneous tumour experiment

In the presence of murine pancreatic cancer cells I found a reduction in phagocytic and migratory functions of BMDMs in which Raptor had been deleted, I next wanted to evaluate whether there are differences within a tumour microenvironment when Raptor is absent in macrophages. I thereby performed an *in vivo* subcutaneous tumour experiment by injecting 4 mice each from *Raptor WT/WT; Csf1r Cre-ERT* (WT) and *Raptor f/f; Csf1r Cre-ERT* (KO) with the murine pancreatic cell line, TB32048, and assessed the cellular composition of the tumour microenvironment, along with lymphoid and myeloid cells in spleen and blood. This is to observe whether the presence of tumour will have an effect on leukocyte counts that are found in either the spleen or blood, which may lead to a significant recruitment of these leukocytes to the tumour site either for pro or anti-tumour

purposes. Once tumours were 1.2 cm in diameter, mice were culled and tumour, spleen, and blood were collected. Tumour and spleen were weighed. FACS was used to assess B cells (CD19), T cells (CD3) cells, and their subsets CD4 and CD8. I also quantified expression of F480 for macrophages and the expression of MHCII. This subcutaneous tumour experiment gave me preliminary data since not all mice developed tumours. Moreover, the FACS data for the tumours were impossible to interpret due to the high percentage of cell death observed. Therefore, I was only able to analyse results for blood and spleen.

There was no significant difference between tumour and spleen weights from WT and KO mice (Figure 5.11 A and B). In the blood there was no significant difference in B and T cells (Figure 5.12 A and B), but there was a significant reduction in the amount of CD4 T cells in KO mice compared to their WT counterparts (Figure 5.12 C). There was no difference in CD8 T cells either for both WT and KOs (Figure 5.12 D).

There were no differences in the B and T cell populations or the subset populations of T cells in spleens from WT and KO mice (Figure 5.13 A-D). However, spleens of KO mice show a significant reduction in macrophages as compared to the WT mice (Figure 5.13 E). There was no significant difference in the MHCII population either in WT and KO mice (Figure 5.13 F).

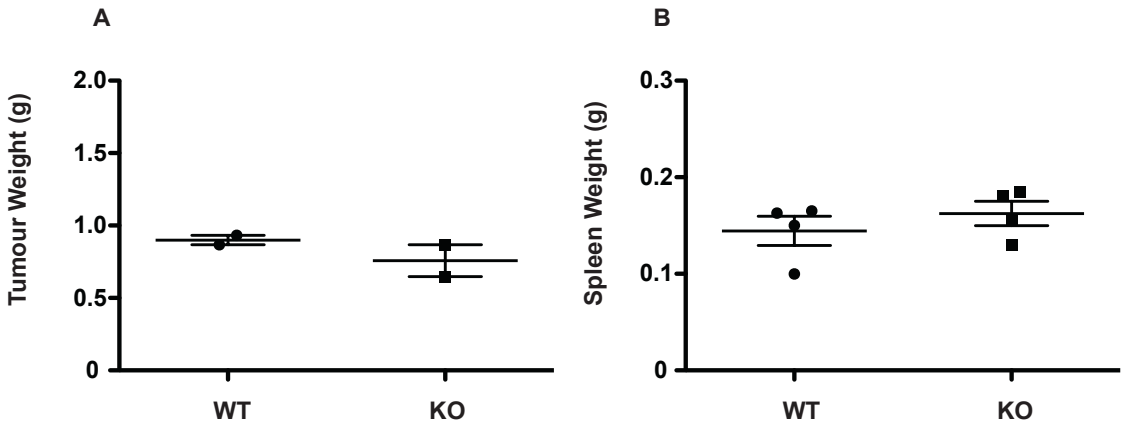

Figure 5.11 Subcutneous tumour experiment: tumour and spleen weights

WT and KO mice were given I.P injections of tamoxifen once per day for 3 consecutive days a week prior the starting of the subcutaneous experiment Mice from WT and KOs were injected with 1x105 of murine pancreatic cancer cells (TB32048) subcutaneously. All mice were given tamoxifen once per week for 3 consecutive days by oral gavage, until end of the experiment in order to sustain KO status in their myeloid cells. After tumours reached 1.2 cm, mice were culled and tumour and spleen were weighed. There was no significant difference in tumour or spleen weights from either WT or KO mice (A and B). Tumour (n=2); spleen (n=3). Student's t-test was used to check for statistical significance.

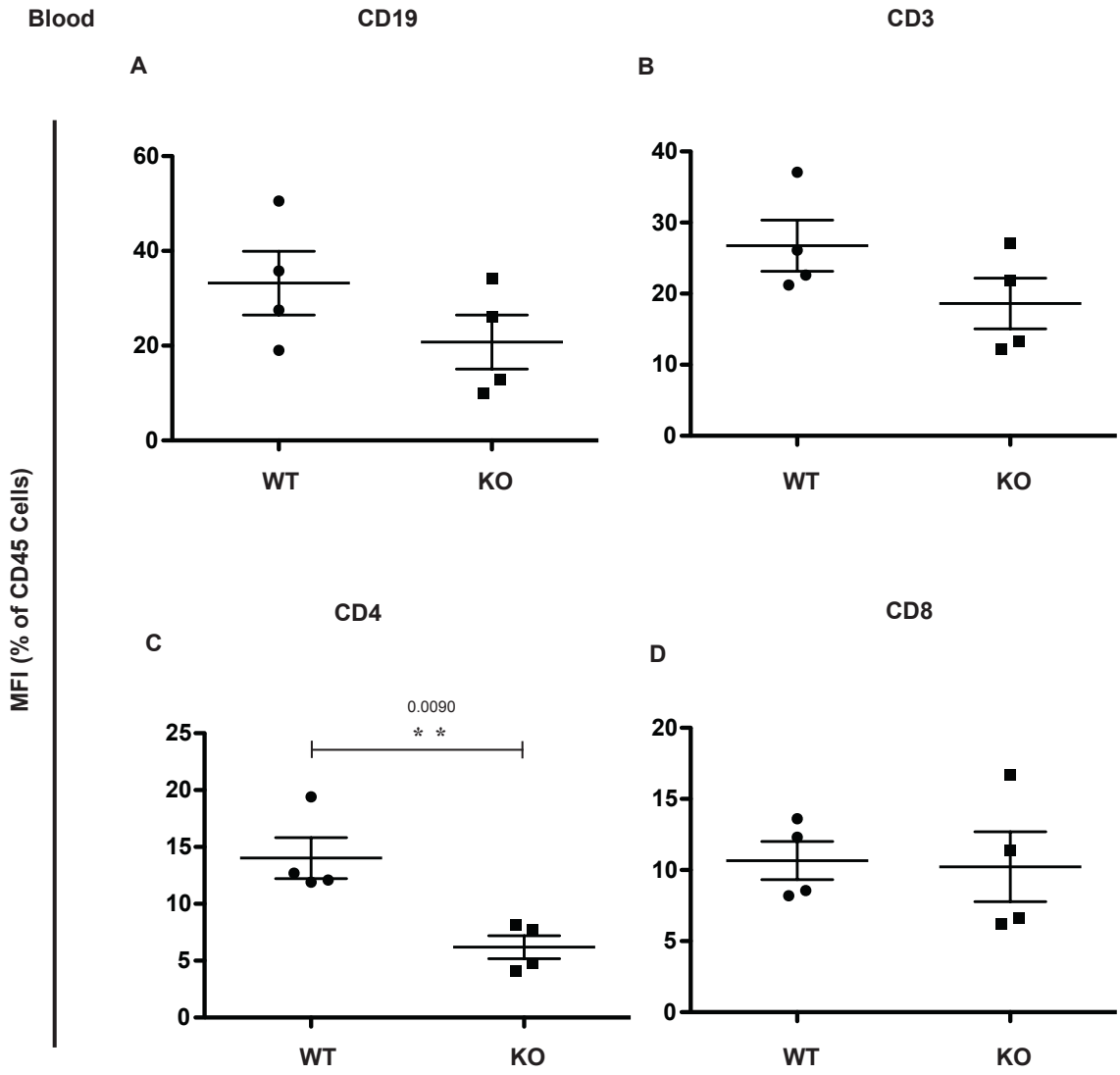

Figure 5.12 Subcutaneous tumour experiment: Effects on blood cells in absence of Raptor

WT and KO mice were given I.P injections of tamoxifen once per day for 3 consecutive days a week prior the starting of the subcutaneous experiment. Mice were injected with $1x10^5$ of murine pancreatic cancer cells (TB32048) subcutaneously. All mice were given tamoxifen once per week for 3 consecutive days by oral gavage, until end of the experiment in order to sustain KO status. After tumours reached 1.2 cm, mice were culled and blood was collected. FACS was performed and cells were quantified. There was no difference in the peripheral blood B cell (CD19) and T cell (CD3) populations (A and B), but there was a significant decrease in the CD4 population of KO mice in comparison to WT mice (C). CD8 showed no difference in the population between WT and KO (D). (n=4) Student's t-test was used to check for statistical significance: p-value of <0.005 (**) is statistically significant.

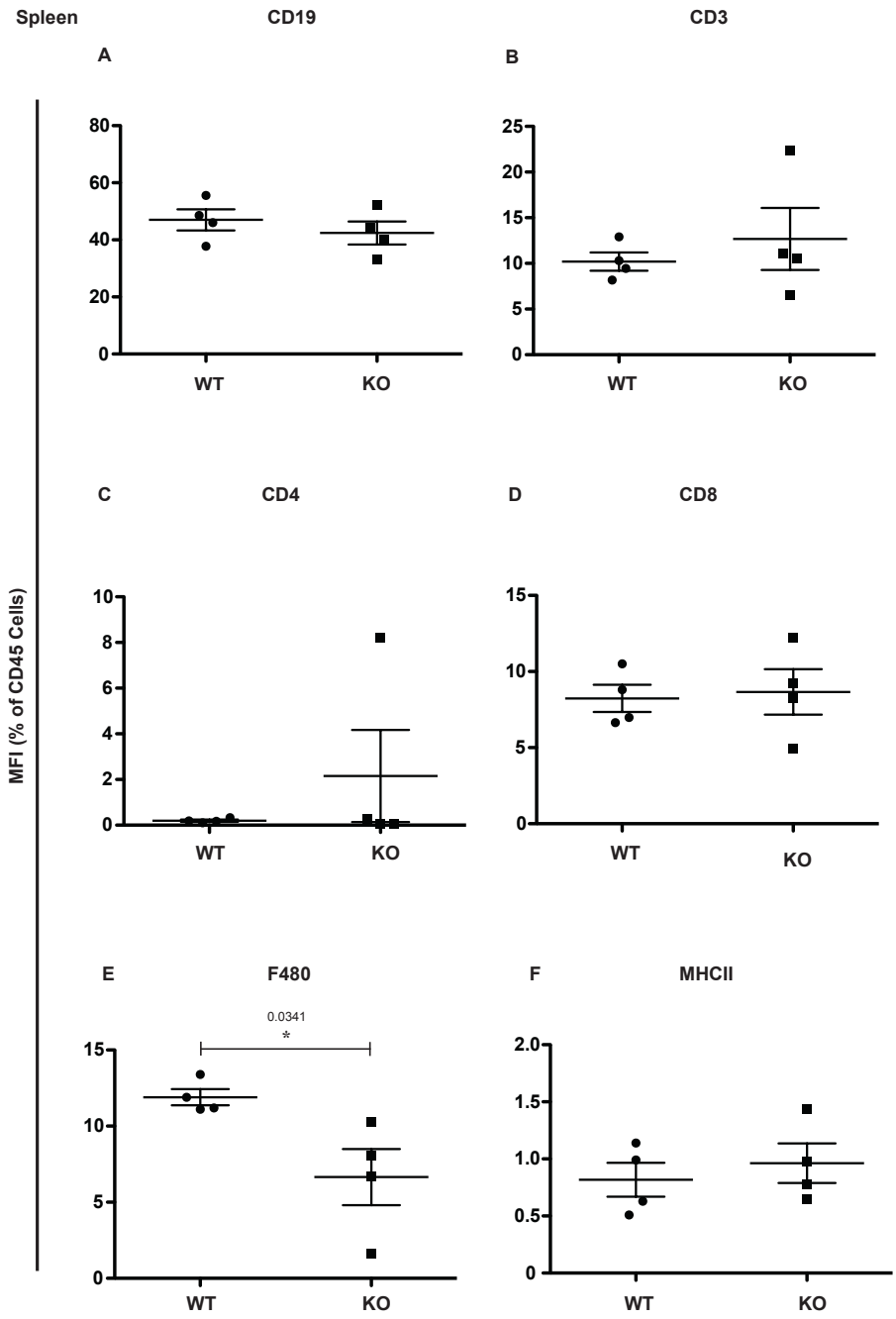

Figure 5.13 Subcutaneous tumour experiment: Effects on splenic cells in absence of Raptor

WT and KO mice were given I.P injections of tamoxifen once per day for 3 consecutive days a week prior the starting of the subcutaneous experiment. Mice were injected with $1x10^5$ of murine pancreatic cancer cells (TB32048) subcutaneously. All mice were given tamoxifen once per week for 3 consecutive days by oral gavage until end of the experiment in order to sustain KO status. After tumours reached 1.2 cm, mice were culled and spleen was collected. FACS was performed and cells were quantified. There was no difference in the B cell (CD19) and T cell (CD3) populations (A and B), or the T cell subsets CD4 and CD8 (C and D), but there was a significant decrease in the F480 population of KO mice in comparison to WT mice (E). MHCII showed no difference in the population between WT and KO (F). (n=4) Student's t-test was used to check for statistical significance: p-value of <0.05 is statistically significant (*).

5.7.2 Orthotopic tumour experiment

Implanting tumour cells directly into the organ provides a more realistic organotypic interaction between the tumour cells and the microenvironment surrounding the organ. Therefore, I decided to perform an orthotopic experiment by injecting murine pancreatic tumour cells (TB32048) directly into the pancreas. In order to perform this experiment, 5 mice from both WT and KO were recruited. Dr. Sarah Spear a post doc in the Centre for Cancer and Inflammation performed the surgery. Unfortunately, two WT mice and one KO mouse had to be culled before the experiment came to an end as mice were showing signs and symptoms of infection. Their behaviour showed characteristics of weakness, pain, and discomfort, as they were barely moving and were not consuming any of their food. They were culled for humane purposes.

Once the tumours were palpable and had reached 1.2cm (approximately), all the mice were culled and tumour, spleen, and blood were collected. Tumours and spleen were weighed. Tumours, spleen, and blood were then stained for FACS analysis (refer to section 5.7.1) in order to compare cell populations and to evaluate whether absence of Raptor within myeloid cells would have an effect on these populations and the tumour microenvironment in general. The results show that there was no significant weight change in tumours or spleen from WT or KO mice (Figure 5.14 A and B). Infiltrating tumour leukocyte populations were quantified and there are no significant differences in B (CD19) and T (CD3) cell populations between WT and KO mice (Figure 5.15 A and B). There was a significant decrease in CD4 T cells in the tumours from KO mice in comparison to their WT counterparts (Figure 5.15 C) but CD8 T cells showed no differences between WT and KO mice (Figure 5.15 D). Also the macrophage population (F480) and MHCII populations showed no differences between WT and KO mice (Figure 5.15 E and F).

Spleen cell populations were also quantified showing a reduction in the B cell population of KO mice in comparison to the WT mice (Figure 5.16 A). All other populations (T cells, T cell subsets, macrophages, and MHCII) showed no significant differences between WT and KO mice (Figure 5.16 B-F). Results for blood cell populations show a reduction in B, T, and CD4 T cells, in KO mice in comparison to WT counterparts (Figure 5.17 A-C). There was no significant change in the CD8 T cell, macrophage, or MHCII populations (Figure 5.17 D-F). The findings in this experiment show that there

are differences between WT and KO mice and suggest that in the absence of Raptor the tumour microenvironment as well as spleen and blood are affected. Since these results are based on preliminary data it is difficult to properly address reasons for these reductions and this experiment must be repeated at least two more times to get clearer picture of whether or not these results will reproduce.

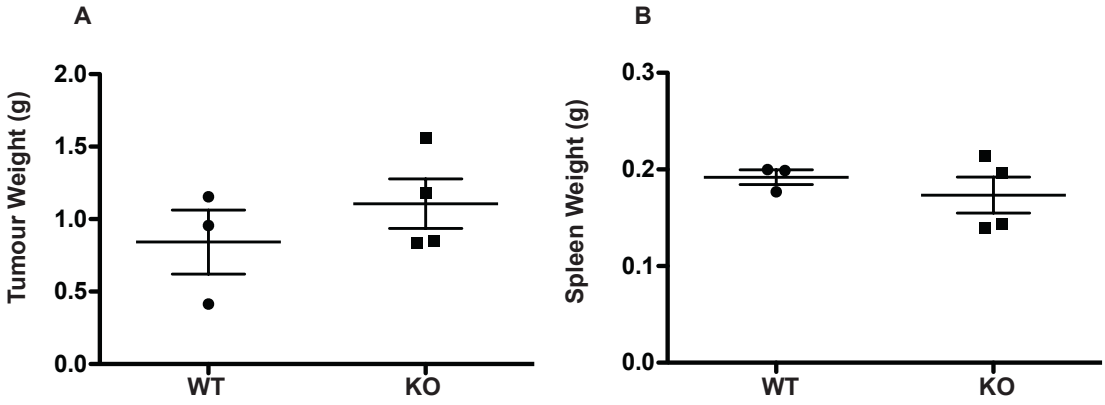

Figure 5.14 Orthotopic tumour experiment: tumour and spleen weights

WT and KO mice were given I.P injections of tamoxifen once per day for 3 consecutive days a week prior the starting of the orthotopic experiment. Mice were injected with $5x10^3$ of murine pancreatic cancer cells (TB32048) orthotopically directly into the pancreas. All mice were given tamoxifen once per week for 3 consecutive days by oral gavages, until end of the experiment in order to sustain KO status. After tumours reached 1.2 cm, mice were culled and tumour and spleen were weighed. There was no significant difference in tumour or spleen weights from either WT or KO mice (A and B). Student's t-test was used to check for statistical significance (tumour n=3; spleen n=4).

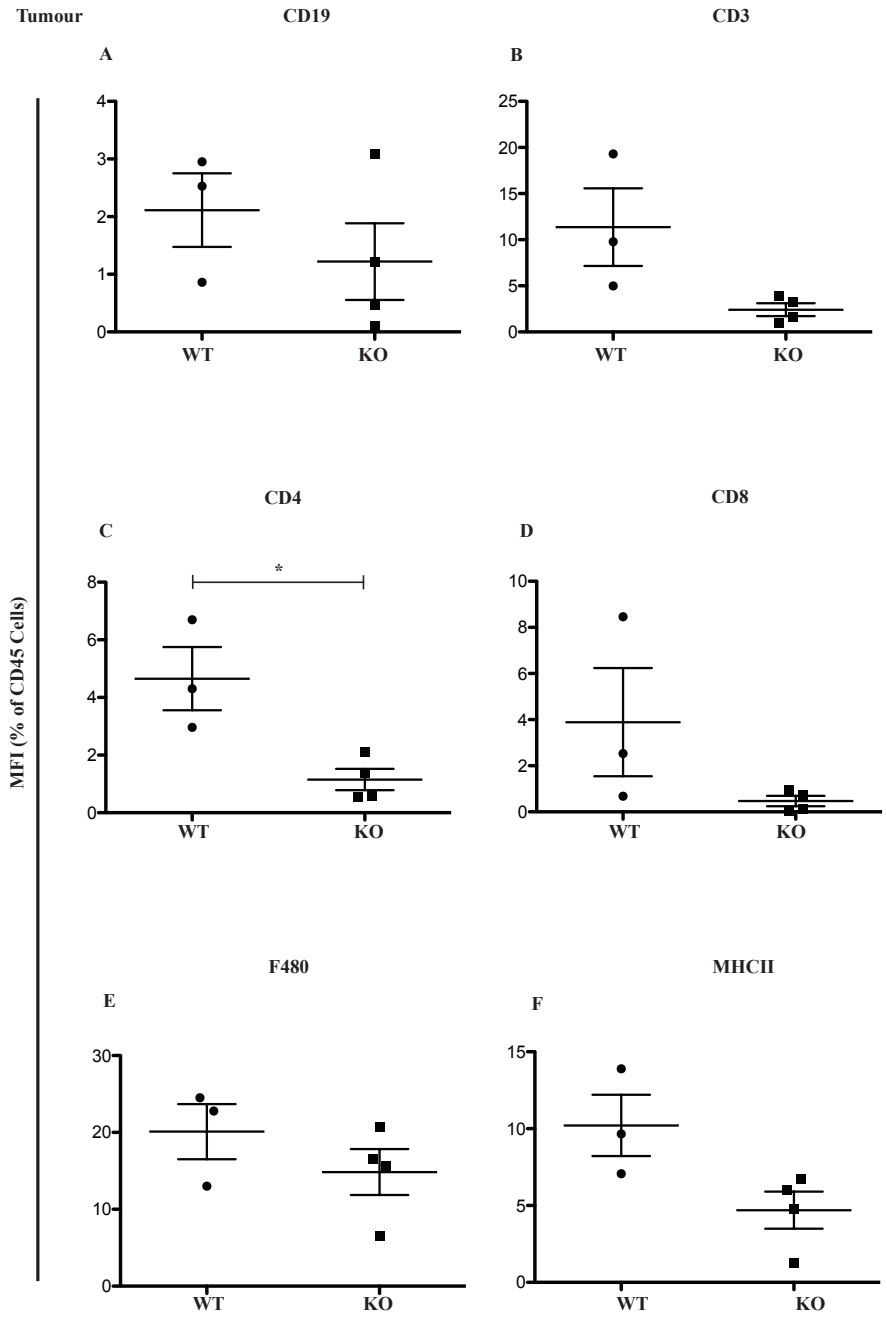

Figure 5.15 Orthotopic tumour experiment: Effects on tumour cells in absence of Raptor

WT and KO mice were given I.P injections of tamoxifen once per day for 3 consecutive days a week prior the starting of the orthotopic experiment. Mice were injected with $5x10^3$ of murine pancreatic cancer cells (TB32048) orthotopically directly into the pancreas. All mice were given tamoxifen once per week for 3 consecutive days by oral gavages, until end of the experiment in order to sustain KO status. After tumours reached 1.2 cm, mice were culled and tumour was collected. FACS was performed and cells were quantified. There was no difference in the B cell (CD19) and T cell (CD3) populations (A and B), but there was a significant decrease in the CD4 population of KO mice in comparison to WT mice (C). CD8 showed no difference in the population between WT and KO (D). Macrophage (F480) population and MHCII showed no differences between WT and KO mice (E and F). WT: (n=3); KO: (n=4) Student's t-test was used to check for statistical significance: p-value of <0.05 is statistically significant (*).

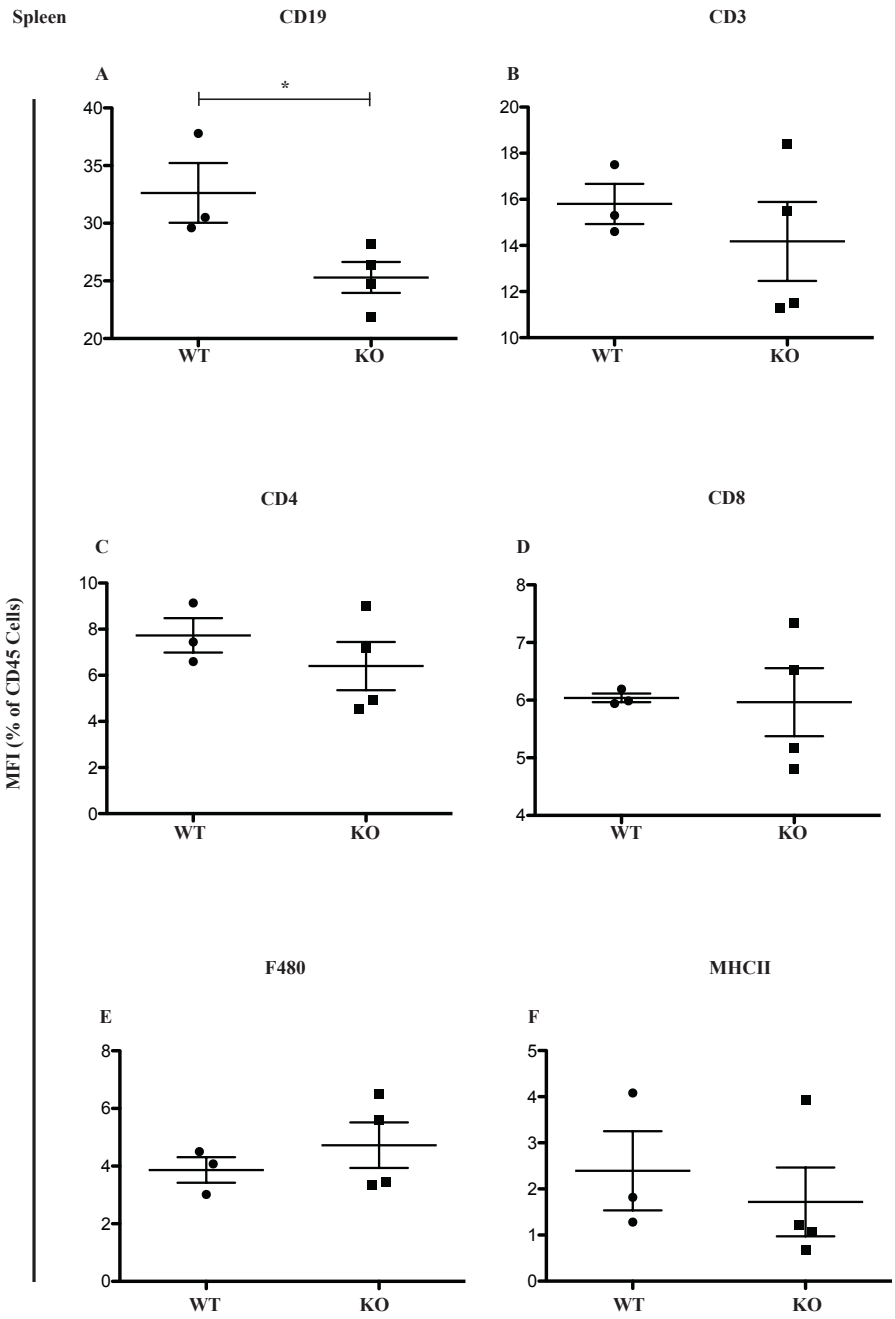

Figure 5.16 Orthotopic tumour experiment: Effects on splenic cells in absence of Raptor

WT and KO mice were given I.P injections of tamoxifen once per day for 3 consecutive days a week prior the starting of the orthotopic experiment. Mice were injected with $5x10^3$ of murine pancreatic cancer cells (TB32048) orthotopically directly into the pancreas. All mice were given tamoxifen once per week for 3 consecutive days by oral gavages, until end of the experiment in order to sustain KO status. After tumours reached 1.2 cm, mice were culled and spleen was collected. FACS was performed and cells were quantified. There was a significant reduction in the B cell (CD19) from KO mice in comparison to the WT (A). There was no significant change in all the rest of the cell populations quantified (T cell (CD3) populations and T cell subset CD4 and CD8, macrophages (F480) and MHCII) between WT and KO mice (B-F). WT: (n=3); KO: (n=4). Student's t-test was used to check for statistical significance: p-value of <0.05 is statistically significant (*).

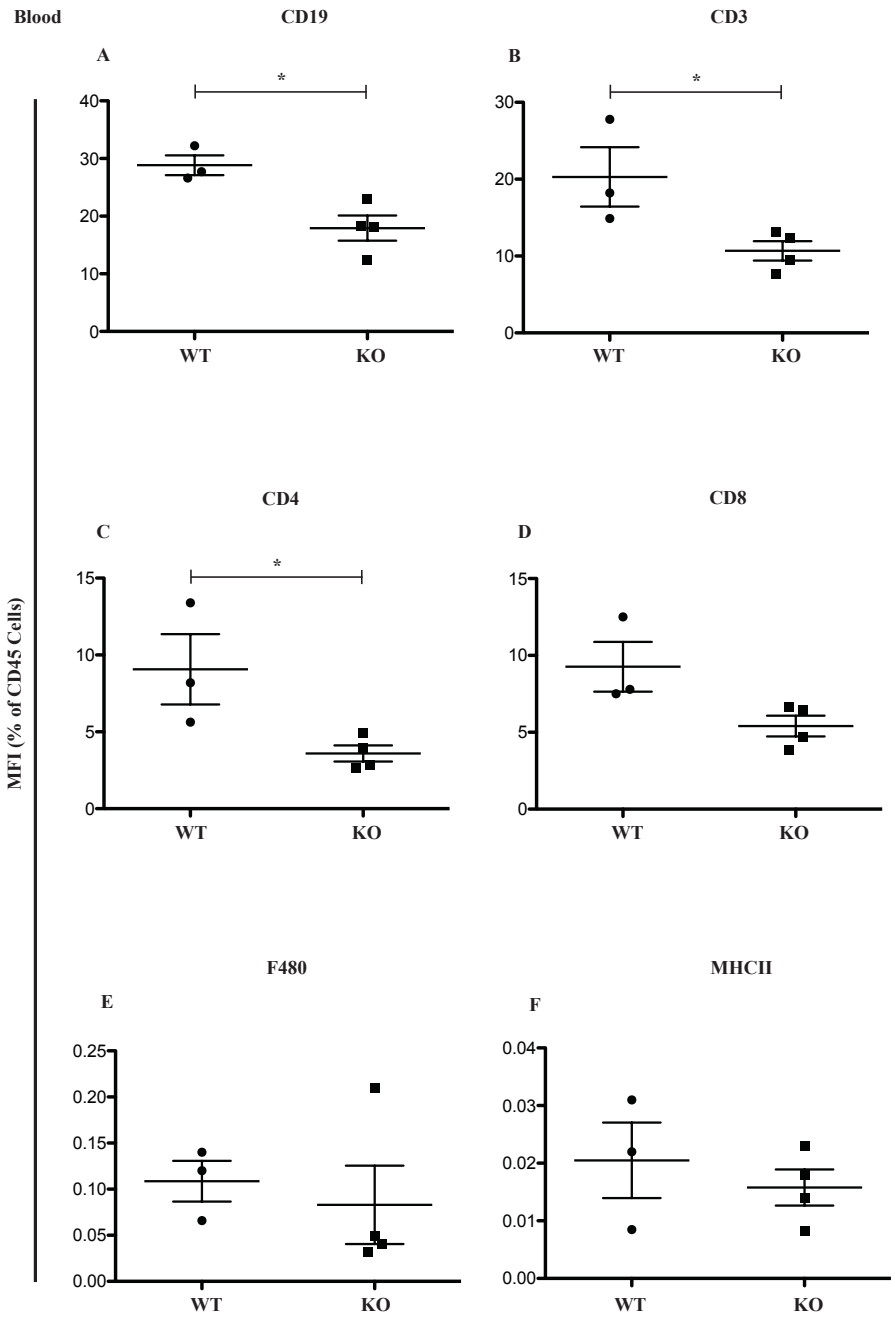

Figure 5.17 Orthotopic tumour experiment: Effects on blood cells in absence of Raptor

WT and KO mice were given I.P injections of tamoxifen once per day for 3 consecutive days a week prior the starting of the orthotopic experiment. Mice were injected with $5x10^3$ of murine pancreatic cancer cells (TB32048) orthotopically directly into the pancreas. All mice were given tamoxifen once per week for 3 consecutive days by oral gavages, until end of the experiment in order to sustain KO status. After tumours reached 1.2 cm, mice were culled and blood was collected. FACS was performed and cells were quantified. There was a significant reduction in the B cell (CD19) population from KO mice in comparison to the WT (A). There was significant reduction in the T cell population and its subset CD4 in KO mice compared to their WT counterparts (B and C). There was no significant change in all the rest of the cell populations quantified (CD8, macrophages (F480) and MHCII) between WT and KO mice (D-F). WT: (n=3); KO: (n=4) Student's t-test was used to check for statistical significance: p-value of <0.05 is statistically significant (*).

5.7.3 Cell populations found in spleen and blood in absence of tumour

Data from both the subcutaneous and orthotopic tumour models were compared to data I obtained from *Raptor WT/WT; Csf1r Cre-ERT* (WT) and *Raptor f/f; Csf1r Cre-ERT* (KO) given I.P injections of tamoxifen once for 3 consecutive days but without any tumour cell injections. These mice were culled on the 4th day and spleen and blood samples were collected in order to compare cell populations of WT and KO mice.

Spleens from Raptor KO mice showed a significant decrease in B cell populations in comparison to their WT counterparts (Figure 5.18 A), this result has also been seen in spleen samples of the orthotopic tumour model (Figure 5.16 A). Mice from Raptor KO have also shown a significant increase in the CD8 T cell population in KO mice compared to the WTs (Figure 5.18 D). This result may be due to CD8 T cell sequestration in the spleen caused by the absence of Raptor. Other cell populations showed no significant differences between WT and KO mice (Figure 5.18 B, C, E, F). Blood samples showed no significant differences in cell populations from both WT and KO mice (Figure 5.19 A-F).

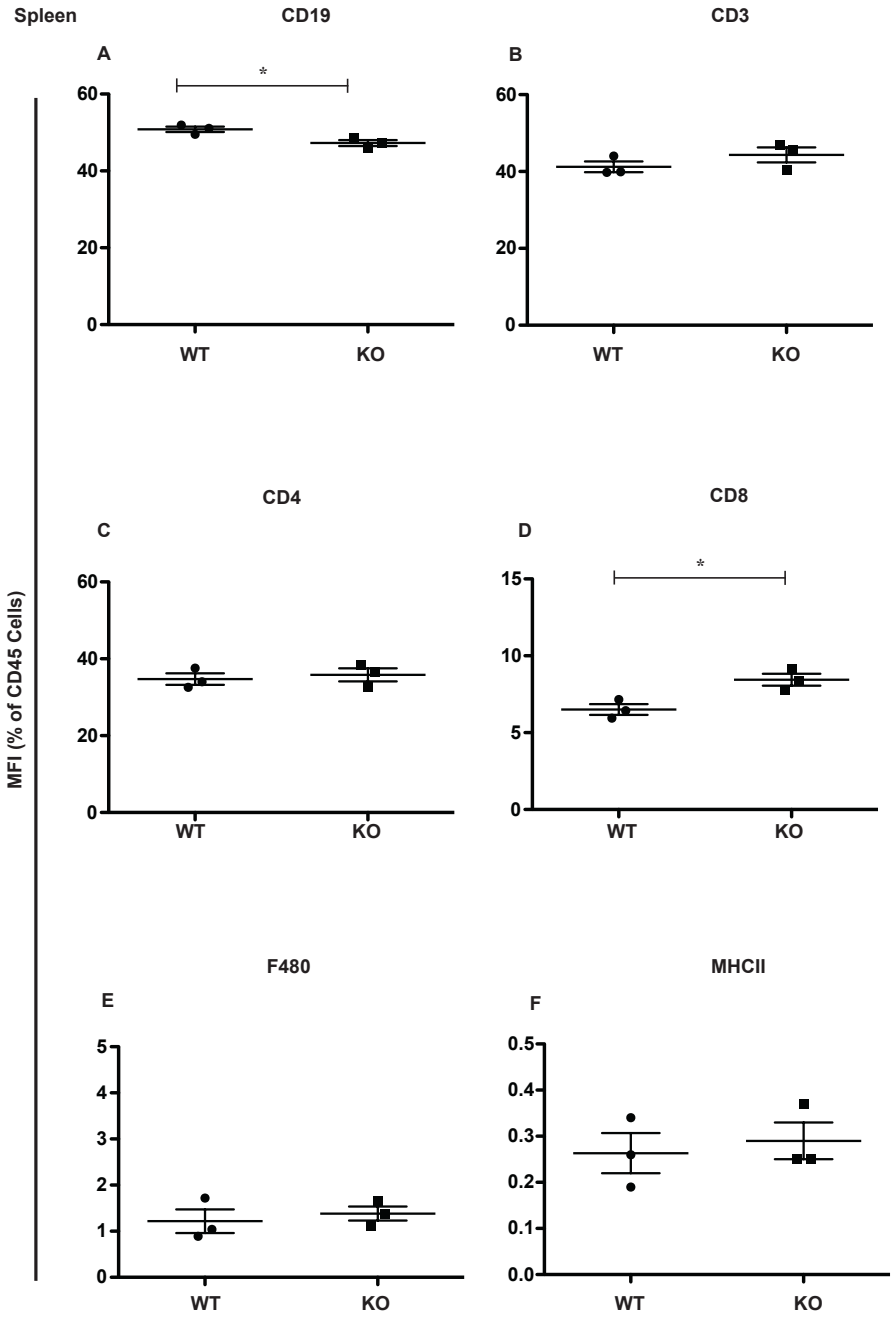

Figure 5.18 Effects on splenic cells in absence of Raptor

WT and KO mice were given I.P injections of tamoxifen once per day for 3 consecutive days, Spleen was collected and FACS was performed and cells were quantified. There was a significant reduction in the B cell (CD19) population from KO mice in comparison to the WT (A). There was no significant reduction in the T cell population and its subset CD4 in KO mice compared to their WT counterparts (B and C). There was a significant increase in the CD8 T cell population observed in the KOs compared to the WTs (D). There were no significant changes in the macrophage population or in the MHCII populations (E and F). WT: (n=3); KO: (n=4). Student's t-test was used to check for statistical significance: p-value of <0.05 is statistically significant (*).

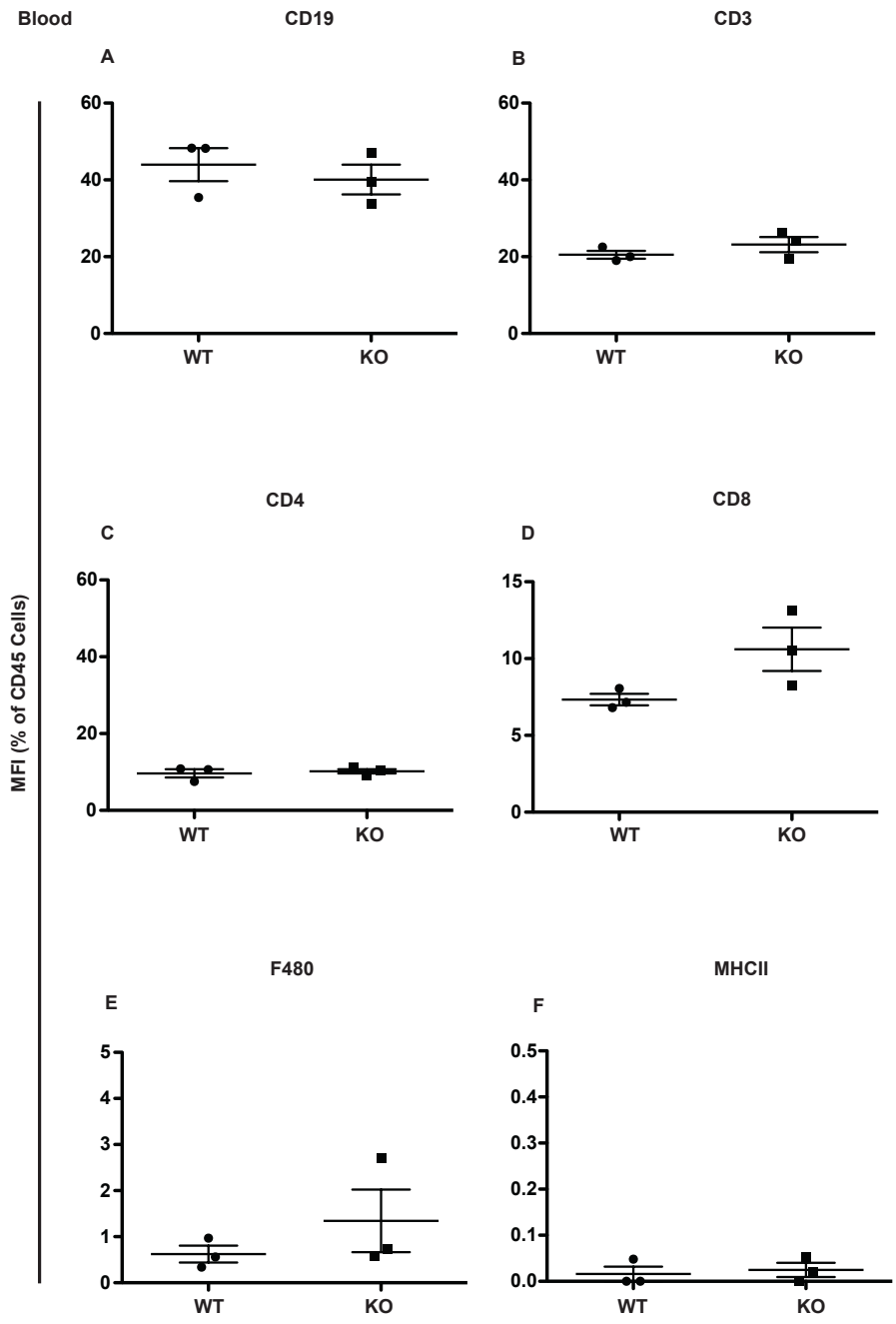

Figure 5.19 Effects on blood cells in absence of Raptor

Mice from WT and KOs were given I.P injections of tamoxifen once per day for 3 consecutive days, Spleen was collected and FACS was performed and cells were quantified. There was no significant reduction in any of the cell populations analysed (A-F). WT: (n=3); KO: (n=4). Student's t-test was used to check for statistical significance.

5.7.4 Result summary of cell populations using different mouse models

I have made a comparison between cell populations from different mouse models in the absence of Raptor either with or without injection of pancreatic tumour cells. It should also be mentioned that orthotopic tumour models are likely to be more clinically relevant since tumour cells are implanted directly into the organ of interest (in my case the pancreas). The orthotopic tumour model is said to have a more realistic microenvironment compared to the subcutaneous site, and may differ in tumour growth kinetics as well.

Model	Cell Populations
Raptor KO model	↓CD19 ↑CD8 (spleen)
Subcutaneous Tumour Model	↓CD4 (blood) ↓F480 (spleen)
Orthotopic tumour Model	↓CD19, CD3, CD4 (blood) ↓CD19 (spleen) ↓CD4 (tumour)

Table 5.1 Differences in leukocyte populations in mice with myeloid cells without Raptor

5.8 Discussion

This chapter included experiments that were performed in order to evaluate how the absence of Raptor may affect macrophage functionality. To my knowledge, there is little information in the literature on the role of Raptor in macrophage phagocytosis. A post doctorate colleague, Dr. Maryam Jangani has been working on Rictor protein that is part of mTORC2 and has seen a reduction of phagocytic capabilities of BMDMs from macrophages in which RICTOR has been deleted (*m.jangani personal communication*). RICTOR is known to play a central role in cytoskeletal reorganisation, through activation of mTORC2 [210], therefore I wanted to investigate whether Raptor may also have a role in macrophage phagocytic ability. I was able to show that in KO BMDMs there was a significant reduction in phagocytic capabilities as BMDMs were unable to engulf both fluorescent beads and apoptotic cancer cells at the same levels when compared to BMDM WT counterparts. This reduction in phagocytic activity may be due to several reasons, which may be attributed to cytoskeletal defects and/or defective cell surface receptors on the BMDMs. In order to address whether this reduction of phagocytic ability in absence of Raptor was due to a cytoskeletal defect, BMDMs were stained with phalloidin which

binds to F-actin and both WT and KO BMDMs were compared for cell size and F-actin intensity and distribution. There was a non-significant reduction of cell size in KO BMDMs in comparison to the WT BMDMs in non-stimulated and stimulated conditions. The mean intensity also showed no significant reduction in non-stimulated and LPS/IFNγ stimulated conditions for KO BMDMs compared to WT. Results for integrated density show a significant reduction in KO BMDMs in comparison with WT in LPS/IFNγ stimulated conditions. These results point to a probable cytoskeleton defect in KO BMDMs. I wanted to assess F/G actin ratios in order to evaluate F-actin polymerisation, since polymerisation is an important mechanism that allows macrophages to phagocytose and allows macrophage movement. The F/G actin ratio shows no difference in polymerisation occurring in general at basal levels and in LPS/IFNγ stimulated conditions within KO BMDMs compared to the WTs. I have interpreted the result this way since G-actin is in the form of monomers, these monomers become filaments of F-actin as polymerisation occurs and F-actin is the active form that is needed for macrophage phagocytosis and motility. If F-actin is reduced, that means less polymerisation is happening and therefore there are more G-actin monomers.

I also wanted to look at receptors in these BMDMs and to investigate whether absence of Raptor may affect them. Results show that there were nonsignificant decreases at basal levels of KO BMDMs compared to WTs for CD64, CD16/32, and CD86, as for CD206 there was a significant decrease at both basal and LPS/IFNγ stimulated conditions. These results show that in the absence of Raptor there are changes in the cytoskeleton and receptors.

Another feature that is important for macrophage function is migration. I assessed migratory capability of WT and KO BMDMs towards fibroblasts and cancer cells. In regards to migration of BMDMs towards fibroblasts there were no significant differences in non-stimulated or stimulated conditions between WT and KOs. Results for BMDM migration towards cancer cells shows that as they are stimulated with either LPS/IFNγ or IL-4/IL-13 there is a reduction seen in KO BMDMs in comparison to WT. These results may only prove the fact that cancer cells secrete factors into the tumour microenvironment that lead to migration of different types of macrophages, some that lead to tumour progression which are of an M2 phenotype and those that are pro-inflammatory which assume an M1 phenotype.

I have also performed preliminary *in vivo* transplantable tumour subcutaneous and orthotopic experiments in mice *Raptor WT/WT; Csf1r Cre-ERT* (WT) and *Raptor f/f; Csf1r Cre-ERT* (KO). I faced many complications with these *in vivo* experiments and therefore it must be noted that repetition of these experiments must be performed in order to increase n numbers and also to make sure that results would reproduce in the next experiments. The preliminary results show that in cases of both subcutaneous and orthotopic experiments there were no significant decreases in tumour or spleen weights. Pertaining to the subcutaneous tumour model, there were significant reductions in the CD4 T cell populations in the blood samples of Raptor KO mice compared to WT mice. Significant reductions were also observed in macrophage populations of the spleen from Raptor KO mice. In regards to the orthotopic tumour model there were significant reductions in all of the B, total T and CD4 T cell populations in the blood samples of Raptor KO mice compared to WT counterparts. These findings could suggest that in the absence of Raptor the tumour microenvironment releases more inflammatory cytokines, therefore there may may be an increase in T regulatory cells present to reduce this inflammation by increasing immunomodulatory cytokine secretions. These immunomodulatory cytokines would lead decreases in CD4 T cell populations. These results also show that macrophages are decreased in the spleen along with B cells, which may be due to mTORC1 regulating macrophages, and an impairment of this regulation would result in the inability of macrophages to secrete proper cytokines used by B cells for their differentiation. In order to have a clear understanding of what is happening to tumours and the microenvironment a repetition of these experiments must be performed.

There is no well-defined understanding of mTOR and its complexes in macrophage migration and functionality and therefore it was important to attempt these experiments to shed light on how mTOR may regulate these aspects in macrophages. What I have observed was that in the absence of Raptor macrophage function was compromised as shown in the reduction of macrophage phagocytic abilities and in the reduction of their migratory capabilities. These functional defects may be due to cytoskeletal impairments and/or reductions in their overall receptors. This was also shown to affect the tumour microenvironment and surrounding cells, which will have an impact on how tumours grow and proliferate. I think that Raptor plays an important role in macrophage function and tumour progression and more experiments should be performed to confirm preliminary findings.

6 Discussion and Plans for Future Work

6.1 Raptor and myeloid cells

mTOR, known as the master growth regulator, senses environmental and nutritional cues such as growth factors, amino acids, energy levels and stress signals from the cells' surroundings integrating them in order to promote growth [211]. This is achieved by phosphorylating key substrates that lead to anabolic processes such as mRNA translation, protein and lipid synthesis [212]. Over the past few years there have been many reports suggesting a central role for the mTOR pathway in diseases such as diabetes, cancer, and neurodegeneration [213] [214] [215]. Deregulation of the mTOR pathway in pancreatic cancer has been implicated in progression to the most invasive form [157]. Present knowledge of pancreatic cancer and its tumour microenvironment has placed great emphasis on TAMs as critical cells in providing the appropriate milieu needed for tumour advancement [216] [217]. Targeting TAMs has been shown to influence the tumour microenvironment, by reducing the immunosuppressive setting provided by TAMs while facilitating a more pro-inflammatory background leading to tumour regression [218] [219]. Despite the current evidence of the mTOR pathway and TAMs being important in pancreatic cancer development, there have not been many studies investigating the link between mTOR and macrophages and evaluation of the extent to which mTOR regulates macrophages, which potentially may have an effect on the tumour microenvironment and thereby tumour progression. This thesis describes *in vitro* and *in vivo* experiments using myeloid cells that lack Raptor (*Raptor f/f; Csf1r Cre-ERT*), which is a key protein in mTORC1 needed for cell survival and development [220]. These experiments were performed to:

1. Characterise the role of Raptor of the mTORC1 complex in myeloid cell maturation, differentiation, and function.
2. Explore the effect of Raptor KO on macrophage polarisation.
3. Explore the effect of Raptor KO on macrophage signalling.
4. Explore the role that myeloid cells lacking Raptor have on the pancreatic tumour microenvironment.

This chapter will discuss the degree to which this thesis has addressed the above aims, the future work that is needed to clarify some of the experimental findings and will outline any additional experiments that could be conducted in regards to the conclusions.

6.1.1 Effects of Raptor on BMDM differentiation and maturation

In vitro experiments were performed using murine bone marrow cells and cultured BMDMs to investigate whether Raptor plays a role in their maturation and differentiation. Mice from *Raptor WT/WT; Csf1r Cre-ERT* (WT) and *Raptor f/f; Csf1r Cre-ERT* (KO) were used to investigate differences in the common myeloid progenitors on chosen differentiation days. By evaluating expression of specific lineage markers, I found that there were no significant differences in the common myeloid progenitors between WT and KO BMDMs. I also investigated whether there would be differences in how these myeloid cells were maturing into macrophages by assessing F4/80 expression. Again there were no significant differences between WT and KO BMDMs. Therefore, I concluded that Raptor does not have a role in macrophage differentiation and maturation. This conclusion is very interesting given the fact that Wang *et al* have published that with a RHEB deletion in macrophages they were able to observe decreased numbers of macrophages from the KOs as compared to WTs [179]. They have also observed decreased differentiation from monocyte to macrophages in their KOs [179], making me speculate that RHEB is a more potent protein within mTORC1 as it is the positive regulator of the complex which lies upstream and furthermore any disruption to RHEB may generate more significant effects on the complex, hence the regulation of monocyte differentiation and maturation.

6.1.2 Effects of Raptor on BMDM polarisation

Further to the *in vitro* studies mentioned in section 6.1.1 with BMDMs, I decided to evaluate the impact Raptor may have on BMDM polarisation. Mice from *Raptor WT/WT; Csf1r Cre-ERT* (WT) and *Raptor f/f; Csf1r Cre-ERT* (KO) were used, and qPCRs were performed on these BMDMs. mRNA levels of different M1(*TNFα, IL-12β, IL-6, iNOS*) and M2 (*IL-10 and MRC1*) genes were investigated, showing Raptor KOs in general had significantly higher levels of M1 genes (*TNFα, IL-12β, IL-6*) in comparison to their WT counterparts both of which were stimulated with LPS/IFNγ or IL-4/IL-13. These results emphasise that once Raptor is lost within BMDMs, inflammatory cytokine mRNA levels increase thereby suggesting a polarisation of these LPS/IFNγ stimulated BMDMs into an M1 phenotype. It has been shown previously by Byles *et al*, Weichhart *et al* and Zhu *et al* that disrupting mTORC1 either genetically or pharmacologically leads to an increase in inflammatory cytokine production in myeloid cells [87 89 88]. However, when I assessed M1

and M2 cytokine secretion from the same BMDMs stimulated with LPS/IFNγ or IL-4/IL-13 translation and secretion of inflammatory cytokines was not observed to the same extent. Most of the M1 cytokines (IL12(p40) and IL-6) were significantly increased in WT BMDMs stimulated with LPS/IFNγ, in comparison to Raptor KOs, apart from TNFα secretion, which was significantly increased at the latest time point for KO BMDMs. The only argument that I would be able to provide for these results is that Raptor KO BMDMs have defective translational abilities; thereby cytokine production is not sustained properly as observed in cytokine production of the WT counterparts, all with the exception of TNFα.

In parallel to the work I have described in this thesis, Dr Maryam Jangani, a postdoc in the lab, has been investigating the role of Rictor on myeloid cells using the same genetic approach. Dr. Jangani used the C57Bl/6 mouse strain to obtain an inducible model that deleted Rictor part of mTORC2 within myeloid compartments, these mice were either *Rictor WT/WT; Csf1r Cre-ERT* (WT) or *Rictor f/f; Csf1r Cre-ERT* (KO). Rictor plays a main role in actin cytoskeletal organisation [45]. Dr. Jangani used BMDMs to assess the role Rictor plays on myeloid cell regulation and function. I compared Raptor KO protein secretion results to those obtained with Rictor KO BMDMs. The Rictor KO BMDMs secreted significantly higher amounts of TNFα, IL12(p70), IL-6 and NOS2 compared to their WT counterparts after LPS/IFNγ stimulation (*m.jangani personal communication*). This was reassuring since mTORC2 does not have a role in protein translation and therefore my results are specific to Raptor that is known to play a major role in protein translation [10 221]. Moreover, I would assume if inflammatory cytokine secretions from Raptor KO BMDMs were higher than their WT counterparts, this would provide a basis in order to manipulate the tumour microenvironment to become more inflammatory. As macrophages would polarise into an M1 phenotype secreting inflammatory cytokines that would reduce the likelihood of tumour progression, instead of cytokines secreted by macrophages found within the tumour environment that are of the M2 phenotype. It is well established that these M2 macrophages release immunomodulatory cytokines, that drive tumour growth [222 223].

6.1.3 Effects of Raptor absence on BMDM signalling pathways

I decided to explore further the mechanistic aspects of BMDM signalling stimulated with LPS/IFNγ in the absence of Raptor. I evaluated intracellular signalling downstream

mTORC1 in the absence of Raptor by observing phosphorylation of S6 (S23S/236). Phosphorylation of S6 was weak, almost negligible in the absence of Raptor compared to WT BMDMs, which is what I was expecting since Raptor is an important constituent of the mTORC1 complex and disruption will influence downstream signalling abilities. This result confirms the KO status of my BMDMs, highlighting that Raptor absence impacts downstream signalling in BMDMs.

I also wanted to investigate whether there would be differences in signalling through the PI3K/Akt axis, since Breuleux *et al* showed that when mTORC1 is inhibited by RAD001 (an mTORC1 inhibitor) more phosphorylation of Akt (S473) occurs [224]. My findings contradicted their results, as I found similarities in Akt phosphorylation between both BMDMs of WT and KOs with only slight reductions of phosphorylation in KO BMDMs. I would assume that for Akt to have approximately similar phosphorylation levels within BMDMs from both WT and Raptor KOs this could be due to Raptor not having such a potent influence on PI3K/Akt signalling as RAD001 had and therefore increase in phosphorylation was not observed indicating Raptor does not affect upstream mTORC1 signalling as much as mTORC1 inhibitors. Furthermore, Breuleux *et al* used tumour cell lines not primary myeloid cells and this may also play a major role in how signalling pathways are activated in comparison to what may be occurring in BMDMs absence of a tumour microenvironment.

I next assessed the ERK signalling pathway as it also feeds into the mTOR pathway by phosphorylating TSC1/2 allowing RHEB to activate mTORC1. I evaluated phosphorylation of ERK (T202/Y206) and found that phosphorylation decreases in KO BMDMs as compared to WT BMDMs. This result is in disagreement to previous findings of Carracedo *et al* where it was observed that by inhibiting mTORC1 through rapamycin or RAD001 in either epithelial cells (breast) or cancer cells (breast) leads to a feedback activation of MEK/ERK signalling [188]. This increased signalling was said to be dependent on the S6K/PI3K/Ras pathway. Despite their findings that were contradictory to my own, I would speculate that Raptor absence has the opposite effect on ERK signalling, as it does not impact upstream signalling thereby generating insignificant inhibitory signs that would usually trigger feedback activation of the ERK pathway thus the reductions I observe on ERK phosphorylation. It may also be due to the difference in

cells used for either experiments as Carracedo *et al* used epithelial cells while I was working on primary myeloid cells.

STAT3 becomes phosphorylated during increased fluxes of growth factors and cytokines, mainly through activation of mTORC1. I have investigated phosphorylation levels of STAT3 (Y705) in absence of Raptor and observed as mTORC1 activation was inhibited, STAT3 phosphorylation was reduced in comparison to WT BMDMs. This result is supported by *Li et al* where their findings showed as mTORC1 was inhibited STAT3 phosphorylation was reduced [190].

As I found that BMDMs in the absence of Raptor to show increased amounts of inflammatory cytokine production at the level of transcription, which might lead them to adopt a more M1 phenotype, I was interested in examining the NFκB signalling pathway to detect whether there would be increased activation through the phosphorylation of the negative regulator of the pathway. Increased IκBα phosphorylation (S32) of KO BMDMs was observed in comparison to WT counterparts, which corresponds to an increase in NFκB signalling activation, this result also has been observed by Weichhart *et al* [89]. Dr. Jangani has also examined phosphorylation levels of S6 on Rictor KOs and found decreased phosphorylation levels in comparison with WT counterparts. Despite this decrease in S6 phosphorylation levels, it remains much higher than phosphorylation levels found with Raptor KOs. Observing her findings pertaining to Akt phosphorylation there was a decrease in phosphorylated Akt from both Rictor WT and KO BMDMs (a slight more reduction in the Rictor KOs). It was not surprising to observe these differences between Akt phosphorylation from Raptor KO and Rictor KO, as mTORC2 targets Akt by downstream signalling, leading to activation of Akt, while mTORC1 does not target Akt. This Rictor KO reduction in phosphorylated Akt levels is an important confirmation of the Rictor KO status (*m.jangani personal communication*).

Taken together these results show that Raptor plays a major role in mTORC1 downstream signalling. It also shows that there is an increase in NFκB signalling which suggests that these BMDMs are polarised to an M1-like phenotype making them more inflammatory as has been also interpreted by Weichhart et al.

6.1.4 Effects of Raptor absence on BMDM function

A series of experiments were then performed to evaluate BMDM function in the absence of Raptor. Investigating phagocytic activity of BMDMs using either fluorescence beads or apoptotic cancer cells showed that in absence of Raptor there was a significant reduction in phagocytosis in comparison to WT BMDM counterparts. My findings are in line with what have been shown in literature using rapamycin as an mTORC1 inhibitor instead of genetic inhibition of the complex as I have done [5] [225]. I was interested in elucidating on what could be the cause of such a reduced phagocytic ability in the absence of Raptor, pursuing two options of cytoskeletal abnormalities or Fc receptor impairment. I checked for cytoskeletal abnormalities by observing whether there were changes occurring in F-actin between BMDMs of KOs in comparison with their WT counterparts. I showed that as these BMDMs were stimulated with LPS/IFNγ there were significant reductions within the integrated density of Raptor KO BMDMs as compared to WTs. This finding in itself is interesting since it shows that F-actin distribution is affected between WT and KOs, suggesting impairment to cytoskeletal rearrangements in the KO BMDMs. I was also interested in looking at F-actin polymerisation in Raptor KO BMDMs. I assessed F-actin polymerisation by acquiring results from an F/G ratio, which demonstrates the capacity of G-actin monomers to polymerise into the active form known as F-actin. My findings show that there were no reductions in the amount of F-actin polymerisation. According to data obtained by integrated density these data are suggestive of cytoskeleton impairment, which was thought provoking, since it is an established fact that mTORC2 is the complex that plays a major role in cytoskeleton rearrangements [210] [226]. Therefore, to observe that mTORC1 also plays a part in this regulation as seen with Raptor absence was interesting. Comparing my data to Dr. Jangani's data (Rictor KO in BMDMs) they were similar to each other, as she has also observed significant reductions in phagocytic abilities within Rictor KO BMDMs in comparison to WTs. Although her F-actin polymerisation data was preliminary (n=1) it showed F-actin polymerisation was reduced in her Rictor BMDM KOs compared to WT counterparts (*m.jangani personal communication*) but more experiments must be performed to increase n numbers in order to prove reductions were truly found.

I subsequently performed experiments to observe whether Raptor may have an effect on the Fc receptors, as phagocytosis is Fc receptor mediated. Looking at non-stimulated

BMDMs there were significant reductions in Fc gamma receptors (FcγRs) CD16/32 and CD64 on BMDMs from Raptor KOs as compared to WTs. This significant reduction was lost as BMDMs were stimulated with LPS/IFNγ. I found this result quite unexpected since I would suspect as these BMDMs become simulated, larger differences in FcγRs would be observed between KOs and WTs. Moreover, I assessed other BMDM receptors, finding significant reductions in mannose receptors of KO compared to WT BMDMs in both non stimulated and LPS/IFNγ stimulated conditions. These findings suggest that in the absence of Raptor these receptors are affected, which may be caused by reduced transcription or increased amounts of receptor internalisation and proteasomal degradation. I compared Raptor KO to Rictor KO BMDM FcγR data, Rictor absence showed reduced expressions of CD64 and CD86 in comparison to the WT counterparts. Dr. Jangani also showed that in the absence of Rictor there were similar expressions of CD16/32 and CD206 between Rictor WTs and KOs (*m.jangani personal communication*), suggesting that Raptor and Rictor influence BMDM receptors in different ways.

Furthermore, I examined the role of Raptor on BMDM migration; while there were no significant differences in migratory capabilities of WT or KO BMDMs towards fibroblasts, I did observe significant reductions in migration of KOs towards cancer cells, while stimulated with LPS/IFNγ as well as IL-4/IL-13. This suggests that cancer cells are producing chemokines that are used to attract BMDMs but in the absence of Raptor, BMDMs are incapable of responding to the chemotactic stimulus appropriately despite stimulation with either LPS/IFNγ or IL-4/IL-13. Dr. Jangani also assessed BMDM migratory capability in absence of Rictor, in which she found reductions in migration of Rictor KO BMDMs towards both fibroblasts and tumour cells. This result was quite interesting as previously stated mTORC2 plays a major role in cell cytoskeletal rearrangements, therefore if Rictor (a major component of the complex) is absent cell motility should be affected. This result also shows that Rictor absence impacts motility more than absence of Raptor on BMDMs (*m.jangani personal communication*).

6.1.5 Role of macrophages in the absence of Raptor in a pancreatic tumour microenvironment

Following previous *in vitro* experiments evaluating impact of Raptor on BMDMs I wanted to assess effects of Raptor absence within macrophages in a pancreatic tumour

microenvironment. Therefore, I performed preliminary *in vivo* experiments using subcutaneous and orthotopic murine tumour models. I would have liked to obtain well-defined results from these experiments but due to lack of time and mice availability, I was unable to perform more than one experiment of each condition. These first *in vivo* experiments showed that tumours containing Raptor KO myeloid cells were no different from WT controls at least in terms of tumour weight. Observing the subcutaneous tumour model, there were significant reductions in the CD4 T cell populations in the blood samples of Raptor KO mice. There were also significant reductions in the macrophage populations observed in the spleen samples of Raptor KO mice. In regards to the orthotopic tumour model there were significant reductions in the B cell populations, total T cell populations and also the CD4 T cell populations in the blood samples of Raptor KO mice. There was a significant reduction in the B cell population found in spleen samples of Raptor KO mice. These findings suggest that within the tumour microenvironment of Raptor KO mice, there is an increase in inflammatory cytokines, therefore I speculate that there may be an increase in T regulatory cells present in the niche to reduce this inflammation by increasing immunomodulatory cytokine secretions, leading to decreases in the CD4 T cell populations. These results also propose that macrophages are decreased in the spleen along with B cells which may be due to the fact that mTORC1 is needed for macrophage regulation and once macrophage regulation is impaired it is unable to secrete proper cytokines used by B cells for their differentiation. Hence this demonstrates the importance of Raptor in macrophages and the impact it holds on the pancreatic tumour microenvironment as shown from the set of results from these two models. Dr. Jangani performed two subcutaneous tumour experiments with the same cancer cells. Her results show that there were significant increases in blood monocytes in Rictor KO mice. There were also significant decreases in the B cell population in blood samples of Rictor KO mice. After tumour digestion it was shown that there was significant increases in the macrophage population of Rictor KO mice, suggesting an increase in macrophage infiltration within the tumour microenvironment (*m.jangani personal communication*).

6.1.6 Summary of results obtained from mice with either Raptor or Rictor KO

In this chapter I have compared my results to those obtained in mice in which Rictor was deleted in the myeloid cell compartment. The table below summarises the similarities and differences in the results obtained with these two approaches (Table 6.1).

	mTORC1 Inhibition	**mTORC2 Inhibition**
Genetic Model	*Raptor f/f; Csf1r Cre-ERT*	*Rictor f/f; Csf1r Cre-ERT*
mRNA Cytokine Expression	↑*TNFα, IL-12b, IL-6*	↑*TNFα, IL-12b, IL-6*
Cytokine Secretion	↑TNFα	↑iNOS, IL-12(p70), IL-6
Downstream Signalling	↓S6 ↓STAT3 ↑NFκB	↓S6↓Akt ↓FOXO
Phagocytosis	↓ towards fluorescence beads ↓ towards cancer cells	↓towards fluorescence beads N/A towards cancer cells
Migration	↓towards cancer cells	↓towards fibroblasts ↓towards cancer cells
F/G actin Ratio	NS	↓(n=1)
Fc Receptors and other receptors	↓CD64, CD16/32, CD206	↓CD64, CD86
Subcutaneous Tumour Model	↓CD4 (blood) ↓F480 (spleen)	↑Monocytes (blood) ↓ B cells (blood) ↑F480 (tumour)
Orthotopic Tumour Model	↓CD19, CD3, CD4 (blood) ↓CD19 (spleen)	N/A

Table 6.1 Summary of results comparing mice with either Raptor or Rictor KO in myeloid cells (NS: non significant ; N/A: not available)

As would be expected Table 6.1, shows some similarities and some differences between Raptor and Rictor KO myeloid cells. In both cases there is an increase in inflammatory cytokine mRNA after LPS/IFNγ stimulation, but differences in protein secretion were evident although increases seen are in pro-inflammatory cytokines. Downstream intracellular signalling shows a decrease in S6 phosphorylation, but downstream targets of mTORC1 and mTORC2 are affected in different ways. Both phagocytosis and migration are impaired which may be due to cytoskeletal and Fc receptor changes.

In summary my findings have shown that Raptor impacts macrophage polarisation and functionality. Furthermore, it affects downstream signalling pathways by inhibiting activation of mTORC1. However, Raptor does not influence macrophage differentiation and maturation status, which suggests Raptor effects are imposed after maturation of macrophages. Nevertheless, more experiments are needed to substantiate these findings as will be described in the next section.

6.2 Plans for Future Work

In this section I would like to describe particular areas that I would want to pursue to further understand the role of Raptor and the mTORC1 pathway in macrophages.

6.2.1 Effects of Raptor absence on BMDM metabolism

These experiments would be undertaken using the Seahorse XF Analyzer on *in vitro* BMDMs.

I would like to investigate whether Raptor has an impact on BMDM metabolism as it is well established that mTORC1 activation is related to cell growth and survival [213] [185]. I WT and KO BMDMs are either left unstimulated, or stimulated with either LPS/IFNγ or IL-4/IL-13. This would provide results pertaining to the glycolytic pathway together with oxygen consumption rates.

6.2.2 Antigen presentation capabilities of BMDMs in absence of Raptor

These experiments would be undertaken using *in vitro* BMDMs co-cultured with T cells (obtained from cell sorting from WT mice).

I would like to assess if Raptor impacts antigen presentation in BMDMs. I would use WT and KO BMDMs either left unstimulated, or stimulated with LPS/IFNγ and culture them with T cells. T cell activation markers would be evaluated by FACS analysis.

6.2.3 *In vivo* LPS-induced inflammation experiment

These experiments would be undertaken using mice from WT and Raptor Ko in myeloid cells. I would inject a non-lethal dose of LPS into the mice, before end point I would cull the mice and inflammatory cytokines would be assessed using a cytokine array kit. These cytokine array kits would provide a more diverse cytokine range, and I would personalise the kit for specific inflammatory cytokines and chemokines, in order to compare differences between WT and Raptor KO mice.

6.2.4 Orthotopic tumour model

I would repeat the orthotopic tumour model two more times with a larger cohort of mice in order to ensure that the results I have obtained in the preliminary experiments are reproducible. It would be important to do detailed studies on the tumour microenvironment including FACS analysis of leukocyte populations and immunohistochemistry.

7 References

1. Zoncu, R., Efeyan, A. & Sabatini, D. M. mTOR: from growth signal integration to cancer, diabetes and ageing. *Nat. Rev. Mol. Cell Biol.* **12,** 21–35 (2011).
2. Delgoffe, G. M. & Powell, J. D. MTOR: Taking cues from the immune microenvironment. *Immunology* **127,** 459–465 (2009).
3. Mills, R. E. & Jameson, J. M. T cell dependence on mTOR signaling. *Cell Cycle* **8,** 545–548 (2009).
4. Weichhart, T. *et al.* The multiple facets of mTOR in immunity. *Trends Immunol.* **30,** 218–26 (2009).
5. Thomson, A. W., Turnquist, H. R. & Raimondi, G. Immunoregulatory functions of mTOR inhibition. *Nat. Rev. Immunol.* **9,** 324–37 (2009).
6. Schmitz, F. *et al.* Mammalian target of rapamycin (mTOR) orchestrates the defense program of innate immune cells. *Eur. J. Immunol.* **38,** 2981–2992 (2008).
7. Guertin, D. A. & Sabatini, D. M. The pharmacology of mTOR inhibition. *Sci Signal* **2,** pe24 (2009).
8. VÉZINA, C., KUDELSKI, A. & SEHGAL, S. N. Rapamycin (AY-22,989), a new antifungal antibiotic. I. Taxonomy of the producing streptomycete and isolation of the active principle. *J. Antibiot. (Tokyo).* **28,** 721–726 (1975).
9. Sabatini, D. M. mTOR and cancer: insights into a complex relationship. *Nat. Rev. Cancer* **6,** 729–734 (2006).
10. Kim, D. H. *et al.* mTOR interacts with raptor to form a nutrient-sensitive complex that signals to the cell growth machinery. *Cell* **110,** 163–175 (2002).
11. Oshiro, N. *et al.* Dissociation of raptor from mTOR is a mechanism of rapamycin-induced inhibition of mTOR function. *Genes to Cells* **9,** 359–366 (2004).
12. Harding, M. W., Galat, a, Uehling, D. E. & Schreiber, S. L. A receptor for the immunosuppressant FK506 is a cis-trans peptidyl-prolyl isomerase. *Nature* **341,** 758–760 (1989).
13. Laplante, M. & Sabatini, D. M. mTOR signaling at a glance. *J Cell Sci* **122,** 3589–3594 (2009).
14. Fonseca, B. D., Smith, E. M., Lee, V. H. Y., MacKintosh, C. & Proud, C. G. PRAS40 is a target for mammalian target of rapamycin complex 1 and is required for signaling downstream of this complex. *J. Biol. Chem.* **282,** 24514–24524 (2007).

15. Peterson, T. R. *et al.* DEPTOR Is an mTOR Inhibitor Frequently Overexpressed in Multiple Myeloma Cells and Required for Their Survival. *Cell* **137,** 873–886 (2009).
16. Abraham, R. T. & Wiederrecht, G. J. Immunopharmacology of rapamycin. *Annu. Rev. Immunol.* **14,** 483–510 (1996).
17. Abraham, R. T. Mammalian target of rapamycin: immunosuppressive drugs uncover a novel pathway of cytokine receptor signaling. *Curr Opin Immunol* **10,** 330–336 (1998).
18. Sarbassov, D. D. *et al.* Prolonged Rapamycin Treatment Inhibits mTORC2 Assembly and Akt/PKB. *Mol. Cell* **22,** 159–168 (2006).
19. Sengupta, S., Peterson, T. R. & Sabatini, D. M. Regulation of the mTOR Complex 1 Pathway by Nutrients, Growth Factors, and Stress. *Molecular Cell* **40,** 310–322 (2010).
20. Yamagata, K. *et al.* rheb, a growth factor- and synaptic activity-regulated gene, encodes a novel ras-related protein. *J. Biol. Chem.* **269,** 16333–16339 (1994).
21. Caron, E. *et al.* A comprehensive map of the mTOR signaling network. *Mol. Syst. Biol.* **6,** 453 (2010).
22. Saucedo, L. J. *et al.* Rheb promotes cell growth as a component of the insulin/TOR signalling network. *Nat. Cell Biol.* **5,** 566–571 (2003).
23. Ma, L., Chen, Z., Erdjument-Bromage, H., Tempst, P. & Pandolfi, P. P. Phosphorylation and functional inactivation of TSC2 by Erk: Implications for tuberous sclerosis and cancer pathogenesis. *Cell* **121,** 179–193 (2005).
24. Sancak, Y. *et al.* The Rag GTPases bind raptor and mediate amino acid signaling to mTORC1. *Science* **320,** 1496–501 (2008).
25. Kim, E., Goraksha-Hicks, P., Li, L., Neufeld, T. P. & Guan, K.-L. Regulation of TORC1 by Rag GTPases in nutrient response. *Nat. Cell Biol.* **10,** 935–45 (2008).
26. Sancak, Y. *et al.* Ragulator-rag complex targets mTORC1 to the lysosomal surface and is necessary for its activation by amino acids. *Cell* **141,** 290–303 (2010).
27. Powell, J. D. & Delgoffe, G. M. The Mammalian Target of Rapamycin: Linking T Cell Differentiation, Function, and Metabolism. *Immunity* **33,** 301–311 (2010).
28. Colombetti, S., Basso, V., Mueller, D. L. & Mondino, A. Prolonged TCR/CD28 engagement drives IL-2-independent T cell clonal expansion through signaling mediated by the mammalian target of rapamycin. *J. Immunol.* **176,** 2730–2738 (2006).

29. Stephenson, L. M., Park, D.-S., Mora, A. L., Goenka, S. & Boothby, M. Sequence motifs in IL-4R alpha mediating cell-cycle progression of primary lymphocytes. *J. Immunol.* **175,** 5178–85 (2005).
30. Motoshima, H., Goldstein, B. J., Igata, M. & Araki, E. AMPK and cell proliferation – AMPK as a therapeutic target for atherosclerosis and cancer. *J Physiol* **5741,** 63–71 (2006).
31. Hardie, D. G. AMP-activated/SNF1 protein kinases: conserved guardians of cellular energy. *Nat. Rev. Mol. Cell Biol.* **8,** 774–785 (2007).
32. Inoki, K. *et al.* TSC2 Integrates Wnt and Energy Signals via a Coordinated Phosphorylation by AMPK and GSK3 to Regulate Cell Growth. *Cell* **126,** 955–968 (2006).
33. Brugarolas, J. *et al.* Regulation of mTOR function in response to hypoxia by REDD1 and the TSC1/TSC2 tumor suppressor complex. *Genes Dev.* **18,** 2893–2904 (2004).
34. Deyoung, M. P., Horak, P., Sofer, A., Sgroi, D. & Ellisen, L. W. Hypoxia regulates TSC1/2-mTOR signaling and tumor suppression through REDD1-mediated 14-3-3 shuttling. *Genes Dev.* **22,** 239–251 (2008).
35. Sarbassov, D. D., Guertin, D. A., Ali, S. M. & Sabatini, D. M. Phosphorylation and regulation of Akt/PKB by the rictor-mTOR complex. *Science* **307,** 1098–101 (2005).
36. Lawlor, M. A. & Alessi, D. R. PKB/Akt: a key mediator of cell proliferation, survival and insulin responses? *J. Cell Sci.* **114,** 2903–10 (2001).
37. Powell, J. D., Pollizzi, K. N., Heikamp, E. B. & Horton, M. R. Regulation of immune responses by mTOR. *Annu. Rev. Immunol.* **30,** 39–68 (2012).
38. Ma, X. M. & Blenis, J. Molecular mechanisms of mTOR-mediated translational control. *Nat. Rev. Mol. Cell Biol.* **5,** 827–835 (2004).
39. Yu, L. *et al.* Autophagy termination and lysosome reformation regulated by mTOR. *Nature* **465,** 942–946 (2010).
40. Jung, C. H., Ro, S. H., Cao, J., Otto, N. M. & Kim, D. H. MTOR regulation of autophagy. *FEBS Letters* **584,** 1287–1295 (2010).
41. Beugnet, A., Tee, A. R., Taylor, P. M. & Proud, C. G. Regulation of targets of mTOR (mammalian target of rapamycin) signalling by intracellular amino acid availability. *Biochem. J.* **372,** 555–66 (2003).
42. Raught, B. *et al.* Phosphorylation of eucaryotic translation initiation factor 4B

Ser422 is modulated by S6 kinases. *EMBO J.* **23,** 1761–1769 (2004).

43. Dorrello, N. V. *et al.* S6K1- and betaTRCP-mediated degradation of PDCD4 promotes protein translation and cell growth. *Science* **314,** 467–471 (2006).
44. Kamada, Y. *et al.* Tor-mediated induction of autophagy via an Apg1 protein kinase complex. *J. Cell Biol.* **150,** 1507–1513 (2000).
45. Dos, D. S. *et al.* Rictor, a novel binding partner of mTOR, defines a rapamycin-insensitive and raptor-independent pathway that regulates the cytoskeleton. *Curr. Biol.* **14,** 1296–1302 (2004).
46. Jacinto, E. *et al.* Mammalian TOR complex 2 controls the actin cytoskeleton and is rapamycin insensitive. *Nat. Cell Biol.* **6,** 1122–1128 (2004).
47. Loewith, R. *et al.* Two TOR complexes, only one of which is rapamycin sensitive, have distinct roles in cell growth control. *Mol. Cell* **10,** 457–468 (2002).
48. Guertin, D. A. *et al.* Ablation in Mice of the mTORC Components raptor, rictor, or mLST8 Reveals??that mTORC2 Is Required for Signaling to Akt-FOXO and PKC??, but Not S6K1. *Dev. Cell* **11,** 859–871 (2006).
49. Zhang, X., Tang, N., Hadden, T. J. & Rishi, A. K. Akt, FoxO and regulation of apoptosis. *Biochimica et Biophysica Acta - Molecular Cell Research* **1813,** 1978–1986 (2011).
50. García-Martínez, J. M. & Alessi, D. R. mTOR complex 2 (mTORC2) controls hydrophobic motif phosphorylation and activation of serum- and glucocorticoid-induced protein kinase 1 (SGK1). *Biochem. J.* **416,** 375–385 (2008).
51. Brunet, A. *et al.* Protein kinase SGK mediates survival signals by phosphorylating the forkhead transcription factor FKHRL1 (FOXO3a). *Mol. Cell. Biol.* **21,** 952–65 (2001).
52. Ikenoue, T., Inoki, K., Yang, Q., Zhou, X. & Guan, K.-L. Essential function of TORC2 in PKC and Akt turn motif phosphorylation, maturation and signalling. *EMBO J.* **27,** 1919–31 (2008).
53. Samuels, Y. & Ericson, K. Oncogenic PI3K and its role in cancer. *Curr. Opin. Oncol.* **18,** 77–82 (2006).
54. Cully, M., You, H., Levine, A. J. & Mak, T. W. Beyond PTEN mutations: the PI3K pathway as an integrator of multiple inputs during tumorigenesis. *Nat. Rev. Cancer* **6,** 184–192 (2006).
55. Wander, S. A., Hennessy, B. T. & Slingerland, J. M. Next-generation mTOR inhibitors in clinical oncology: How pathway complexity informs therapeutic

strategy. *Journal of Clinical Investigation* **121,** 1231–1241 (2011).

56. Decker, T. *et al.* Rapamycin-induced g1 arrest in cycling B-CLL cells is associated with reduced expression of cyclin D3, cyclin E, cyclin A, and survivin. *Blood* **101,** 278–285 (2003).
57. Luo, Y. *et al.* Rapamycin resistance tied to defective regulation of p27Kip1. *Mol. Cell. Biol.* **16,** 6744–6751 (1996).
58. Guba, M. *et al.* Rapamycin inhibits primary and metastatic tumor growth by antiangiogenesis: involvement of vascular endothelial growth factor. *Nat. Med.* **8,** 128–35 (2002).
59. Medzhitov, R. Origin and physiological roles of inflammation. *Nature* **454,** 428–435 (2008).
60. Coussens, L. M. & Werb, Z. Inflammation and cancer. *Nature* **420,** 860–867 (2002).
61. Medzhitov, R. Inflammation 2010: New Adventures of an Old Flame. *Cell* **140,** 771–776 (2010).
62. Kawai, T. & Akira, S. The role of pattern-recognition receptors in innate immunity: update on Toll-like receptors. *Nat. Immunol.* **11,** 373–84 (2010).
63. Rossol, M. *et al.* LPS-induced Cytokine Production in Human Monocytes and Macrophages. *Crit. Rev. Immunol.* **31,** 379–446 (2011).
64. Sica, A. & Mantovani, A. Macrophage plasticity and polarization: In vivo veritas. *Journal of Clinical Investigation* **122,** 787–795 (2012).
65. Mosser, D. M. & Edwards, J. P. Exploring the full spectrum of macrophage activation. *Nat. Rev. Immunol.* **8,** 958–69 (2008).
66. Murray, P. J. & Wynn, T. A. Protective and pathogenic functions of macrophage subsets. *Nat. Rev. Immunol.* **11,** 723–737 (2011).
67. Biron, C. A. Role of early cytokines, including alpha and beta interferons (IFN-alpha/beta), in innate and adaptive immune responses to viral infections. *Semin. Immunol.* **10,** 383–390 (1998).
68. Gessner, A., Mohrs, K. & Mohrs, M. Mast cells, basophils, and eosinophils acquire constitutive IL-4 and IL-13 transcripts during lineage differentiation that are sufficient for rapid cytokine production. *J. Immunol.* **174,** 1063–1072 (2005).
69. Voehringer, D. Protective and pathological roles of mast cells and basophils. *Nat. Rev. Immunol.* **13,** 362–75 (2013).
70. Raveney, B. J. E., Copland, D. A., Calder, C. J., Dick, A. D. & Nicholson, L. B.

TNFR1 signalling is a critical checkpoint for developing macrophages that control of T-cell proliferation. *Immunology* **131,** 340–349 (2010).

71. Harvey, B. P., Gee, R. J., Haberman, A. M., Shlomchik, M. J. & Mamula, M. J. Antigen presentation and transfer between B cells and macrophages. *Eur. J. Immunol.* **37,** 1739–1751 (2007).
72. Carrasco, Y. R. & Batista, F. D. B Cells Acquire Particulate Antigen in??a Macrophage-Rich Area at the Boundary between the Follicle and??the Subcapsular Sinus of the Lymph Node. *Immunity* **27,** 160–171 (2007).
73. Geissmann, F. *et al.* Development of monocytes, macrophages, and dendritic cells. *Science* **327,** 656–61 (2010).
74. Haldar, M. & Murphy, K. M. Origin, development, and homeostasis of tissue-resident macrophages. *Immunol. Rev.* **262,** 25–35 (2014).
75. Gordon, S. & Taylor, P. R. Monocyte and macrophage heterogeneity. [Nat Rev Immunol. 2005] - PubMed result. *Nat. Rev. Immunol.* **5,** 953–64 (2005).
76. Geissmann, F., Gordon, S., Hume, D. A., Mowat, A. M. & Randolph, G. J. Unravelling mononuclear phagocyte heterogeneity. *Nat Rev Immunol* **10,** 453–460 (2010).
77. Hume, D. A. Macrophages as APC and the dendritic cell myth. *J. Immunol.* **181,** 5829–5835 (2008).
78. Gordon, S. & Martinez, F. O. Alternative activation of macrophages: Mechanism and functions. *Immunity* **32,** 593–604 (2010).
79. Mahmoud, S. M. *et al.* Tumour-infiltrating macrophages and clinical outcome in breast cancer. *J Clin Pathol* **65,** 159–163 (2012).
80. Mantovani, A. & Sica, A. Macrophages, innate immunity and cancer: balance, tolerance, and diversity. *Curr Opin Immunol* **22,** 231–237 (2010).
81. Davis, M. J. *et al.* Macrophage M1/M2 polarization dynamically adapts to changes in cytokine microenvironments in Cryptococcus neoformans infection. *MBio* **4,** e00264-13 (2013).
82. Biswas, S. K. & Mantovani, A. Macrophage plasticity and interaction with lymphocyte subsets: cancer as a paradigm. *Nat Immunol* **11,** 889–896 (2010).
83. Martinez, F. O. *et al.* Genetic programs expressed in resting and IL-4 alternatively activated mouse and human macrophages: similarities and differences. *Blood* **121,** e57-69 (2013).
84. Chawla, A. Control of macrophage activation and function by PPARs. *Circulation*

Research **106,** 1559–1569 (2010).

85. Van den Bossche, J. *et al.* Arginase-1-independent polyamine production stimulates the expression of IL-4-induced alternatively activated macrophage markers while inhibiting LPS-induced expression of inflammatory genes. *J. Leukoc. Biol.* **91,** 685–99 (2012).
86. Vats, D. *et al.* Oxidative metabolism and PGC-1?? attenuate macrophage-mediated inflammation. *Cell Metab.* **4,** 13–24 (2006).
87. Byles, V. *et al.* The TSC-mTOR pathway regulates macrophage polarization. *Nat. Commun.* **4,** 2834 (2013).
88. Zhu, L. *et al.* TSC1 controls macrophage polarization to prevent inflammatory disease. *Nat. Commun.* **5,** 4696 (2014).
89. Weichhart, T. *et al.* The TSC-mTOR Signaling Pathway Regulates the Innate Inflammatory Response. *Immunity* **29,** 565–577 (2008).
90. Rokutanda, S. *et al.* Akt regulates skeletal development through GSK3, mTOR, and FoxOs. *Dev. Biol.* **328,** 78–93 (2009).
91. Festuccia, W. T., Pouliot, P., Bakan, I., Sabatini, D. M. & Laplante, M. Myeloid-specific rictor deletion induces M1 macrophage polarization and potentiates in vivo pro-inflammatory response to lipopolysaccharide. *PLoS One* **9,** (2014).
92. Xie, S. *et al.* Identification of a role for the PI3K/AKT/mTOR signaling pathway in innate immune cells. *PLoS One* **9,** (2014).
93. Chen, W. *et al.* Macrophage-induced tumor angiogenesis is regulated by the TSC2-mTOR pathway. *Cancer Res.* **72,** 1363–1372 (2012).
94. Ai, D. *et al.* Disruption of mammalian target of rapamycin complex 1 in macrophages decreases chemokine gene expression and atherosclerosis. *Circ. Res.* **114,** 1576–1584 (2014).
95. Allen, A. *et al.* The novel cyclophilin binding compound, sanglifehrin A, disassociates G1 cell cycle arrest from tolerance induction. *J. Immunol.* **172,** 4797–4803 (2004).
96. Powell, J. D., Lerner, C. G. & Schwartz, R. H. Inhibition of cell cycle progression by rapamycin induces T cell clonal anergy even in the presence of costimulation. *J. Immunol.* **162,** 2775–2784 (1999).
97. Palmer, C. S., Ostrowski, M., Balderson, B., Christian, N. & Crowe, S. M. Glucose metabolism regulates T cell activation, differentiation, and functions. *Frontiers in Immunology* **6,** (2015).

98. Vander Heiden, M. G., Cantley, L. C. & Thompson, C. B. Understanding the Warburg effect: the metabolic requirements of cell proliferation. *Science* **324,** 1029–33 (2009).

99. Jones, R. G. & Thompson, C. B. Revving the Engine: Signal Transduction Fuels T Cell Activation. *Immunity* **27,** 173–178 (2007).

100. Frauwirth, K. a & Thompson, C. B. Regulation of T lymphocyte metabolism. *J. Immunol.* **172,** 4661–4665 (2004).

101. Bong, S. J. *et al.* AICAR suppresses IL-2 expression through inhibition of GSK-3 phosphorylation and NF-AT activation in Jurkat T cells. *Biochem. Biophys. Res. Commun.* **332,** 339–346 (2005).

102. Hidayat, S. *et al.* Inhibition of amino acid-mTOR signaling by a leucine derivative induces G1 arrest in Jurkat cells. *Biochem. Biophys. Res. Commun.* **301,** 417–423 (2003).

103. Zhang, S. *et al.* Constitutive reductions in mTOR alter cell size, immune cell development, and antibody production. *Blood* **117,** 1228–1238 (2011).

104. Benhamron, S. & Tirosh, B. Direct activation of mTOR in B lymphocytes confers impairment in B-cell maturation andloss of marginal zone B cells. *Eur. J. Immunol.* **41,** 2390–2396 (2011).

105. Donahue, a. C. & Fruman, D. A. Proliferation and Survival of Activated B Cells Requires Sustained Antigen Receptor Engagement and Phosphoinositide 3-Kinase Activation. *J. Immunol.* **170,** 5851–5860 (2003).

106. Sakata, A., Kuwahara, K., Ohmura, T., Inui, S. & Sakaguchi, N. Involvement of a rapamycin-sensitive pathway in CD40-mediated activation of murine B cells in vitro. in *Immunology Letters* **68,** 301–309 (1999).

107. Donahue, A. C. & Fruman, D. A. Distinct signaling mechanisms activate the target of rapamycin in response to different B-cell stimuli. *Eur. J. Immunol.* **37,** 2923–2936 (2007).

108. Monson, N. L. *et al.* Differentiation Stage-Specific Requirement in Hypoxia-Inducible Factor-1–Regulated Glycolytic Pathway during Murine B Cell Development in Bone Marrow.pdf. *J. Neuroinflammation* **11,** 22 (2014).

109. Ellis, H. Anatomy of the pancreas. *Surgery* **25,** 72–73 (2007).

110. Mahadevan, V. Anatomy of the pancreas and spleen. *Surg. (United Kingdom)* **34,** 261–265 (2016).

111. Coupland, V. H. *et al.* Incidence and survival for hepatic, pancreatic and biliary

cancers in England between 1998 and 2007. *Cancer Epidemiol* **36,** e207-14 (2012).

112. Jemal, A. *et al.* Cancer statistics, 2009. *CA Cancer J Clin* **59,** 225–249 (2009).
113. Burris 3rd, H. A. *et al.* Improvements in survival and clinical benefit with gemcitabine as first-line therapy for patients with advanced pancreas cancer: a randomized trial. *J Clin Oncol* **15,** 2403–2413 (1997).
114. Brat, D. J., Lillemoe, K. D., Yeo, C. J., Warfield, P. B. & Hruban, R. H. Progression of pancreatic intraductal neoplasias to infiltrating adenocarcinoma of the pancreas. *Am J Surg Pathol* **22,** 163–169 (1998).
115. Hruban, R. H. *et al.* An illustrated consensus on the classification of pancreatic intraepithelial neoplasia and intraductal papillary mucinous neoplasms. *Am J Surg Pathol* **28,** 977–987 (2004).
116. Maitra, A. & Hruban, R. H. Pancreatic cancer. *Annu. Rev. Pathol.* **3,** 157–88 (2008).
117. Morris, J. P., Wang, S. C. & Hebrok, M. KRAS, Hedgehog, Wnt and the twisted developmental biology of pancreatic ductal adenocarcinoma. *Nat. Rev. Cancer* **10,** 683–95 (2010).
118. Feig, C. *et al.* The pancreas cancer microenvironment. *Clinical Cancer Research* **18,** 4266–4276 (2012).
119. Filipazzi, P., Huber, V. & Rivoltini, L. Phenotype, function and clinical implications of myeloid-derived suppressor cells in cancer patients. *Cancer Immunol Immunother* **61,** 255–263 (2012).
120. Kundu, J. K. & Surh, Y. J. Inflammation: gearing the journey to cancer. *Mutat Res* **659,** 15–30 (2008).
121. Wu, Y. & Zhou, B. P. TNF-alpha/NF-kappaB/Snail pathway in cancer cell migration and invasion. *Br J Cancer* **102,** 639–644 (2010).
122. Balkwill, F. & Mantovani, A. Inflammation and cancer: back to Virchow? *Lancet* **357,** 539–545 (2001).
123. Wesolowski, R., Markowitz, J. & Carson 3rd, W. E. Myeloid derived suppressor cells - a new therapeutic target in the treatment of cancer. *J Immunother Cancer* **1,** 10 (2013).
124. McKay, C. J., Glen, P. & McMillan, D. C. Chronic inflammation and pancreatic cancer. *Best Pr. Res Clin Gastroenterol* **22,** 65–73 (2008).
125. Yachida, S. *et al.* Clinical significance of the genetic landscape of pancreatic cancer and implications for identification of potential long-term survivors. *Clin*

Cancer Res **18,** 6339–6347 (2012).

126. Clark, C. E. *et al.* Dynamics of the immune reaction to pancreatic cancer from inception to invasion. *Cancer Res.* **67,** 9518–9527 (2007).
127. Tang, Y. *et al.* An increased abundance of tumor-infiltrating regulatory t cells is correlated with the progression and prognosis of pancreatic ductal adenocarcinoma. *PLoS One* **9,** (2014).
128. Mantovani, A. The growing diversity and spectrum of action of myeloid-derived suppressor cells. *Eur. J. Immunol.* **40,** 3317–3320 (2010).
129. Gros, A. *et al.* Myeloid cells obtained from the blood but not from the tumor can suppress T-cell proliferation in patients with melanoma. *Clin Cancer Res* **18,** 5212–5223 (2012).
130. Gabrilovich, D. I., Ostrand-Rosenberg, S. & Bronte, V. Coordinated regulation of myeloid cells by tumours. *Nat Rev Immunol* **12,** 253–268 (2012).
131. Stromnes, I. M. *et al.* Targeted depletion of an MDSC subset unmasks pancreatic ductal adenocarcinoma to adaptive immunity. *Gut* **63,** 1769–81 (2014).
132. Lewis, C. E. & Pollard, J. W. Distinct role of macrophages in different tumor microenvironments. *Cancer Res* **66,** 605–612 (2006).
133. Allavena, P., Sica, A., Solinas, G., Porta, C. & Mantovani, A. The inflammatory micro-environment in tumor progression: the role of tumor-associated macrophages. *Crit Rev Oncol Hematol* **66,** 1–9 (2008).
134. Galdiero, M. R., Garlanda, C., Jaillon, S., Marone, G. & Mantovani, A. Tumor associated macrophages and neutrophils in tumor progression. *J Cell Physiol* **228,** 1404–1412 (2013).
135. Mielgo, A. & Schmid, M. C. Impact of tumour associated macrophages in pancreatic cancer. *BMB Reports* **46,** 131–138 (2013).
136. Lin, E. Y., Nguyen, A. V, Russell, R. G. & Pollard, J. W. Colony-stimulating factor 1 promotes progression of mammary tumors to malignancy. *J Exp Med* **193,** 727–740 (2001).
137. Shojaei, F. & Ferrara, N. Role of the microenvironment in tumor growth and in refractoriness/resistance to anti-angiogenic therapies. *Drug Resist Updat* **11,** 219–230 (2008).
138. Erkan, M. *et al.* The activated stroma index is a novel and independent prognostic marker in pancreatic ductal adenocarcinoma. *Clin Gastroenterol Hepatol* **6,** 1155–1161 (2008).

139. Hanahan, D. & Weinberg, R. A. Hallmarks of cancer: the next generation. *Cell* **144,** 646–674 (2011).
140. Pardoll, D. Does the immune system see tumors as foreign or self? *Annu Rev Immunol* **21,** 807–839 (2003).
141. Mytar, B. *et al.* Tumor cell-induced deactivation of human monocytes. *J Leukoc Biol* **74,** 1094–1101 (2003).
142. Qian, B. Z. & Pollard, J. W. Macrophage Diversity Enhances Tumor Progression and Metastasis. *Cell* **141,** 39–51 (2010).
143. Chen, J. J. *et al.* Tumor-associated macrophages: the double-edged sword in cancer progression. *J Clin Oncol* **23,** 953–964 (2005).
144. Li, H., Fan, X. & Houghton, J. Tumor microenvironment: The role of the tumor stroma in cancer. *Journal of Cellular Biochemistry* **101,** 805–815 (2007).
145. Nielsen, M. F. B., Mortensen, M. B. & Detlefsen, S. Key players in pancreatic cancer-stroma interaction: Cancer-associated fibroblasts, endothelial and inflammatory cells. *World Journal of Gastroenterology* **22,** 2678–2700 (2016).
146. Toullec, A. *et al.* Oxidative stress promotes myofibroblast differentiation and tumour spreading. *EMBO Mol. Med.* **2,** 211–230 (2010).
147. Orimo, A. & Weinberg, R. A. Heterogeneity of stromal fibroblasts in tumors. *Cancer Biology and Therapy* **6,** 618–619 (2007).
148. Wen, S., Niu, Y., Yeh, S. & Chang, C. BM-MSCs promote prostate cancer progression via the conversion of normal fibroblasts to cancer-associated fibroblasts. *Int. J. Oncol.* **47,** 719–727 (2015).
149. Nagasaki, T., Hara, M., Shiga, K. & Takeyama, H. Relationship between inflammation and cancer progression: Recent advances in interleukin-6 signaling and its blockage in cancer therapy. *Receptors & Clinical Investigation* **1,** 10–14800/rci.202 (2014).
150. Eser, S., Schnieke, A., Schneider, G. & Saur, D. Oncogenic KRAS signalling in pancreatic cancer. *Br. J. Cancer* **111,** 817–22 (2014).
151. Grutzmann, R. *et al.* Gene expression profiles of microdissected pancreatic ductal adenocarcinoma. *Virchows Arch.* **443,** 508–517 (2003).
152. Hingorani, S. R. *et al.* Preinvasive and invasive ductal pancreatic cancer and its early detection in the mouse. *Cancer Cell* **4,** 437–450 (2003).
153. Schlieman, M. G., Fahy, B. N., Ramsamooj, R., Beckett, L. & Bold, R. J. Incidence, mechanism and prognostic value of activated AKT in pancreas cancer.

Br J Cancer **89,** 2110–2115 (2003).

154. Bellizzi, A. M., Bloomston, M., Zhou, X. P., Iwenofu, O. H. & Frankel, W. L. The mTOR pathway is frequently activated in pancreatic ductal adenocarcinoma and chronic pancreatitis. *Appl Immunohistochem Mol Morphol* **18,** 442–447 (2010).
155. Arlt, A. *et al.* Role of NF-kappaB and Akt/PI3K in the resistance of pancreatic carcinoma cell lines against gemcitabine-induced cell death. *Oncogene* **22,** 3243–3251 (2003).
156. Roy, R. & Maraveyas, A. Chemoradiation in pancreatic adenocarcinoma: a literature review. *Oncologist* **15,** 259–269 (2010).
157. Morran, D. C. *et al.* Targeting mTOR dependency in pancreatic cancer. *Gut* **63,** 1481–9 (2014).
158. Metchnikoff, I. & Prize, N. Mini - review : Macrophage Polarization. *Biorad* **2,** 1–8 (2015).
159. Lu, Y. C., Yeh, W. C. & Ohashi, P. S. LPS/TLR4 signal transduction pathway. *Cytokine* **42,** 145–151 (2008).
160. Guha, M. & Mackman, N. LPS induction of gene expression in human monocytes. *Cellular Signalling* **13,** 85–94 (2001).
161. Hayes, M. P., Freeman, S. L. & Donnelly, R. P. IFN-[gamma] priming of monocytes enhances LPS-induced TNF production by augmenting both transcription and mRNA stability. *Cytokine* **7,** 427–435 (1995).
162. Stein, M., Keshav, S., Harris, N. & Gordon, S. Interleukin 4 potently enhances murine macrophage mannose receptor activity: a marker of alternative immunologic macrophage activation. *J. Exp. Med.* **176,** 287–92 (1992).
163. Martinez, F. O. & Gordon, S. The M1 and M2 paradigm of macrophage activation: time for reassessment. *F1000Prime Rep.* **6,** 13 (2014).
164. Gordon, S., Plüddemann, A. & Martinez Estrada, F. Macrophage heterogeneity in tissues: Phenotypic diversity and functions. *Immunol. Rev.* **262,** 36–55 (2014).
165. Pan, H., O'Brien, T. F., Zhang, P. & Zhong, X.-P. The Role of TSC1 in Regulating Innate Immunity. *J Immunol* (2012). doi:10.4049/jimmunol.1102187
166. Xu, K., Liu, P. & Wei, W. MTOR signaling in tumorigenesis. *Biochimica et Biophysica Acta - Reviews on Cancer* **1846,** 638–654 (2014).
167. Akashi, K., Traver, D., Miyamoto, T. & Weissman, I. L. A clonogenic common myeloid progenitor that gives rise to all myeloid lineages. *Nature* **404,** 193–197 (2000).

168. Kondo, M., Weissman, I. L. & Akashi, K. Identification of clonogenic common lymphoid progenitors in mouse bone marrow. *Cell* **91,** 661–672 (1997).
169. Manz, M. G., Miyamoto, T., Akashi, K. & Weissman, I. L. Prospective isolation of human clonogenic common myeloid progenitors. *Proc. Natl. Acad. Sci. U. S. A.* **99,** 11872–11877 (2002).
170. Francke, A., Herold, J., Weinert, S., Strasser, R. H. & Braun-Dullaeus, R. C. Generation of mature murine monocytes from heterogeneous bone marrow and description of their properties. *J. Histochem. Cytochem.* **59,** 813–25 (2011).
171. Wang, C. *et al.* Characterization of murine macrophages from bone marrow, spleen and peritoneum. *BMC Immunol* **14,** 6 (2013).
172. Manzanero, S. Generation of mouse bone marrow-derived macrophages. *Methods Mol. Biol.* **844,** 177–181 (2012).
173. Mantovani, A. *et al.* The chemokine system in diverse forms of macrophage activation and polarization. *Trends in Immunology* **25,** 677–686 (2004).
174. Martinez, F. O., Helming, L. & Gordon, S. Alternative Activation of Macrophages: An Immunologic Functional Perspective. *Annu. Rev. Immunol.* **27,** 451–483 (2009).
175. Gordon, S. Alternative activation of macrophages. *Nat. Rev. Immunol.* **3,** 23–35 (2003).
176. Dowling, R. J. *et al.* mTORC1-mediated cell proliferation, but not cell growth, controlled by the 4E-BPs. *Science (80-.).* **328,** 1172–1176 (2010).
177. Katholnig, K. *et al.* Immune responses of macrophages and dendritic cells regulated by mTOR signalling. *Biochem. Soc. Trans.* **41,** 927–33 (2013).
178. Dowling, R. J. O., Topisirovic, I., Fonseca, B. D. & Sonenberg, N. Dissecting the role of mTOR: Lessons from mTOR inhibitors. *Biochimica et Biophysica Acta - Proteins and Proteomics* **1804,** 433–439 (2010).
179. Wang, X. *et al.* Rheb1-mTORC1 maintains macrophage differentiation and phagocytosis in mice. *Exp. Cell Res.* **344,** 219–228 (2016).
180. Inoki, K., Li, Y., Xu, T. & Guan, K. L. Rheb GTPase is a direct target of TSC2 GAP activity and regulates mTOR signaling. *Genes Dev* **17,** 1829–1834 (2003).
181. Lavin, Y., Mortha, A., Rahman, A. & Merad, M. Regulation of macrophage development and function in peripheral tissues. *Nat. Rev. Immunol.* **15,** 731–744 (2015).
182. Lisi, L., Navarra, P., Feinstein, D. L. & Dello Russo, C. The mTOR kinase

inhibitor rapamycin decreases iNOS mRNA stability in astrocytes. *J. Neuroinflammation* **8,** 1 (2011).

183. Zhou, D. *et al.* Macrophage polarization and function with emphasis on the evolving roles of coordinated regulation of cellular signaling pathways. *Cellular Signalling* **26,** 192–197 (2014).
184. Hackstein, H., Taner, T., Logar, A. J. & Thomson, A. W. Rapamycin inhibits macropinocytosis and mannose receptor-mediated endocytosis by bone marrow-derived dendritic cells. *Blood* **100,** 1084–1087 (2002).
185. Cornu, M., Albert, V. & Hall, M. N. MTOR in aging, metabolism, and cancer. *Current Opinion in Genetics and Development* **23,** 53–62 (2013).
186. Lee, D. F. & Hung, M. C. All roads lead to mTOR: Integrating inflammation and tumor angiogenesis. *Cell Cycle* **6,** 3011–3014 (2007).
187. Kim, J.-H., Yoon, M.-S. & Chen, J. Signal transducer and activator of transcription 3 (STAT3) mediates amino acid inhibition of insulin signaling through serine 727 phosphorylation. *J. Biol. Chem.* **284,** 35425–35432 (2009).
188. Carracedo, A. *et al.* Inhibition of mTORC1 leads to MAPK pathway activation through a PI3K-dependent feedback loop in human cancer. *J. Clin. Invest.* **118,** 3065–3074 (2008).
189. Busch, S., Renaud, S. J., Schleussner, E., Graham, C. H. & Markert, U. R. mTOR mediates human trophoblast invasion through regulation of matrix-remodeling enzymes and is associated with serine phosphorylation of STAT3. *Exp. Cell Res.* **315,** 1724–1733 (2009).
190. Li, H., Lee, J., He, C., Zou, M.-H. & Xie, Z. Suppression of the mTORC1/STAT3/Notch1 pathway by activated AMPK prevents hepatic insulin resistance induced by excess amino acids. *Am. J. Physiol. Endocrinol. Metab.* **306,** E197-209 (2014).
191. Dan, H. C. *et al.* Akt-dependent regulation of NF-??B is controlled by mTOR and Raptor in association with IKK. *Genes Dev.* **22,** 1490–1500 (2008).
192. Shih, V. F.-S., Tsui, R., Caldwell, A. & Hoffmann, A. A single NFκB system for both canonical and non-canonical signaling. *Cell Res.* **21,** 86–102 (2011).
193. García-García, E. & Rosales, C. Signal transduction during Fc receptor-mediated phagocytosis. *J. Leukoc. Biol.* **72,** 1092–1108 (2002).
194. Aderem, a & Underhill, D. M. Mechanisms of phagocytosis in macrophages. *Annu. Rev. Immunol.* **17,** 593–623 (1999).

195. Castellano, F., Chavrier, P. & Caron, E. Actin dynamics during phagocytosis. *Semin. Immunol.* **13,** 347–55 (2001).
196. Harrison, R. E. & Grinstein, S. Phagocytosis and the microtubule cytoskeleton. *Biochem. Cell Biol.* **80,** 509–515 (2002).
197. Flannagan, R. S., Jaumouillé, V. & Grinstein, S. The cell biology of phagocytosis. *Annu. Rev. Pathol.* **7,** 61–98 (2012).
198. Gordon, S., Plüddemann, A. & Mukhopadhyay, S. Sinusoidal immunity: Macrophages at the lymphohematopoietic interface. *Cold Spring Harb. Perspect. Biol.* **7,** (2015).
199. Allen, W. E., Zicha, D., Ridley, A. J. & Jones, G. E. A role for Cdc42 in macrophage chemotaxis. *J. Cell Biol.* **141,** 1147–1157 (1998).
200. Park, H., Ishihara, D. & Cox, D. Regulation of tyrosine phosphorylation in macrophage phagocytosis and chemotaxis. *Archives of Biochemistry and Biophysics* **510,** 101–111 (2011).
201. Pixley, F. J. Macrophage migration and its regulation by CSF-1. *International Journal of Cell Biology* (2012). doi:10.1155/2012/501962
202. Schmidt, A. & Hall, M. N. Signaling To the Actin Cytoskeleton. *Annu. Rev. Cell Dev. Biol* **14,** 305–38 (1998).
203. Kanno, S., Furuyama, A. & Hirano, S. A murine scavenger receptor MARCO recognizes polystyrene nanoparticles. *Toxicol. Sci.* **97,** 398–406 (2007).
204. Sedgwick, J. D., Ford, a L., Foulcher, E. & Airriess, R. Central nervous system microglial cell activation and proliferation follows direct interaction with tissue-infiltrating T cell blasts. *J. Immunol.* **160,** 5320–5330 (1998).
205. Hart, S. P., Dransfield, I. & Rossi, A. G. Phagocytosis of apoptotic cells. *Methods* **44,** 280–285 (2008).
206. Eitzen, G. Actin remodeling to facilitate membrane fusion. *Biochimica et Biophysica Acta - Molecular Cell Research* **1641,** 175–181 (2003).
207. Strieter, R. M. *et al.* Monocyte chemotactic protein gene expression by cytokine-treated human fibroblasts and endothelial cells. *Biochem Biophys Res Commun* **162,** 694–700 (1989).
208. Green, C. E. *et al.* Chemoattractant signaling between tumor cells and macrophages regulates cancer cell migration, metastasis and neovascularization. *PLoS One* **4,** (2009).
209. Sica, A., Allavena, P. & Mantovani, A. Cancer related inflammation: The

macrophage connection. *Cancer Letters* **267,** 204–215 (2008).

210. Sen, B. *et al.* MTORC2 regulates mechanically induced cytoskeletal reorganization and lineage selection in marrow-derived mesenchymal stem cells. *J. Bone Miner. Res.* **29,** 78–89 (2014).
211. Dunlop, E. A. & Tee, A. R. Mammalian target of rapamycin complex 1: Signalling inputs, substrates and feedback mechanisms. *Cellular Signalling* **21,** 827–835 (2009).
212. Laplante, M. & Sabatini, D. M. Regulation of mTORC1 and its impact on gene expression at a glance. *J. Cell Sci.* **126,** 1713–1719 (2013).
213. Laplante, M. & Sabatini, D. M. mTOR signaling in growth control and disease. *Cell* **149,** 274–293 (2013).
214. Chiang, G. G. & Abraham, R. T. Targeting the mTOR signaling network in cancer. *Trends in Molecular Medicine* **13,** 433–442 (2007).
215. Hoeffer, C. A. & Klann, E. mTOR signaling: At the crossroads of plasticity, memory and disease. *Trends in Neurosciences* **33,** 67–75 (2010).
216. Komura, T. *et al.* Inflammatory features of pancreatic cancer highlighted by monocytes/macrophages and CD4+ T cells with clinical impact. *Cancer Sci.* **106,** 672–686 (2015).
217. Helm, O. *et al.* Tumor-associated macrophages exhibit pro- and anti-inflammatory properties by which they impact on pancreatic tumorigenesis. *Int. J. Cancer* **135,** 843–861 (2014).
218. Zhu, Y. *et al.* CSF1/CSF1R blockade reprograms tumor-infiltrating macrophages and improves response to T-cell checkpoint immunotherapy in pancreatic cancer models. *Cancer Res.* **74,** 5057–5069 (2014).
219. Mitchem, J. B. *et al.* Targeting tumor-infiltrating macrophages decreases tumor-initiating cells, relieves immunosuppression, and improves chemotherapeutic responses. *Cancer Res.* **73,** 1128–1141 (2013).
220. Wang, X. & Proud, C. G. MTORC1 signaling: What we still dont know. *Journal of Molecular Cell Biology* **3,** 206–220 (2011).
221. Holz, M. K., Ballif, B. A., Gygi, S. P. & Blenis, J. mTOR and S6K1 mediate assembly of the translation preinitiation complex through dynamic protein interchange and ordered phosphorylation events. *Cell* **123,** 569–580 (2005).
222. Hao, N. B. *et al.* Macrophages in tumor microenvironments and the progression of tumors. *Clinical and Developmental Immunology* **2012,** (2012).

223. Mantovani, A., Sozzani, S., Locati, M., Allavena, P. & Sica, A. Macrophage polarization: Tumor-associated macrophages as a paradigm for polarized M2 mononuclear phagocytes. *Trends in Immunology* **23,** 549–555 (2002).
224. Breuleux, M. *et al.* Increased AKT S473 phosphorylation after mTORC1 inhibition is rictor dependent and does not predict tumor cell response to PI3K/mTOR inhibition. *Mol. Cancer Ther.* **8,** 742–53 (2009).
225. Fox, R. *et al.* PSGL-1 and mTOR regulate translation of ROCK-1 and physiological functions of macrophages. *EMBO J.* **26,** 505–515 (2007).
226. Huang, W. *et al.* mTORC2 controls actin polymerization required for consolidation of long-term memory. *Nat. Neurosci.* **16,** 441–8 (2013).